THE ASTROPHYSICAL JOURNAL

AN INTERNATIONAL REVIEW OF SPECTROSCOPY AND ASTRONOMICAL PHYSICS

VOLUME 86 OCTOBER 1937 NUMBER 3

ON THE MASSES OF NEBULAE AND OF CLUSTERS OF NEBULAE

F. ZWICKY

ABSTRACT

Present estimates of the masses of nebulae are based on observations of the *luminosities* and *internal rotations* of nebulae. It is shown that both these methods are unreliable; that from the observed luminosities of extragalactic systems only lower limits for the values of their masses can be obtained (sec. i), and that from internal rotations alone no determination of the masses of nebulae is possible (sec. ii). The observed internal motions of nebulae can be understood on the basis of a simple mechanical model, some properties of which are discussed. The essential feature is a central core whose internal *viscosity* due to the gravitational interactions of its component masses is so high as to cause it to rotate like a solid body.

In sections iii, iv, and v three new methods for the determination of nebular masses are discussed, each of which makes use of a different fundamental principle of physics.

Method iii is based on the *virial theorem* of classical mechanics. The application of this theorem to the Coma cluster leads to a minimum value $\overline{M}=4.5\times 10^{10}M_{\odot}$ for the average mass of its member nebulae.

Method iv calls for the observation among nebulae of certain *gravitational lens* effects.

Section v gives a generalization of the principles of ordinary *statistical mechanics* to the whole system of nebulae, which suggests a new and powerful method which ultimately should enable us to determine the masses of all types of nebulae. This method is very flexible and is capable of many modes of application. It is proposed, in particular, to investigate the distribution of nebulae in individual great clusters.

As a first step toward the realization of the proposed program, the Coma cluster of nebulae was photographed with the new 18-inch Schmidt telescope on Mount Palomar. Counts of nebulae brighter than about $m=16.7$ given in section vi lead to the gratifying result that the distribution of nebulae in the Coma cluster is very similar to the distribution of luminosity in globular nebulae, which, according to Hubble's investigations, coincides closely with the theoretically determined distribution of matter in isothermal gravitational gas spheres. The high central condensation of the Coma cluster, the very gradual decrease of the number of nebulae per unit volume at great distances from its center, and the hitherto unexpected enormous extension of this cluster become here apparent for the first time. These results also suggest that the current classification of nebulae into relatively few *cluster nebulae* and a majority of

field nebulae may be fundamentally inadequate. From the preliminary counts reported here it would rather follow that practically *all* nebulae must be thought of as being grouped in clusters—a result which is in accord with the theoretical considerations of section v.

In conclusion, a comparison of the relative merits of the three new methods for the determination of nebular masses is made. It is also pointed out that an extensive investigation of great clusters of nebulae will furnish us with decisive information regarding the question whether physical conditions in the known parts of the universe are merely fluctuating around a stationary state or whether they are continually and systematically changing.

The determination of the masses of extragalactic nebulae constitutes at present one of the major problems in astrophysics. Masses of nebulae until recently were estimated either from the luminosities of nebulae or from their internal rotations. In this paper it will be shown that both these methods of determining nebular masses are unreliable. In addition, three new possible methods will be outlined.

I. MASSES FROM LUMINOSITIES OF NEBULAE

The observed absolute luminosity of any stellar system is an indication of the approximate amount of luminous matter in such a system. In order to derive trustworthy values of the masses of nebulae from their absolute luminosities, however, detailed information on the following three points is necessary.

1. According to the mass-luminosity relation, the conversion factor from absolute luminosity to mass is different for different types of stars. The same holds true for any kind of luminous matter. In order to determine the conversion factor for a nebula as a whole, we must know, therefore, in what proportions all the possible luminous components are represented in this nebula.

2. We must know how much dark matter is incorporated in nebulae in the form of cool and cold stars, macroscopic and microscopic solid bodies, and gases.

3. Finally, we must know to what extent the apparent luminosity of a given nebula is diminished by the internal absorption of radiation because of the presence of dark matter.

Data are meager[1] on point 1. Accurate information on points 2

[1] It should, however, be mentioned that certain spiral nebulae seem to be stellar systems similar in composition to the local Kapteyn system of our galaxy. For such systems the conversion factors may with some confidence be set equal to the conversion factor of the Kapteyn system. See also E. Hubble, *Ap. J.*, **64**, 148, 1929.

and 3 is almost entirely lacking. Estimates of the masses of nebulae from their observed luminosities are therefore incomplete and can at best furnish only the lowest limits for the values of these masses.

II. MASSES FROM INTERNAL ROTATIONS OF NEBULAE

It has apparently been taken for granted by some astronomers[2] that from observations on the internal rotations good values for the masses M_N of nebulae could be derived. Values of the order of $M_N = 10^9\ M_\odot$ up to $M_N = 4 \times 10^{10}\ M_\odot$ were obtained in this way,[2] where $M_\odot = 2 \times 10^{33}$ gr is the mass of the sun. A closer scrutiny of the behavior of suitably chosen mechanical models of stellar systems, unfortunately, soon reveals the fact that the masses of such systems, for a given distribution of average angular velocities throughout the system, are highly indeterminate, and vice versa. This conclusion may, for instance, be derived from the consideration of two limiting models of a nebula as a mechanical system.

A. MODEL OF A NEBULA WHOSE "INTERNAL VISCOSITY" IS NEGLIGIBLE

This model consists of a heavy and small nucleus of mass M_0 around which a given number, n, of stars of average mass $M_s \ll M_0/n$ describe planetary orbits. The mutual gravitational interactions between these outlying stars are negligible, and the system may therefore be said to have an internal "viscosity" equal to zero. It is obvious that under these circumstances we may build up models that satisfy almost any specifications in regard to total mass, total luminosity, and internal distribution of luminosity as well as distribution of the average angular velocities. We may, for instance, distribute our n stars over the six-dimensional manifold of all possible planetary orbits (including the epochs or phases) in such fashion that the average angular velocity of the resulting system S_0 is zero in every point. Since all these orbits are essentially non-interacting, we may reverse the sense of rotation (direction of stellar motion) in an arbitrary number of these orbits. In this way a system S of specified distribution of average angular velocities may be constructed whose remaining characteristics, such as the mass, the luminosity,

[2] E. Hubble, *The Realm of Nebulae* (New Haven: Yale University Press, 1936), p. 179; also *Ap. J.*, **69**, 150, 1929.

and the external shape, are identical with those of S_0. Thus, the observed angular velocities in themselves give no clue regarding the mass of the system.

B. MODEL OF A NEBULA WHOSE INTERNAL VISCOSITY IS VERY GREAT

This model is built up of stars, dust, and gases in such fashion that the gravitational interactions between the various components, as well as direct impacts, influence the path of every component mass in a radical way. Many changes in energy and momentum of every component mass will take place during time intervals that are short compared with the time an unperturbed mass of the same initial velocity would consume to traverse the system.

Conditions of motion in this model are analogous to the conditions of motion of elementary particles in a star. This model of a nebula, therefore, will rotate like a solid body, regardless of what its total mass and the distribution of mass over different regions of the system may be. The conclusion which has sometimes been put forward,[2] that constant angular velocity necessarily implies uniform distribution of mass, is obviously erroneous. Furthermore, it is again seen that the rate of rotation of a stellar system has no very direct bearing on its total mass.

C. ACTUAL NEBULAE

Good mechanical models of actual nebulae may presumably be constructed by combining the distinctive features of the two limiting cases described in the preceding sections. Such a combined model will possess a central, highly viscous core whose relative dimensions are not negligible but are comparable with the extension of the whole system. If the outlying, and among themselves little interacting, components of the nebula had no connection with the central core, we might, at a given instant, observe average angular velocities Ω which, as a function of the distance r from the center of rotation, would be given by

$$\Omega(r) = \Omega_0 = \text{const.} \longleftrightarrow \text{for } r < r_0 \,, \tag{1}$$

where r_0 is the radius of the core. For $r > r_0$, the angular velocity $\Omega(r)$ would be essentially arbitrary. In reality, however, the viscosity will not drop abruptly to zero at $r = r_0$. From an inspection

of the distribution of the outlying masses in many nebulae it would seem that these masses at some previous time must have formed part of the central core. They may have been ejected from this core because they acquired high kinetic energy through many close encounters, or they may be the result of a partial disruption of the core by tidal actions caused by encounters with other nebulae (Jeans). At the moment these outlying masses have passed the boundary of the core, their average tangential velocities must have been of the order $r_0\Omega_0$. Assuming that these masses in regions $r > r_0$ are essentially subject only to the gravitational attraction of a central spherical core and that the interactions among themselves may be neglected (the internal viscosity of the outlying system is equal to zero), the average angular velocity $\Omega(r)$ outside the core will be approximately given as

$$\Omega(r) = \frac{r_0^2\Omega_0}{r^2} \qquad \text{for } r > r_0 \, . \tag{2}$$

This relation simply expresses the fact that a mass m which, on being ejected from the core with a tangential velocity v_t relative to this core, describes an orbit whose angular momentum,

$$mr^2\omega = m[r_0 v_t + r_0^2\Omega_0] = c \, , \tag{3}$$

is a constant. If the average $\overline{v_t}$ for many particles leaving the core is zero, the average angular velocity $\overline{\omega} = \Omega$ of all the particles in a given point is obtained from

$$r^2\overline{\omega} = r^2\Omega(r) = r_0^2\Omega_0 \, , \tag{4}$$

which is the same as (2). Unfortunately, relation (2) is superficially very similar to the relation obeyed by the angular velocities ω_c of a system of circular planetary orbits around a heavy central mass M. For such an orbit we have

$$mr\omega_c^2 = \frac{\Gamma m M}{r^2} \tag{5}$$

or

$$\omega_c = \frac{(\Gamma M)^{1/2}}{r^{3/2}} \, , \tag{6}$$

where Γ is the universal gravitational constant. The similarity of the dependence on r in (2) and (6) will in reality become still greater, since the rate of decrease of $\Omega(r)$ with increasing values of r will in actual nebulae be more gradual than that given by (2), owing to the fact that the internal viscosity will not vanish abruptly at $r = r_0$ but will disappear gradually with increasing r. The observed angular velocities in the outlying regions of nebulae actually show a dependence on r which resembles the relation (6). This relation was, therefore, sometimes erroneously used for the determination of the mass M. The preceding discussion, however, indicates that the observed angular velocities may be adequately accounted for on the basis of the considerations resulting in relation (2) rather than in relation (6). This again shows clearly that it is not possible to derive the masses of nebulae from observed rotations without the use of additional information, since the relation (2) does not contain the mass M at all.

D. FURTHER DISCUSSION OF THE ROTATION OF NEBULAE

From the analysis of an appropriate mechanical model of actual nebulae we have derived in the preceding section the following approximate dependence on r of the average tangential velocity V_t:

$$V_t = r\Omega_0 \qquad \text{for } r < r_0 \tag{7}$$

$$V_t = \frac{r_0^2\Omega_0}{r} \qquad \text{for } r > r_0 \, . \tag{8}$$

This dependence is pictured in Figure 1 . The observed curves $V_t(r)$ are similar to the schematic curve of Figure 1. From this similarity we infer that the cores of nebulae possess considerable internal viscosity. The problem of deducing theoretical values for this viscosity therefore arises. It will be interesting to see whether the gravitational interactions in dense stellar systems are sufficient to account for the fact that such systems rotate like solid bodies, or if it is necessary to introduce matter in the form of dust particles and gases.

The point of view adopted in the preceding discussion automatically eliminates the discrepancy which was thought to exist, with respect to the distribution of mass in nebulae as derived from data on

internal rotations, on the one side, and from the shape and the distribution of the isophotal contours, on the other. The tremendous increase of surface brightness from the edge, $r = r_0$, of the core of nebulae to their center, $r = 0$, indicates a correspondingly large increase of mass density. The erroneous idea[2] that the constancy of the angular velocity throughout the core necessitates the assumption of a constant mass density therefore created an apparently insoluble paradox. This paradox, however, disappears as soon as we introduce the idea of an internal gravitational viscosity of stellar systems, which equalizes the angular velocity throughout such systems re-

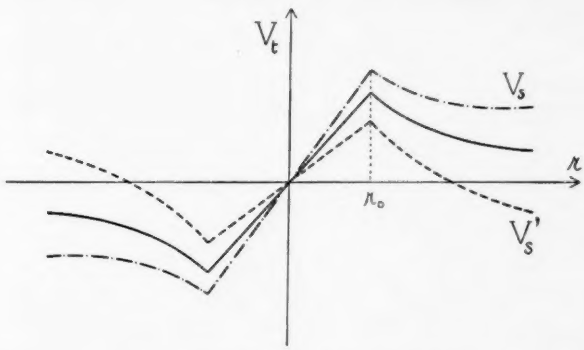

FIG. 1.—Velocity of rotation in nebulae

gardless of the distribution of mass. How this viscosity may be expressed in terms of the gravitational interactions of stars will be discussed in another place.

One further interesting problem presents itself. The distribution of matter in a stellar system which has an internal viscosity as high as we have assumed it to be in the cores of nebulae should rapidly converge toward stationary conditions. The determination of the density distribution in such a system should be analogous to the determination of the density distribution in gravitating gas spheres. R. Emden's analysis[3] of such spheres may, therefore, prove useful in the study of globular and elliptical nebulae as well as in the study of cores of spiral nebulae.

In concluding this section the question may be raised whether

[3] *Gaskugeln* (Leipzig, 1907).

data on the internal rotation of nebulae, supplemented by certain additional information, make possible the determination of nebular masses. This question, in principle, must be answered in the affirmative. For instance, data on internal velocities combined with the virial theorem discussed in the next section may ultimately furnish good values for the masses of globular and elliptical nebulae as well as the cores of certain spirals. In the case of open spirals, an investigation of the geometrical structure of the spiral arms, combined with

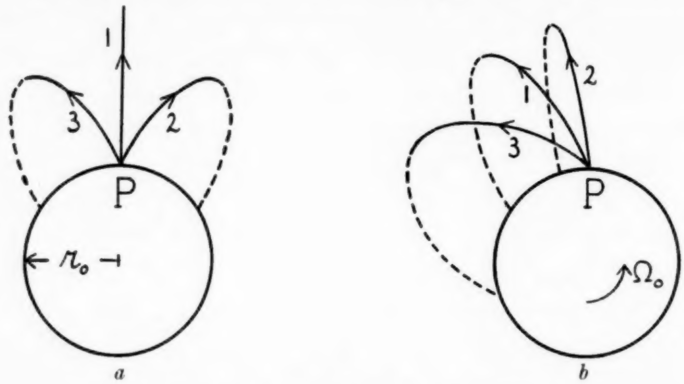

FIG. 2.—Rotation of nebulae and shape of spiral arms

velocity data, promises to be helpful. In this connection a few remarks may be in order regarding the possibility of the formation of spiral arms in our simple mechanical model of nebulae.

Consider the two alternatives pictured in Figure 2: (*a*) a nonrotating core, that is, $\Omega_0 = 0$, and (*b*) a rotating core, $\Omega_0 \neq 0$. Suppose that some disturbance, such as tidal action, causes the ejection from the core of a number of stars at P. The resulting orbits of three stars, 1, 2, and 3, are schematically indicated in Figure 2. For $\Omega_0 \neq 0$ distinct spiral arms may be formed, provided a sufficient number of stars are ejected whose radial and tangential velocity components v_r and v_t relative to the core are in certain favorable relations to the peripheral velocity $r_0\Omega_0$ of the core.

It should be remarked that the orbits 1, 2, 3, etc., in Figure 2*b* are ellipses only if outside the core the corresponding masses are no longer acted upon by the forces which originally caused their ejection from the core. If, for example, the ejection is brought about by

the close encounter of the nebula with another nebula, tidal actions will continue until the second nebula has moved far away and our simple model must be correspondingly modified. It may suffice here to point out that in addition to the creation of angular momentum in a nebula, a close encounter may also set up radial pulsation in this nebula. This pulsation will not, in general, be spherically symmetrical. As a first approximation we can schematically characterize it by what might be called the "tidal ellipsoid" or "ellipsoid of pulsation." The magnitudes and signs of the radial velocities which are induced along the principal axes of this ellipsoid by the passing second nebula approximately determine the character of the resulting pulsation in the nebula under consideration.

The probable existence of pulsation in many nebulae further complicates the interpretation of differences in the observed velocities V_s along the line of sight of various parts of a nebula. If we have pulsation, V_s differs from the value of V_t owing to rotation alone, by amounts which depend on the position of the tidal ellipsoid relative to the two vectors which define the line of sight and the axis of rotation. In two obvious, simple cases the functions $V_s(r)$ may graphically assume the forms represented by the two dotted curves (V_s and V_s') in Figure 1.

The possible existence of pulsation also suggests that we cannot, without additional knowledge, interpret ellipsoidal shapes of nebulae as being due to rotation alone. Values of the masses of nebulae which are derived on the assumption that elliptical nebulae are stellar systems in rotational equilibrium must therefore be viewed with suspicion.

Before embarking on any detailed analysis of spiral structures it will be advisable to obtain first qualitative information concerning the shape of the spiral arms in relation to the sense of rotation of the core. Promising results in this direction have already been secured by Dr. W. Baade of the Mount Wilson Observatory, who has found that the tips of the spiral arms of the Andromeda nebula are curved in the direction determined by the sense of rotation of the core, as pictured in Figure 2*b*. I am indebted to Dr. Baade for a private communication of this unpublished result.

Summing up, we may say that present data on internal rotations

furnish, at best, minimum values $M_{\min}$ for the masses of the nebulae. Such minimum values are obtained if we assume that nebulae are stable systems whose components have velocities v inferior to the velocity of escape v_e from the system. Therefore

$$v_e \geqslant v_{\max} \geqslant r_0\Omega_0 . \tag{9}$$

But

$$v_e = \left(\frac{2\Gamma M_0}{r_0}\right)^{1/2} , \tag{10}$$

where M_0, r_0, and Ω_0 are the mass, the radius, and the angular velocity of the core. Consequently, the mass M of the nebula is

$$M > M_0 \geqslant \frac{r_0^3\Omega_0^2}{2\Gamma} . \tag{11}$$

For example, in the case of NGC 4594 we have $r_0 \geqslant 4.3 \times 10^{21}$ cm and $r_0\Omega_0 \cong 4 \times 10^7$ cm/sec, which gives

$$M > 5 \times 10^{43} \text{ gr} = 2.5 \times 10^{10} M_\odot . \tag{12}$$

The data used are taken from the paper on NGC 4594 by F. G. Pease,[4] who, in 1916, measured the spectroscopic rotation of this nebula. Pease also was the first to point out that the central parts of nebulae rotate like solid bodies.

Since the determination of nebular masses is of considerable importance in modern astrophysics, three new methods for the solution of this problem are briefly outlined in the following pages. Two of these I have proposed already in previous communications.[5, 6] The third, in a restricted form, has been applied thus far only to clusters of stars.[7] Its applicability to clusters of nebulae remains to be investigated. The purpose of this paper is to discuss the basic principles on which the new methods rest.

[4] *Proc. Nat. Acad.*, **2**, 517, 1916.

[5] F. Zwicky, *Helv. physica acta*, **6**, 110, 1933.

[6] F. Zwicky, *Phys. Rev.*, **51**, 290, 1937, and **51**, 679, 1937.

[7] H. von Zeipel, *Jubilaeumsnummer d. A. N.*, p. 33, 1921.

III. THE VIRIAL THEOREM APPLIED TO CLUSTERS OF NEBULAE

If the total masses of clusters of nebulae were known, the average masses of cluster nebulae could immediately be determined from counts of nebulae in these clusters, provided internebular material is of the same density inside and outside of clusters.

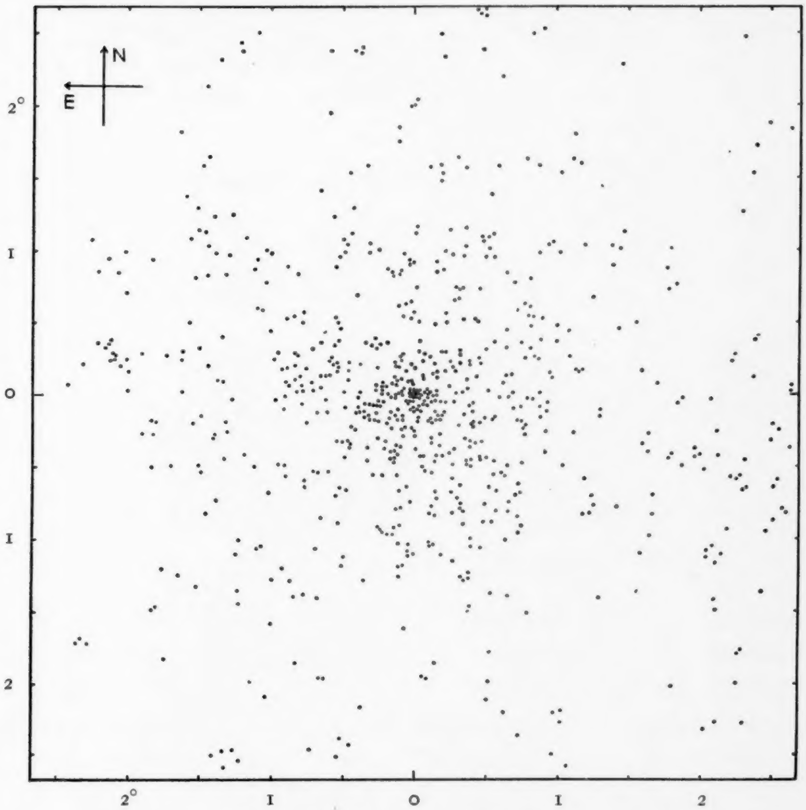

FIG. 3.—The Coma cluster of nebulae

As a first approximation, it is probably legitimate to assume that clusters of nebulae such as the Coma cluster (see Fig. 3) are mechanically stationary systems. With this assumption, the virial theorem of classical mechanics gives the total mass of a cluster in terms of the average square of the velocities of the individual nebulae which constitute this cluster.[5] But even if we drop the assumption that clus-

ters represent stationary configurations, the virial theorem, in conjunction with certain additional data, allows us to draw important conclusions concerning the masses of nebulae, as will now be shown.

Suppose that the radius vector from a fixed point in the cluster to the nebula (σ) of mass M_σ is $\vec{r}_\sigma$. For the fixed point we conveniently chose the center of mass of the whole cluster. The fundamental law of motion of the nebula (σ) is

$$M_\sigma \frac{d^2\vec{r}_\sigma}{dt^2} = \vec{F}_\sigma , \tag{13}$$

where $\vec{F}_\sigma$ is the total force acting on M_σ. Scalar multiplication of this equation with $\vec{r}_\sigma$ gives

$$\tfrac{1}{2} \frac{d^2}{dt^2} (M_\sigma r_\sigma^2) = \vec{r}_\sigma \cdot \vec{F}_\sigma + M_\sigma \left(\frac{d\vec{r}_\sigma}{dt}\right)^2 . \tag{14}$$

Summation over all the nebulae of the cluster leads to

$$\tfrac{1}{2} \frac{d^2\Theta}{dt^2} = Vir + 2K_T , \tag{15}$$

where $\Theta = \sum_\sigma M_\sigma r_\sigma^2$ is the polar moment of inertia of the cluster, $Vir = \sum_\sigma \vec{r}_\sigma \cdot \vec{F}_\sigma$ is the virial of the cluster, and K_T is the sum of the kinetic energies of translation of the individual nebulae. If the cluster under consideration is stationary, its polar moment of inertia Θ fluctuates around a constant value Θ_0, such that the time average of its derivatives with respect to time is zero. Denoting time averages by a bar, we have in this case

$$\overline{Vir} = -2\overline{K_T} . \tag{16}$$

On the assumption that Newton's inverse square law accurately describes the gravitational interactions among nebulae, it follows that

$$Vir = E_p , \tag{17}$$

where

$$E_p = - \sum_{\sigma, \nu} \frac{\Gamma M_\sigma M_\nu}{r_{\sigma\nu}} \longleftrightarrow \sigma < \nu \tag{18}$$

is the total potential energy of the cluster due to the gravitational interactions of its member nebulae. Equation (16) thus takes on the well-known form

$$- \overline{E_p} = 2\overline{K_T} = \overline{\sum_\sigma M_\sigma v_\sigma^2} = \sum_\sigma M_\sigma \overline{v_\sigma^2} , \tag{19}$$

where v_σ is the velocity of the mass M_σ. In order to arrive at a quantitative estimate of the total mass $\mathcal{M}$ of a globular cluster of nebulae, we assume as a first approximation that these nebulae are, on the average, uniformly distributed inside a sphere of radius R. In this case

$$E_p = \frac{-3\Gamma\mathcal{M}^2}{5R} . \tag{20}$$

We may also write

$$\sum M_\sigma \overline{v_\sigma^2} = \mathcal{M}\overline{\overline{v^2}} , \tag{21}$$

where the double bar indicates a double average taken over time and over mass. Therefore, from (19), (20), and (21),

$$\mathcal{M} = \frac{5R\overline{\overline{v^2}}}{3\Gamma} . \tag{22}$$

This relation (22) can also be derived if we take the time average of equation (14) which holds for an individual nebula. The time average of the left side of (14) disappears if the mass M_σ is a member of a stationary system. Thus we have

$$\overline{vir_\sigma} = - 2\overline{k_{\sigma T}} = - M_\sigma \overline{v_\sigma^2} , \tag{23}$$

where vir_σ is the virial of the nebula (σ) and $k_{\sigma T}$ is its kinetic energy. Now, in a sphere of mass $\mathcal{M}$ and radius R, the density ρ, if uniform, is equal to $\rho = 3\mathcal{M}/4\pi R^3$. The force $\vec{F}_\sigma(r)$ which acts on M_σ is therefore

$$\vec{F}_\sigma(r) = \frac{-\Gamma\mathcal{M}M_\sigma\vec{r}_\sigma}{R^3} , \tag{24}$$

and the virial

$$vir_\sigma = \vec{r}_\sigma \cdot \vec{F}_\sigma = \frac{-\Gamma \mathcal{M} M_\sigma r_\sigma^2}{R^3}, \tag{25}$$

which, combined with (23), results in

$$\frac{\Gamma \mathcal{M} \overline{r_\sigma^2}}{R^3} = \overline{v_\sigma^2}. \tag{26}$$

Since it has been assumed that all the nebulae combined produce a uniform distribution of matter throughout the sphere, the average nebula spends equal times in equal volumes, and we have

$$\overline{\overline{r^2}} = \frac{3}{4\pi R^3} \int_0^R r^2 \times 4\pi r^2 dr = \frac{3R^2}{5}, \tag{27}$$

where the double bar again designates a double average with respect to time and mass. Consequently,

$$\mathcal{M} = \frac{5R\overline{\overline{v^2}}}{3\Gamma}, \tag{28}$$

as before.

From the distribution of the brighter nebulae in the Coma cluster pictured in Figure 3 it is apparent that the assumption of uniform distribution is not fulfilled. But it is also evident that the actual potential energy E_p will have a value which, in order of magnitude, is correctly given by (20). Even if we crowded all the cluster nebulae into a sphere of radius $R/2$, the value of E_p would only be doubled. Also, we can increase E_p only very little if we assume that the M_σ's run through a wide range of values. For instance, if we assumed that practically the whole mass $\mathcal{M}$ of the cluster were concentrated in only two or three nebulae of mass $\mathcal{M}/2$ or $\mathcal{M}/3$, respectively, and that these masses had mutual distances as small as $R/10$, we should arrive at values for the potential energy:

$$E_p^1 = \frac{-2.5\Gamma \mathcal{M}^2}{R} \text{ and } E_p^1 = \frac{-\frac{10}{3}\Gamma \mathcal{M}^2}{R}. \tag{29}$$

These values are of the same order of magnitude as in (20). The following inequalities must therefore be considered as conservative estimates for the possible maximum values of the average kinetic energy and the minimum values of the total mass $\mathscr{M}$:

$$2\overline{K_T} = -\overline{E_p} < \frac{5\Gamma\mathscr{M}^2}{R} \tag{30}$$

and

$$\mathscr{M} > \frac{R\overline{\overline{v^2}}}{5\Gamma}\,. \tag{31}$$

We apply this relation to the Coma cluster of nebulae whose radius is of the order of 2×10^6 light-years. From the observational data we do not know directly the velocities v of the individual nebulae relative to the center of mass of the cluster. Only the velocity components v_s along the line of sight from the observer are known from the observed spectra of cluster nebulae. For a velocity distribution of spherical symmetry, however, we have

$$\overline{\overline{v^2}} = 3\overline{\overline{v_s^2}}\,. \tag{32}$$

Therefore

$$\mathscr{M} > \frac{3R\overline{\overline{v_s^2}}}{5\Gamma}\,. \tag{33}$$

From the observations of the Coma cluster so far available we have, approximately,[5]

$$\overline{\overline{v_s^2}} = 5 \times 10^{15}\text{cm}^2\,\text{sec}^{-2}\,. \tag{34}$$

This average has been calculated as an average of the velocity squares alone without assigning to them any mass weights, as actually should be done according to (21). It seems, however, as Sinclair Smith[8] has shown for the Virgo cluster, that the velocity dispersion for bright nebulae is about the same as that for faint nebulae. Assuming this to be true also for the Coma cluster, it follows that the

[8] *Ap. J.*, **83**, 499, 1936.

mass-weighted means of v^2 and the straight means are essentially the same. Furthermore, in calculating (34) we have used velocities which belong to the bright nebulae, since only these have been measured. If brightness can be taken as a qualitative indication of mass, the error in substituting (34) for (21) cannot be great. We must, nevertheless, remember that, strictly speaking, the determination of $\mathcal{M}$ by the virial theorem is subject to the difficulty of calculating $\overline{\overline{v^2}}$ through the application of an averaging process which involves the as yet unknown masses. The mass $\mathcal{M}$, as obtained from the virial theorem, can therefore be regarded as correct only in order of magnitude.

Combining (33) and (34), we find

$$\mathcal{M} > 9 \times 10^{46}\mathrm{gr} . \tag{35}$$

The Coma cluster contains about one thousand nebulae. The average mass of one of these nebulae is therefore

$$\overline{M} > 9 \times 10^{43}\ \mathrm{gr} = 4.5 \times 10^{10}\ M_{\odot} . \tag{36}$$

Inasmuch as we have introduced at every step of our argument inequalities which tend to depress the final value of the mass $\mathcal{M}$, the foregoing value (36) should be considered as the lowest estimate for the average mass of nebulae in the Coma cluster. This result is somewhat unexpected, in view of the fact that the luminosity of an average nebula is equal to that of about 8.5×10^7 suns. According to (36), the conversion factor γ from luminosity to mass for nebulae in the Coma cluster would be of the order

$$\gamma = 500 , \tag{37}$$

as compared with about $\gamma' = 3$ for the local Kapteyn stellar system. This discrepancy is so great that a further analysis of the problem is in order. Parts of the following discussion were published several years ago, when the conclusion expressed in (36) was reached for the first time.[5]

We inquire first what happens if the cluster considered is not st-a

tionary, in which case the virial theorem (16) must be replaced by one of the two inequalities

$$2\overline{K_T} + \overline{Vir} \gtrless 0\,, \tag{38}$$

where the bars denote averages taken over time intervals which are comparable with the time it takes one nebula to traverse the whole system. The smaller sign needs no further consideration, since instead of resulting in equation (19) it leads to the inequality

$$-\,\overline{E_p} > 2\overline{K_T}\,. \tag{39}$$

This, in turn, means that the inequality (33) is further enhanced, and we arrive at a lowest value for the mass $\mathcal{M}$ greater even than (36).

The other alternative is

$$-\,\overline{E_p} < 2\overline{K_T}\,. \tag{40}$$

We may combine this inequality with the principle of conservation of total energy E of the whole cluster

$$\overline{K_T} + \overline{E_p} = E\,, \tag{41}$$

which, added to (40), leads to

$$E > -\overline{K_T}\,. \tag{42}$$

This means that the cluster is expanding. In particular, if $E = 0$ we have

$$\overline{E_p} = -\overline{K_T} \tag{43}$$

instead of $\overline{E_p} = -2\overline{K_T}$, for a stationary system. Equation (43) means that the cluster will ultimately just fly apart. In this case the mass $\mathcal{M}$ of the cluster still has a value of half that arrived at in (36), and the discrepancy between the conversion factors γ and γ' remains materially the same in order of magnitude.

If we wish to reduce the mass $\mathcal{M}$ still further so as to make approximately $\gamma = \gamma'$, we must put $E > 0$ and $K_T \gg -E_p$. By as-

suming this, however, we run into two serious difficulties. In the first place, it is difficult to understand why under these circumstances there are any great clusters of nebulae remaining in existence at all, since the formation of great clusters by purely geometrical chance is vanishingly small, as will be shown in another paper. In the second place, the cluster nebulae, after complete dispersion of a cluster would still possess velocities practically identical with their original velocities. The field nebulae in general, which under the assumed circumstances can hardly have a velocity distribution different from that of former cluster nebulae, should therefore have a dispersion in peculiar velocities comparable to that of cluster nebulae. The average range of peculiar velocities among field nebulae, however, seems to be of the order of 150 km/sec only. This observation, if correct, excludes values of the total energy E which are sufficiently greater than zero to reduce the discrepancy between γ and γ' to a satisfactory degree.[5] It will, nevertheless, be advisable to obtain more data on the velocities of both cluster nebulae and field nebulae in order to arrive at accurate values of the dispersion which characterizes the respective velocity distribution functions.

In addition it will be necessary to develop methods which allow us to determine the relative amounts of internebular material in clusters as well as in the general field.

It should also be noticed that the virial theorem as applied to clusters of nebulae provides for a test of the validity of the inverse square law of gravitational forces. This is of fundamental interest because of the enormous distances which separate the gravitating bodies whose motions are investigated. Since clusters of nebulae are the largest known aggregations of matter, the study of their mechanical behavior forms the last stepping-stone before we approach the investigation of the universe as a whole.

The result (36) taken at face value of course does not mean that the average masses of field nebulae must be as great as those of cluster nebulae. From the general principles discussed in a following section one would rather expect the heaviest nebulae to be favored in the process of clustering.

The distribution of nebulae in the Coma cluster, illustrated in Figure 3, rather suggests that stationary conditions prevail in this cluster. It is proposed, therefore, to study the Coma cluster in more

detail. On the other hand, the virial theorem can hardly be used with much confidence in cases such as the Virgo cluster and the Pisces cluster.[9] These clusters are much more open and asymmetrical than the Coma cluster and their boundaries are thus far ill defined. Accurate values of the gravitational potentials in these clusters are difficult to determine.

In passing it should be noted that the mechanical conditions in clusters of nebulae are in some important respects different from the conditions in clusters of stars. During close encounters of stars only a minute part of their translational energy is transformed into internal energy of these stars, if the extremely rare cases of actual impacts are disregarded. Nebulae act differently. In the first place, close encounters and actual impacts in a cluster of nebulae must occur during time intervals which are not very long compared with the time of passage of one nebula through the entire system. Therefore, a considerable tendency exists toward equipartition of rotational and internal energy of nebulae with their translational energy. Star clusters in some ways are analogous to gas spheres built up of monatomic gases, whereas clusters of nebulae may be likened to gas spheres built up of polyatomic gases. This difference in internal characteristics may lead ultimately to serious consequences, as will be seen from the following line of reasoning.

We again start from the virial theorem (19), in the form in which it may be written for stationary gravitational systems, namely,

$$\overline{E_p} + 2\overline{K_T} = 0 \,. \tag{44}$$

Admitting that on close encounters of nebulae kinetic energy of translation K_T may be transformed into energy of rotation K_R and internal energy E_I of nebulae, we must replace the restricted form (41) of the energy principle by the more general equation

$$\overline{K_T} + \overline{K_R} + \overline{E_I} + \overline{E_p} = E \,. \tag{45}$$

Combining (44) and (45), we have

$$E = -\overline{K_T} + \overline{K_R} + \overline{E_I} \,. \tag{46}$$

[9] F. Zwicky, *Proc. Nat. Acad.*, May, 1937.

Encounters among nebulae tend to establish equipartition among translational, rotational, and internal energies of nebulae, analogous to the equipartition of energy among different degrees of freedom which is so well known in ordinary statistical mechanics. The mechanical conditions in a cluster of nebulae should converge toward a state for which

$$\overline{K_T} = \overline{K_R} . \quad \overline{E_I} = \lambda \overline{K_T} , \tag{47}$$

where $\lambda > 0$. For instance, $\lambda = 1$ if we include in E_I only the kinetic energy of the first three fundamental modes of pulsation of the whole system. The older the system becomes, the more of its many degrees of freedom may be expected to share in the equipartition of energy. Other happenings excluded, the value of λ would, therefore, increase almost indefinitely as the average value $\overline{E_I}$ of E_I is determined for time intervals of increasing length. In any case, admitting (47),

$$E = \lambda \overline{K_T} > 0 . \tag{48}$$

We are thus led to the uncomfortable conclusion that the total energy of a stationary cluster of nebulae should be positive. This is a contradiction in itself, since it means that on the assumption of stationary conditions in a cluster we have proved that the cluster really cannot be stationary but must ultimately fly apart. It would seem, therefore, that clusters of nebulae analogous to gravitational gas spheres[3] which are built up of polyatomic gases could never represent stationary configurations. In reality, however, condition (47) cannot be reached. In contradistinction to the rotational energy of polyatomic molecules at low temperatures, the rotational energy k_R of a nebula cannot become equal to its observed translational energy k_T. Long before the equipartition (47) among the various types of energy can be established by close encounters among nebulae, these nebulae will have been partially or completely disrupted. We are here confronted with processes which are analogous to the dissociation of polyatomic molecules when their average kinetic energy of translation—that is, the temperature of the gas—becomes too high.

The preceding considerations open up interesting new vistas on the change in time of nebular types in clusters where close encoun-

ters are much more frequent than among field nebulae. In the first place, the most compact and most massive nebulae are presumably the least vulnerable to disruption. These nebulae, therefore, are destined to survive the longest. This effect of selective elimination of nebular types may, in part, be responsible for the difference in the representation of types among cluster nebulae as compared with field nebulae. In the second place, we should expect a considerable number of stars, as well as matter in dispersed form from disrupted nebulae, to be scattered through the internebular spaces within clusters. Sufficiently large amounts of internebular matter in clusters might seriously change our estimate (36) of the average value of nebular masses as derived from the preceding application of the virial theorem to clusters of nebulae. It is therefore the intention to undertake a series of observations which may throw some light on the problem of the density of internebular matter in clusters, as compared with the density of matter in the general field. Until such observations have been made it will be well to keep in mind that, although the determination of average nebular masses from the virial theorem may be viewed with considerable confidence, this method is not entirely free from objections which have not yet been satisfactorily dealt with.

In principle the virial theorem may also be applied to describe the mechanical conditions in an individual nebula. Actually a direct application is difficult, since it is not possible to measure separately, as in the case of a cluster of nebulae, the velocities of the individual units of mass which constitute a nebula. The average square velocity (21) might be derived from the shape of the spectral lines in the light from nebulae. Unfortunately, the practical determination of such shapes is at present exceedingly difficult, if not impossible. In addition the spectral lines in the light of nebulae are doubtless of complex origin, and the interpretation even of well-known shapes of lines is by no means an easy task.

IV. NEBULAE AS GRAVITATIONAL LENSES

As I have shown previously,[6] the probability of the overlapping of images of nebulae is considerable. The gravitational fields of a number of "foreground" nebulae may therefore be expected to deflect the

light coming to us from certain background nebulae. The observation of such gravitational lens effects promises to furnish us with the simplest and most accurate determination of nebular masses. No thorough search for these effects has as yet been undertaken. It would seem, perhaps, that if the masses of field nebulae were, on the average, as great as the masses of cluster nebulae obtained in section iii, gravitational lens effects among nebulae should have been long since discovered. Until many plates of rich nebular fields taken under excellent conditions of seeing have been carefully examined it would be dangerous, however, to draw any definite conclusions.

The mathematical analysis of the formation of images of distant nebulae through the action of the gravitational fields of nearer nebulae will be given in detail in an article to be published in the *Helvetica physica acta*.

V. STATISTICAL DISTRIBUTION IN SPACE OF DIFFERENT TYPES OF NEBULAE

It will be shown elsewhere that the number of clusters of nebulae actually observed is far greater than the number that might be expected for a random distribution of non-interacting objects. This tendency of nebulae toward clustering is no doubt due to the action of gravitational forces.

By a bold extrapolation of well-known results of ordinary statistical mechanics we adopt the following working hypothesis as a tentative basis for the interpretation of future observations on the clustering of nebulae.

BASIC PRINCIPLES

1. The system of extragalactic nebulae throughout the known parts of the universe forms a statistically stationary system.

2. Every constellation of nebulae is to be endowed with a probability weight $f(\epsilon)$ which is a function of the total energy ϵ of this constellation. Quantitatively the probability P of the occurrence of a certain configuration of nebulae is assumed to be of the type

$$P = A\left(\frac{V}{V_0}\right) f\left(\frac{\epsilon}{\epsilon_K}\right) . \tag{49}$$

Here V is the volume occupied by the configuration or cluster considered, V_0 is the volume to be allotted, on the average, to any individual nebula in the known parts of the universe, and ϵ is the total energy of the cluster in question, while $\overline{\epsilon_K}$ will probably be found to be proportional to the average kinetic energy of individual nebulae. The function $A(V/V_0)$ can be determined a priori. On the other hand, $f(\epsilon/\overline{\epsilon_K})$ presumably will be found to be a monotonously decreasing function in $\epsilon/\overline{\epsilon_K}$, analogous in type to a Boltzmann factor

$$F = \text{const} \times e^{-\epsilon/\overline{\epsilon}_K} . \tag{50}$$

Assuming the basic principles stated in the preceding to be correct, we may draw the following hypothetical conclusions:

a) The clustering of nebulae is favored by high values of f and is partially checked by low values of the a priori probability A.

b) If, as would appear to be certain, nebulae are not all of the same mass, nebulae of high mass are favored in the process of clustering, since they contribute most to produce high values of the weight function f.

c) As a consequence of *b*, we should expect that the frequency with which different types of nebulae occur will not be the same among field nebulae and among cluster nebulae. In other words, clustering is a process which tends to segregate certain types of nebulae from the remaining types. This may contribute toward the correct interpretation of the well-known fact that cluster nebulae are preponderantly of the globular and elliptical types, whereas field nebulae are mostly spirals. From the arguments put forth in the preceding section as well as in section iii it follows that it is not necessary as yet to call on evolutionary processes to explain why the representation of nebular types in clusters differs from that in the general field. Here, as in the interpretation of other astronomical phenomena, the idea of evolution may have been called upon prematurely. It cannot be overemphasized in this connection that systematic and irreversible evolutionary changes in the domain of astronomy have thus far in no case been definitely established.

d) If cluster nebulae, on the average, are really more massive than

field nebulae, the conclusion suggests itself that globular nebulae may, somewhat unexpectedly, be among the most massive systems. It will be of great interest to check this inference by a search for gravitational lens effects among globular nebulae.

The preceding considerations point toward the possibility of an entirely new approach in the study of masses of nebulae. We may argue somewhat as follows:

The function $A(V/V_0)$, as said before, can be obtained from the theory of probabilities applied to random distributions in space of non-interacting objects. The function A, therefore, is known a priori. The function f may be determined from counts of types of clusters of nebulae (single, double, triple, quadruple nebulae, etc.) in given volumes of space. Such counts will give directly the values of P characteristic for different clusters. The numerical values of the function f follow from $f = P/A$. In order to determine the masses of individual nebulae, we must express the argument $\epsilon/\overline{\epsilon_K}$ of the function f in terms of these masses and then seek to correlate each definite argument with one numerical value of f. To solve this problem of the functional form of f we may proceed as follows:

We first segregate the nebulae into classes of types $T_1, T_2, T_3, \ldots . T_n$. For these types the usual ones, $E_0, E_1, \ldots . E_7, S_a, S_b, S_c$, etc., may, for instance, be chosen. As a first approximation we assume tentatively that the mass $M_\sigma(L)$ of a nebula of a given type T_σ is a function of its luminosity L alone. The argument $\epsilon/\overline{\epsilon_K}$ of the function f may then be formulated mathematically in terms of M_σ, $r_{\sigma\nu}$ and v_σ, where the M_σ are the unknown masses of the various types (T_σ) of nebulae in the cluster and where the velocities v_σ of these nebulae, as well as their mutual distances $r_{\sigma\nu}$, are known from observation. Since the numerical values of f are already known, the functional dependence of these values on the arguments $\epsilon/\overline{\epsilon_K}$ can then be determined by a purely mathematical procedure. Once the form of the function $f(\epsilon/\overline{\epsilon_K})$ is known, the unknown masses follow from our knowledge of $\epsilon/\overline{\epsilon_K}$ expressed in terms of M_σ, v_σ, $r_{\sigma\nu}$. It should be noted, however, that the method just described gives only relative masses M_σ/M_0, measured, for instance, with the mass M_0 of the type T_0 taken as the arbitrary unit. Only if the absolute value of $\overline{\epsilon_K}$ is known or if we have independent knowledge of M_0 can we

derive the absolute values M_σ from the statistics of nebular distribution.

Needless to say, this program, if it can be carried out, provides the most powerful method of determining the masses of all types of nebulae. In addition, it also enables us to determine the statistical weights f. The practical application of this method necessitates a great amount of observational work. In view of this fact, it will perhaps be advantageous to apply the preceding program first in a restricted form by a consideration of the distribution of various types of nebulae in one individual great cluster. The procedure to be applied in this case is analogous to that used successfully by H. von Zeipel[7] in his determination of the masses of different types of stars in certain clusters of stars.

Since it is intended to carry out the investigation just mentioned on the Coma cluster, a few preliminary remarks concerning the distribution of nebulae in this cluster are here given.

VI. THE COMA CLUSTER OF NEBULAE

According to Hubble and Humason,[10] the Coma cluster of nebulae "consists of about 800 nebulae scattered over an area roughly $1^\circ\!.7$ in diameter. . . . . Photographic magnitudes range from about 14.1 to 19.5, with 17.0 as the most frequent value." The distance of the cluster is about 13.8 million parsecs.

In order to get some preliminary data on the distribution of nebulae in the Coma cluster, photographs of this cluster were taken on Mount Palomar with the new 18-inch Schmidt-type telescope of the California Institute of Technology. The faintest nebulae which on limiting exposures (30–60 min) with this telescope can still be clearly distinguished from stars have an apparent magnitude close to 16.5. In Figure 3 dots represent nebulae which can be distinguished on 30-minute exposures on panchromatic films. To avoid crowding of points near the center of the cluster, not all the nebulae in this region are marked which can be seen on the original photographs. The counts given in Table 1 at different distances r from the

[10] E. Hubble and M. L. Humason, *Ap. J.*, **74**, 131, 1931; see also the descriptions of the Coma cluster by M. Wolf, *Heidelberg Pub.*, **1**, 125, 1902, and H. Shapley, *Harvard Bull.*, No. 896, 1934.

center of the Coma cluster include, however, all the nebulae which I have been able to identify on half-hour exposures.

The nebula NGC 4874 (α 12^h56^m, δ $28°20'$, 1930), which lies at (0°, 0°) in Figure 3, was taken to be the approximate center of the cluster, no effort being made to determine a mathematically accurate central point. Concentric circles were then drawn around the adopted center, with radii $r = nr_0$, where n is a whole number running from $n = 1$ to $n = 32$, and $r_0 \cong 5$ minutes of arc. The unit of area to

TABLE 1

COUNTS OF NEBULAE IN THE COMA CLUSTER

r/r_0	n_r	$\log_{10} n_r$	r/r_0	n_r	$\log_{10} n_r$
1/5	50	1.699	12	1.61	0.207
1/3	63	1.799	13	1.20	.079
1/2	52	1.716	14	1.44	.158
1	31	1.491	15	0.66	−.181
			16	0.48	−.319
2	14	1.146	17	0.60	−.222
3	10.8	1.033	18	0.48	−.319
4	6.33	0.801	19	0.43	−.367
5	4.22	0.625	20	0.64	−.194
6	4.10	0.613	22	0.26	−.585
7	1.85	0.267	24	0.36	−.444
8	2.73	0.436	26	0.27	−.569
9	1.76	0.245	28	0.16	−.796
10	2.16	0.334	30	0.25	−.602
11	1.76	0.245	32	0.15	−0.824

which all counts are reduced is $s = \pi r_0^2$, or about 1/46.4 sq. deg. The numbers of nebulae per unit area, n_r, are averages for the ringlike areas which lie between $r = nr_0$ and $r = (n + 1)r_0$. The first four figures in Table 1, however, are averages for the full circles the radii of which are $r = r_0/5$, $r_0/3$, $r_0/2$, and r_0, respectively. The corresponding numbers N_r of nebulae per square degree are $N_r = 46.4\, n_r$.

In Figure 4 values of $\log_{10} n_r$ are plotted against values of r. The full curve is drawn only approximately and does not correspond to any definite mathematical function. From the general character of this curve it is seen immediately that the Coma cluster extends to much greater distances than was originally assumed by Hubble and Humason.[10] At the edge of a circle the diameter of which is 4°5 instead of only 1°7, the average number of nebulae per unit area is

still higher than the corresponding number in the surrounding general field. Since our counts include only the brighter nebulae, it is to be expected that counts made with more powerful telescopes will enable us to follow the extensions of the Coma cluster still farther into the general field.

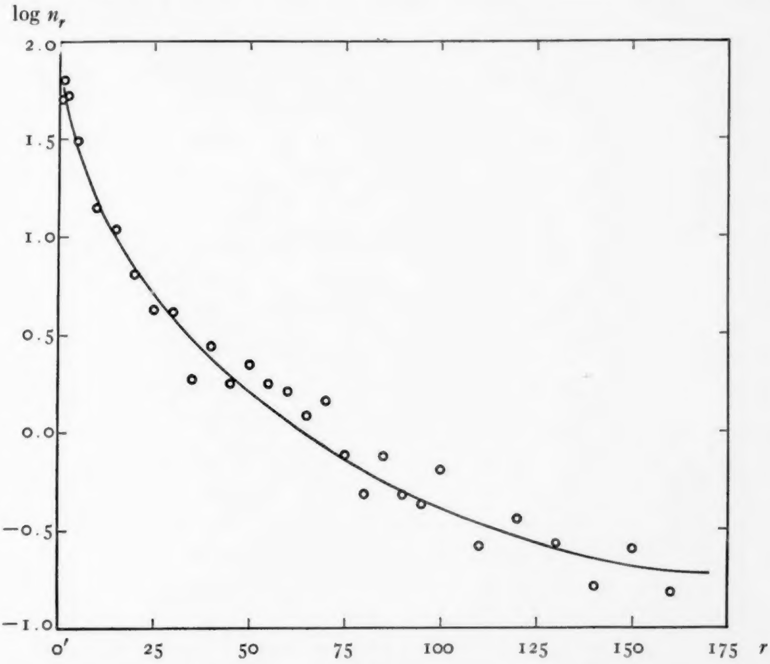

FIG. 4.—Counts of nebulae in the Coma cluster

The high central condensation, the very gradual decrease of the number of nebulae per unit volume at great distances from the center of a cluster, and the great extension of this cluster become here apparent for the first time. It is quite as we should expect from the considerations of section v. According to these considerations, a cluster of nebulae analogous to an isothermal gravitational gas sphere may in some cases be expected to extend indefinitely far into space, until its extension is stopped through the formation of independent clusters in the regions surrounding it.

The actual shape of the distribution curve in Figure 4 is also of great interest. We notice at once the great similarity of this curve

to the luminosity-curves of elliptical nebulae derived by Hubble.[11] According to him, the distribution of the intrinsic luminosity in globular nebulae corresponds very closely to the distribution of mass density in isothermal gas spheres as computed by R. Emden.[3] The same is approximately true for the distribution of the brighter nebulae in the Coma cluster. This result also checks the general conclusions drawn from the basic principles which, according to the discussion in section v, determine the stationary configurations of clusters of nebulae.

The total number $\mathcal{N}$ of nebulae in the Coma cluster that can be identified on photographs taken with the 18-inch Schmidt telescope is obtained as follows: The curve in Figure 4 apparently has a horizontal asymptote which corresponds to a value of n_r not higher than $n_\infty = 0.159$. Thus, the corresponding number N of nebulae in the general field should be $N = 46.4 \times n_\infty = 7.38$. The total number of nebulae counted to the distance $r = 2°40'$ from the center is 834. From this we must subtract $22.3 \times 7.38 = 165$ nebulae, since the area in question covers 22.3 sq. deg. The Coma cluster therefore comprises a number $\mathcal{N}$ of nebulae the brightnesses of which are greater than $m = 16.5$:

$$\mathcal{N}_{16.5} = 670 . \tag{51}$$

Since the most frequent apparent magnitude is about 17, we conclude that $\mathcal{N}_{16.5}$ is less than half the total number $\mathcal{N}$ of nebulae incorporated in the Coma cluster. This number must be at least equal to $\mathcal{N} = 1500$, and it may be even greater.

Finally, a word with respect to the limiting magnitude $m = 16.5$ which we have used in the preceding discussion. According to Hubble,[2] the number N_m of nebulae per square degree which are brighter than m near the galactic pole is given by

$$\log N_m = 0.6m - 9.05 . \tag{52}$$

Since the Coma cluster lies within a few degrees of the galactic pole, we may use relation (52) directly without introducing any correction for partial obscuration. Our counts of nebulae lead to an aver-

[11] E. Hubble, *Ap. J.*, **71**, 131, 1930.

age number of 7.38 nebulae in the general field surrounding the Coma cluster. Inserting $N_m = 7.38$ into the equation (52), we therefore find that $m = 16.6$ represents approximately the limiting magnitude at which it is still possible to distinguish images of average nebulae from those of stars on photographs taken with the 18-inch Schmidt telescope.

VII. COMPARISON OF THE THREE METHODS

Each of the three new methods for the determination of masses of nebulae which have been described makes use of a different fundamental principle of physics. Thus, method iii is based on the virial theorem of classical mechanics; method iv takes advantage of the bending of light in gravitational fields; and method v is developed from considerations analogous to those which result in Boltzmann's principle in ordinary statistical mechanics. Applied simultaneously, these three methods promise to supplement one another and to make possible the execution of exacting tests to the results obtained.

Method iii can be applied advantageously only to clusters. Its application calls for the observation of radial velocities of cluster nebulae. The absolute dimensions of the cluster investigated also must be known.

Method iv involves the observation of gravitational lens effects. Measurements of deflecting angles combined with data on the absolute distance of the "lens nebula" from the observer suffice to determine the mass of the lens nebula. The chances for the successful application of this method grow rapidly with the size of the available telescopes. Since method iii gives only the average masses of cluster nebulae and method v furnishes only the ratios between the masses of different types of nebulae, much depends on whether or not a single image of a nebula, modified through the gravitational field of another nebula, can be found. A single good case of this kind would, so to speak, provide us with the fixed point of Archimedes in our attempt to explore the physical characteristics of nebulae.

Method v is the most powerful of all, since it enables us in principle to find the masses of all types of nebulae, provided the absolute mass of a single type of nebula is known or that we have some independent way of finding a sufficiently accurate value of $\overline{\epsilon_K}$. Method v

also results automatically in the knowledge of the statistical weight functions f which govern the distribution of nebulae. The knowledge of these functions is of interest for two reasons:

1. The weight functions derived from direct observations may be compared with those to be expected theoretically, for different "models" of the universe. Through such a comparison it should be possible to decide whether the universe as a whole is in thermodynamic equilibrium[12, 13] or is continually changing.

2. It will be of particular interest, as proposed previously,[14] to investigate the probability P of the occurrence of clusters of nebulae in our "immediate" extragalactic neighborhood, as well as at great distances. If the universe is, for instance, expanding, we should expect P to be different at different distances from the observer. The fact that a great cluster of nebulae, such as the Coma cluster, seems to represent a statistically stationary configuration suggests that a short time scale with 10^9 years as the characteristic age of the universe is hardly adequate. Considerably longer time intervals would seem to be necessary to insure the formation of a stationary distribution of nebulae in great clusters. A detailed analysis of the problem of the time scale, however, must be postponed until the distribution of nebulae in a greater number of clusters has been investigated.

California Institute of Technology
Pasadena, California
June 1937

[12] P. S. Epstein, *Commentary on the Scientific Writing of J. W. Gibbs* (New Haven: Yale University Press, 1936), **2**, 104.

[13] F. Zwicky, *Proc. Nat. Acad.*, **14**, 592, 1928.

[14] F. Zwicky, *Phys. Rev.*, **48**, 802, 1935.

PHOTOELECTRIC MAGNITUDES AND COLORS OF EXTRAGALACTIC NEBULAE*

JOEL STEBBINS[1] AND ALBERT E. WHITFORD[2]

ABSTRACT

The magnitudes of 165 extragalactic nebulae down to magnitude 15 have been measured with the photoelectric cell; of these, 112 have also been measured for color. The magnitudes, based upon the Harvard visual system, are reduced to the international scale and give a correction of −0.1 to the photographic magnitudes of the Harvard Survey at magnitudes 11–13.

The colors of the nebulae are referred to the color scale of dwarf stars. The nebulae of Hubble's types E, Sa, and Sb are nearly uniform in color; those of type Sc are more varied, owing presumably to the presence of giant stars.

There is a residual color excess for the nebulae, $E = +0.14$ mag. on the international scale, which is possibly due to selective absorption within the nebulae themselves. There is no dependence of color upon magnitude such as would be caused by selective absorption in intergalactic space.

From the colors of nebulae, globular clusters, and B stars it is found that the ratio of selective to total space absorption is smaller in high than in low galactic latitude. The sun is assumed to be immersed in a dark layer of small selectivity near the galactic plane, while clouds of greater selectivity are present in nearly all directions along that plane but not immediately about the sun.

The photoelectric cell furnishes a convenient means for comparing the total light of a diffuse object like a nebula with the light of a single star. The scale of distances for nebulae depends upon their assumed absolute magnitudes, which for near-by nebulae are found by comparing the relative magnitudes of the nebulae and the individual component stars. The photoelectric magnitudes of a dozen of the brightest nebulae have already been published by Whitford,[3] who used the 10-inch telescope with focal diaphragms up to 30′ for some nebulae, but for the Andromeda nebula a $3\frac{1}{2}$-inch lens with a diaphragm more than 2° in diameter. The present work on fainter nebulae was begun by Stebbins in the summer of 1930. With a photocell on the 60-inch reflector it was found possible to measure the

* *Contributions from the Mount Wilson Observatory, Carnegie Institution of Washington*, No. 577.

[1] Research Associate of the Mount Wilson Observatory, Carnegie Institution of Washington.

[2] National Research Fellow, 1933–35.

[3] *Mt. W. Contr.*, No. 543; *Ap. J.*, **83**, 424, 1936.

magnitudes and colors of the central areas of nebulae down to the eleventh or twelfth magnitude. The focal diaphragm was about 3′ in diameter for bright objects, and 1′ or less for faint ones. The work was continued with the same photometer on the 100-inch reflector in 1931 and 1932. From 1933 on, the amplifier was substituted for the electrometer in the installation.

In addition to the nebulae, a few globular clusters were included in the program, and, after several clusters in low galactic latitude had been found to be strongly reddened, other clusters were added to the list; and, finally, all but two or three of the globular clusters observable from Mount Wilson were measured for color. The methods of observation have been described in our paper on the clusters.[4] The measures and reductions of the clusters and nebulae were carried on together, so that the same system of magnitudes holds for both. The advantages of the amplifier over the electrometer were even greater for the nebulae than for the clusters, as the nebulae extend to fainter magnitudes.

COLOR SCALE

With the same photocell and pair of filters there has been no change in the color scale except what was caused by variations of the mirrors of the large reflectors and by possible progressive changes in the cell over the years. For convenience the color scale was first determined from giant stars, but in the summer of 1936 about sixty dwarfs from the *Mount Wilson Catalogue*[5] were observed to establish a scale comparable with the dwarf characteristics of the nebulae.

The colors of the dwarf stars are in Table 1. The data in the first four columns are from the *Draper Catalogue*, except for the few faint stars marked C and 20C, which are from *Cincinnati Publications*, Nos. 18 and 20. The spectrum and the visual absolute magnitude M are from the Mount Wilson list. The last column gives the color index C_2, observed with our light filters and reduced to the standard season of 1932. We designate by C_1 the color index measured with the heavier filters used for the B stars.[6] Most of the stars in Table 1

[4] *Mt. W. Contr.*, No. 547; *Ap. J.*, **84**, 132, 1936.

[5] Adams, Joy, Humason, and Brayton, *Mt. W. Contr.*, No. 511; *Ap. J.*, **81**, 187, 1935.

[6] Stebbins and Huffer, *Pub. Washburn Obs.*, **15**, 218, 1934.

TABLE 1

OBSERVED COLORS OF DWARF STARS

HD	R.A. 1900	Decl. 1900	Vis. m	Spec.	M	C_2
20C 16	0^h11^m8	$+40°23'$	8.7	M0	8.9	$+0^M28$
3125	0 29.4	− 5 6	7.4	G0	3.7	+ .01
3651	0 34.2	+20 43	6.08	K1	5.9	+ .11
3765	0 35.3	+39 39	7.52	K5	6.5	+ .14
4256	0 39.9	+ 1 15	8.14	K5	6.5	+ .16
4307	0 40.5	−13 25	6.11	F8	4.3	− .04
4628	0 43.1	+ 4 46	5.82	K4	6.5	+ .12
5256	0 49.2	+86 47	8.9	G4	4.6	+ .02
6734	1 2.8	+ 1 28	6.69	G5	4.1	+ .08
7983	1 14.0	− 9 27	8.9	G0	4.5	− .05
8110	1 15.4	+15 11	7.53	G6	4.0	+ .10
10126	1 33.9	+27 36	7.9	G6	4.6	+ .03
10307	1 35.7	+42 7	5.10	G0	4.4	− .03
10697	1 39.5	+19 35	6.23	G4	4.7	+ .03
10995	1 42.9	+16 31	7.32	G0	2.8	+ .01
13783	2 9.2	+64 30	8.40	G5	4.9	.00
15596	2 25.4	+17 16	6.41	G5	3.7	+ .13
16160	2 30.6	+ 6 25	5.92	K4	6.7	+ .16
16397	2 32.7	+30 24	7.21	G0	4.1	− .04
18702	2 55.2	+ 5 36	8.2	K1	5.5	+ .09
20165	3 9.4	+ 8 27	7.7	K2	5.9	+ .13
20512	3 12.9	+14 49	7.69	G4	4.2	+ .05
20630	3 14.1	+ 3 0	4.96	G5	4.7	.00
21197	3 20.1	− 5 42	8.1	K6	7.3	+ .23
21531	3 23.3	−20 9	8.2	M0	8.4	+ .27
24206	3 46.2	+22 23	7.8	G5	4.9	+ .02
128165	14 30.2	+53 20	7.37	K5	6.7	+ .16
132142	14 52.3	+54 4	7.9	K0	5.4	+ .05
20C 920	15 8.8	− 3 26	9.6	M0	8.2	+ .14
136064	15 13.5	+67 44	5.23	F9	3.1	− .07
147379	16 16.5	+67 29	8.9	M0	8.7	+ .30
149105	16 27.4	+48 11	7.03	F8	3.7	− .06
149661	16 31.1	− 2 7	5.87	K0	5.4	+ .09
151288	16 41.4	+33 41	8.6	M0	8.7	+ .28
152391	16 47.9	+ 0 11	6.78	G9	5.5	+ .05
153344	16 53.8	+62 16	7.04	G4	4.7	+ .01
154345	16 59.8	+47 12	6.74	K0	5.2	+ .02
154363	16 59.8	− 4 54	7.90	M0	7.8	+ .20
166620	18 6.3	+38 27	6.40	K2	5.9	+ .09
20C 1095	18 32.4	+45 39	9.8	M2	8.5	+0.28

TABLE 1—*Continued*

HD	R.A. 1900	Decl. 1900	Vis. *m*	Spec.	*M*	C_2
184467	19^h29^m5	$+58°23'$	6.70	K5	6.1	$+0^M10$
193202	20 13.8	+76 55	9.3	M0	8.9	+ .31
200779	21 0.4	+ 6 41	8.9	K6	7.4	+ .23
202123	21 8.8	+73 18	8.8	K4	6.8	+ .06
207491	21 44.1	+ 5 15	8.61	K6	7.1	+ .16
210277	22 4.2	− 8 2	6.63	G9	5.1	+ .03
214059	22 30.5	+ 4 52	8.4	G4	4.4	.00
215110	22 37.8	− 0 6	8.0	G4	4.0	+ .09
216259	22 46.4	+13 26	8.0	K4	6.4	+ .08
C 2986	22 47.3	+31 12	9.4	K6	6.9	+ .17
217014	22 52.6	+20 14	5.59	G0	4.3	.00
217580	22 56.7	− 4 23	7.60	K4	6.1	+ .08
220339	23 17.8	−11 19	8.1	K1	5.2	+ .10
221356	23 26.4	− 4 38	6.50	F8	3.6	− .07
221830	23 30.4	+30 27	6.72	G0	4.4	− .04
221914	23 31.0	+17 53	8.0	G5	4.9	+ .01
222860	23 39.2	+ 0 10	8.03	F8	3.3	− .05
222935	23 40.0	+29 0	8.9	K2	5.7	+ .10
C 3124	23 44.0	+ 1 52	9.1	M2	9.2	+0.25

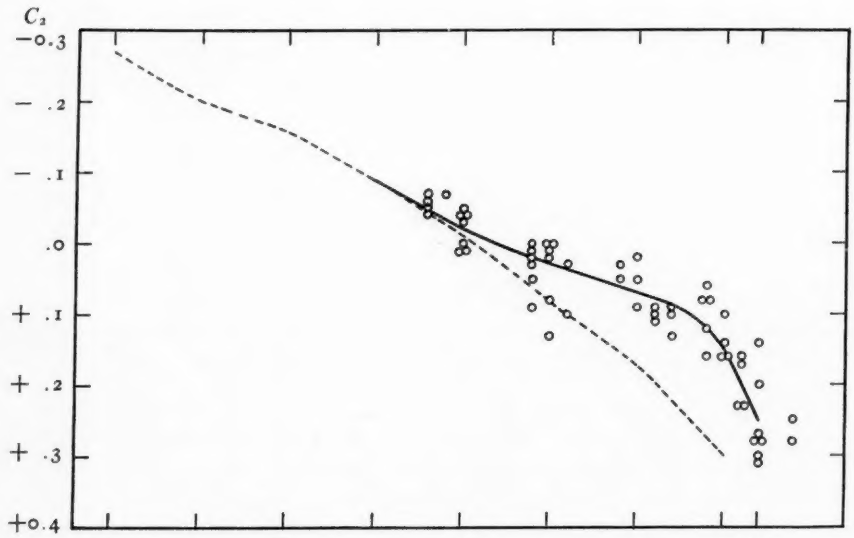

FIG. 1.—Colors of dwarf stars. Heavy line, mean for dwarfs; broken line, mean for giants.

were observed only once. Because of the dispersion of color within a spectral class it seemed better to take additional stars than to repeat the measures of each star. The colors C_2 in Table 1 are shown in Figure 1, and the smoothed means are in Table 2. There is some

TABLE 2

NORMAL COLORS OF GIANT AND DWARF STARS

Spectrum	Color Index, C_2		Spectrum	Color Index, C_2	
	Giants	Dwarfs		Giants	Dwarfs
B5	$-0^{M}.32$	....	G5	$+0^{M}.08$	$+0^{M}.03$
A0	.27	....	K0	.17	.07
A5	.20	....	K5	.30	.15
F0	.16	....	K6	....	.20
F5	.09	$-0^{M}.09$	M	+0.32	+0.24
G0	−0.01	−0.02			

evidence of an absolute-magnitude effect within the spectral classes, particularly in G4, G5, and G6. In G5 the dependence of C_2 upon M is pronounced:

M	C_2	M	C_2
3.7	$+0^{M}.13$	4.9	$+0^{M}.00$
4.1	.08	4.9	.01
4.7	+0.00	4.9	+0.02

In other spectral classes the data are insufficient to show such a relation; but a rough attempt was made to find the color for the mean absolute magnitude of each spectral subdivision, and the curve in Figure 1 was drawn with some allowance for this effect. In Table 2 the previously derived colors for giants are also included.

We are well aware of the compressed scale of our colors, which has a difference of only 0.34 mag. between A0 and K0 for dwarf stars. We found from the Polar Sequence that the relation to the international scale is given by

$$IC = 2.62\, C_2 + \text{Const.}$$

For bright stars we get a probable error of less than ± 0.01 mag. for one observation of color, corresponding to ± 0.02 mag. or ± 0.03 mag. on the international system. The errors for faint nebulae are, of

course, larger. The differences in color between stars with the same spectral lines are already conspicuous on our scale; a combination of cell and filters using more widely separated spectral regions would simply exaggerate these differences in the stars themselves.

STANDARD MAGNITUDES

The photoelectric magnitudes of the nebulae were referred to the Harvard visual magnitudes of stars, mostly between the sixth and the seventh magnitude. The observations of a night usually began

TABLE 3

MAGNITUDES OF STANDARD STARS

Group (1)	HD (2)	Spec. (3)	*HV* (4)	C_1 (5)	*Pe* (6)	Pe_H (7)	$Pe - Pe_H$ (8)	Resid. (9)
I	149631	A5	7.30	-0^M23	7.30	7.37	-0^M07	-0^M06
	149632	A0	6.27	− .24	6.43	6.32	+ .11	+ .12
	151900	F2	6.32	− .12	6.63	6.57	+ .06	+ .07
	156717	A0	6.04	− .23	6.01	6.11	− .10	− .09
	160018	K0	5.92	+0.26	6.75	6.81	−0.06	−0.05
Mean							−0.01	±0.08

Group	$Pe - Pe_H$	Resid.
I	-0^M01	-0^M04
II	.00	− .03
III	+ .01	− .02
IV	+0.11	+0.08
Mean	+0.03	±0.04

with several standard stars measured in the twilight, and other standards were taken from time to time between the measures of the nebulae. Usually the conditions were so good that all the standards observed over several hours could be used as a group; but when there were interruptions, the measures and reductions of the night were broken into several sections. The reductions of the standard stars from visual to photoelectric magnitudes were determined by the measured colors. Since the 100-inch cannot be pointed near the pole, a comparison of some of the standard stars with the North Polar Sequence was made with the 60-inch reflector. As it is not con-

venient to rotate the Newtonian cage of the 60-inch during the night, the southern stars were compared with the Polar Sequence by way of intermediate stars culminating near the zenith, which could be reached with the cage in either the north or the south position. In the tests were two southern groups, I and II, of five stars each, and two intermediate groups, III and IV, of five and six stars, respectively.

In Table 3, HV is the Harvard visual magnitude, C_2 the photoelectric color, Pe the observed photoelectric magnitude referred to our arbitrary zero point of the Polar Sequence, and Pe_H the photoelectric magnitude computed from the visual magnitude by the formula

$$Pe_H = HV + 1.68(C_2 + 0.27) . \tag{1}$$

The mean of $Pe - Pe_H$ for each group is the difference between the zero points from the Polar Sequence and the Harvard visual magnitudes. Taking the average for the four groups, we have

$$Pe = Pe_H + 0.03 . \tag{2}$$

For the polar stars we found

$$Pg_p = Pe - 0.05 + 0.53(C_2 + 0.21) , \tag{3}$$

where Pg_p is the photographic magnitude computed from the photoelectric. The constant -0.05 brings Pg_p into agreement with $I\,Pg$ for the mean of five stars at magnitude 6.0. Substituting (2) in (3), we have

$$Pg_p = Pe_H - 0.02 + 0.53(C_2 + 0.21) . \tag{4}$$

The constant term -0.02 has been determined here from only 21 stars, and it must vary with any systematic errors of the Harvard visual magnitudes over different parts of the sky. The term can be discarded, and we adopt

$$Pg_p = Pe + 0.53(C_2 + 0.21) , \tag{5}$$

where Pe now has the same zero point as Pe_H for any group of stars.

This close agreement in zero point between the Harvard visual

scale and the international photographic scale is accidental. In equation (1) we adopted $C_2 = -0.27$ for an A0 star in a nonobscured region; but because of the selective absorption at the pole, $C_2 = -0.21$ when the international color index $IC = 0.00$. To keep the magnitudes on the international system throughout, we should use 0.21 in place of 0.27 in (1), which would change the constant term in (4) by 0.10. Instead, we let the photoelectric magnitudes remain as they are, and then the photographic magnitudes derived from (5) are nearly enough on the international system. On our scale the zero point of Pg_p is made to agree with IPg at magnitude 6.0. The precision of the magnitudes of the comparison stars is indicated by the residuals in column (9) of Table 3. Usually the average residual for a star is less than ± 0.10 mag.; the means from groups of several stars are good enough for standards for the nebulae.

It might appear better to refer the magnitudes of nebulae to standards in Selected Areas than to the Harvard visual magnitudes of bright stars, but the Harvard stars are easily picked up and are available all over the sky. The manipulation of so large a telescope as the 100-inch is a slow process, and we could not afford to spend valuable time in identifying and checking faint standard stars. From laboratory and other tests in observing the North Polar Sequence with the 60-inch, we found the scale of magnitudes with the photocell to be correct within 0.01 mag. or 0.02 mag. over the range from the second to the twelfth magnitude. Hence the same scale would hold to the thirteenth magnitude with the 100-inch, and the extension to one or two magnitudes still fainter is a small extrapolation.

THE OBSERVATIONS

The present results for extragalactic nebulae are brought together in Table 4. Column (1) gives the *New General Catalogue* number; column (2), the year of observation (measures after the aluminizing of the large mirrors in 1935 are marked "35*a*"). The photoelectric magnitudes in columns (3) to (6) are for the respective diaphragms. Usually the 64″ diaphragm was used first for both the magnitude and the color; then the measures through other diaphragms were made differentially from 64″. In column (7) all measures on the same night were counted as one observation. In column (8) the com-

TABLE 4

MAGNITUDES AND COLORS OF NEBULAE

NGC	Yr.	*Pe* Magnitude				No.	Pg_p	HPg	Pg_p-HPg	Diam.	Type	Spec.	C_2	A.D.	No.	l	b
		42″	64″	128″	163″												
(1)	(2)	(3)	(4)	(5)	(6)	(7)	(8)	(9)	(10)	(11)	(12)	(13)	(14)	(15)	(16)	(17)	(18)
95	35*a*			13.26		2	13.3	13.1	$+0^{M}2$	1′6 1′2	Sc					81°	−52°
128	35*a*				12.66	1	12.8	12.9	− .1	2.5 0.4	SBa					81	60
221	32	10.03	9.71	9.36	9.33	1	9.5	9.5	.0	2.6 2.1	E2	G3	$+0^{M}07$	$\pm0^{M}02$	2	89	22
224	33	9.33				2	9.5	5±		160 40	Sb	G5	+ .12	.02	2	89	20
237	35*a*			13.68		1	13.8	13.2	+ .6	1.8 1.3	Sc					90	63
428	35*a*				12.33	1	12.4	11.9		4.0 2.2	Sc					105	61
470	35*a*			12.64		1	12.7	12.4	+ .3	1.6 1.0	Sbc					107	58
474	35*a*		13.06			1	13.2	12.6	+ .6	0.4 0.4	Eo					107	58
488	35*a*				11.63	1	11.8	11.8		3.0 3.0	Sa					106	56
520	35*a*			12.63		1	12.7	12.4		3.0 0.7	I:					109	58
521	35*a*			12.69		1	12.8	13.0		3.0 2.5	SBb					111	60
524	32	12.60	12.19	11.37	11.23	1	11.4	12.0	− .6	2.6 2.6	So		+ .14	.08	2	106	52
533	35*a*			12.98		1	13.1	13.0		1.0 0.7	E3					111	60
584	32	12.08	11.80	11.51	11.39	2	11.5	11.6	− .1	2.0 1.2	E3		+ .07	±0.07	2	120	66
598	34		11.39			1	11.5	7.8		60 40	Sc	F5	− .07		1	103	31
628	35*a*				11.75	1	11.8	11.2		8.0 8.0	Sc	G2				108	45
718	35*a*			12.55*	12.52	1, 1	12.7	12.7	.0	0.5 0.4	Sab					118	55
720	32		11.60			1	11.8	11.7	+ .1	1.3 0.7	E6	G4	+0.11		1	142	69
741	35*a*		12.82*			1	13.0	13.0	.0	0.8 0.8	Eo					120	53
821	35*a*		12.35*			1	12.5	12.7	−0.2	1.0 0.4	E6					120	−47

* Taken with 60-inch; multiply diameter of diaphragm by 1.7.

TABLE 4—*Continued*

NGC	Yr.	*Pe* Magnitude				No.	Pg_p	HPg	Pg_p-HPg	Diam.	Type	Spec.	C_2	A.D.	No.	l	b
		42″ (3)	64″ (4)	128″ (5)	163″ (6)												
(1)	(2)					(7)	(8)	(9)	(10)	(11)	(12)	(13)	(14)	(15)	(16)	(17)	(18)
877	35a	......	......	12.45*	......	1	12.5	12.4	$+0^M1$	1′.9 1′.3	Sc	....	....	....	....	121°	−43°
936	32	12.24	11.92	11.39	11.31	2	11.5	11.5	....	3.0 2.0	SBa	....	$+0^M12$	$\pm0^M01$	2	136	−54
1023	32	11.60	11.22	10.78	10.68	2	10.9	11.2	....	6.0 1.3	SBa	....	+ .13	.03	2	113	−17
1068	32	10.69	10.39	9.95	9.91	2	10.0	10.0	.0	2.5 1.7	Sbc	....	− .03	.03	2	140	−51
1084	32	12.27	11.63	11.18	11.14	2	11.2	11.2	.0	2.2 0.8	Sc	F5	− .13	.01	2	151	−55
1400	32	12.41	12.05	......	......	1	12.2	12.5	− .3	0.6 0.5	E1	G5	− .02	....	1	177	−49
IC 342	35a	12.73*	......	......	......	1	12.9	......	....	25 ...	Sc	F8e	+ .08	.07	2	106	+11
1407	32	12.01	11.59	10.97	10.84	1	11.0	11.5	− .5	0.7 0.7	Eo	G8	+ .15	....	1	177	−48
IC 356	35a	13.28*	......	......	......	2	13.6	......	....	1.0 1.0	Sa	....	+ .40	.05	2	106	+14
1600	32	12.95	12.41	12.10	11.95	1	12.2	12.7	− .5	1.5 1.0	E3	....	+ .32	....	1	168	−32
1637	32	13.21	12.61	11.86	11.49	1	11.6	11.6	....	3.0 2.5	Sc	....	+ .01	....	1	167	−30
1700	32	12.62	12.32	12.05	12.09	1	12.3	12.4	− .1	0.8 0.5	E4	....	+ .18	....	1	172	−27
2681	32	11.98	11.64	11.28	11.21	1	11.3	11.3	....	3.0 ...	Sa	....	− .01	....	1	135	+41
2841	32	11.74	11.26	10.62	10.42	2	10.6	10.5	....	6.0 1.6	Sb	....	+ .08	.01	2	135	+45
2859	32	12.70	12.41	11.95	11.95	1	12.1	12.2	− .1	1.9 1.2	SBa	G3	+ .08	....	1	159	+47
2903	34, 35	......	10.72*	10.6	......	1, 1	10.7	10.3	....	11.0 5.0	Sc	Fo	− .11	±0.02	2	177	+45
3031	32	......	9.96*	......	......	1	10.1	8.9	....	16 10	Sb	....	+ .09	....	1	108	+42
3166	34	......	11.9	......	......	1	12.0	11.6	....	4.0 4.0	Sc*	....	+ .05	....	1	207	+46
3169	34	......	12.2	......	......	1	12.3	11.9	....	4.0 1.7	Sa	....	+ .06	....	1	207	+47
3294	34	......	......	12.3	......	1	12.3	11.6	....	3.0 1.5	Sc	....	− .19	....	1	150	+61
3377	32	12.42	12.06	11.67	11.58	1	11.7	11.6	+ .1	1.5 0.8	E6	G2e	+ .09	....	1	200	+60
3384	32	11.52	11.27	10.81	10.68	1	10.9	11.3	....	3.0 1.2	SBa	Go	+ .14	....	1	203	+59
3414	32	12.76	12.43	11.97	11.95	1	12.2	12.2	.0	1.8 0.7	SBb	G7	+ .21	....	1	170	+64
3486	34	......	......	11.8	......	1	11.8	11.4	....	3.8 2.5	Sc	G3	− .16	....	1	168	+67
3504	32	12.44	12.00	11.56	11.40	1	11.5	11.7	−0.2	2.0 1.0	SBb	....	+0.01	....	1	170	+67

* listed Sa in ApJ 115 p 286

TABLE 4—*Continued*

NGC	Yr.	*Pe* Magnitude				No.	Pg_p	HPg	Pg_p-HPg	Diam.	Type	Spec.	C_2	A.D.	No.	l	b
		42″	64″	128″	163″												
(1)	(2)	(3)	(4)	(5)	(6)	(7)	(8)	(9)	(10)	(11)	(12)	(13)	(14)	(15)	(16)	(17)	(18)
3512	32	13.78	12.96	...	...	1	13.0	12.8	$+0^{\mathrm{M}}.2$	1′.0 1′.0	Sc	...	...	...	...	170°	+67°
3521	34, 35	...	10.66*	10.5	...	1, 1	10.6	10.3	...	9 4.5	Sc	...	$-0^{\mathrm{M}}.01$	$\pm 0^{\mathrm{M}}.01$	2	223	53
3626	32	12.48	12.14	11.70	11.77	1	11.9	11.8	+ .1	1.9 1.3	Sa	...	+ .01	...	1	200	68
3810	34	...	...	11.8	...	1	11.9	11.8	+ .1	4.2 2.7	Sc	...	− .05	...	1	221	68
4192	35a	...	...	...	11.02*	1	11.1	11.4	...	8.0 2.0	Sb	...	+ .04	...	1	240	75
4216	35a	...	...	...	11.08*	1	11.2	11.3	...	7.0 1.0	Sb	...	...	...	...	242	75
4254	34, 35	...	11.23*	11.15	10.42*	1, 2, 2	10.5	10.5	.0	4.5 4.5	Sc	...	− .09	.01	4	245	75
4259	32	14.65	...	...	...	2	14.8	...	...	0.5 0.2	So	...	...	...	...	255	67
4261	32	...	12.01	...	...	2	12.2	...	...	1.6 1.3	E2	G5	+ .10	...	1	253	67
4261	35a	...	11.80*	11.46*	...	1	11.6	11.7	− .1	1.6 1.3	E2	G5	...	...	...	253	67
4264	32	...	13.70	...		2	13.8	...	...	0.5 0.5	SBa	...	...	...	...	254	69
4268	32	...	13.68	...		2	13.8	...	...	1.0 0.4	So	...	...	...	...	255	67
4270	32	...	13.00	...		2	13.1	12.8	...	1.6 0.6	E7	...	− .01	...	1	254	67
4273	32	...	12.66	...		2	12.6	12.2	...	2.0 1.4	Sbc	F2e	− .29	.08	2	255	67
4281	32	...	12.46	...		2	12.6	12.2	...	2.4 1.2	Sa	G3	+ .08	...	1	255	67
4293	35a	...	...	...	11.37*	1	11.5	11.7	...	5.0 2.0	Sa	...	...	...	...	238	79
4303	34, 35	...	11.04*	10.9	10.38*	1, 1, 1	10.4	10.4	...	6.0 6.0	Sc	Go	− .13	.00	2	255	66
4321	34, 35	11.96*	...	11.49	10.39*	1, 2, 1	10.5	10.8	− .3	5.0 5.0	Sc	F2	− .06	.04	4	245	76
4374	32	11.56	11.14	10.89	10.52	2	10.7	10.9	...	2.9 2.6	E1	G4	+ .12	.04	2	253	74
4382	35a	...	...	...	10.16*	1	10.3	10.5	− .2	4.0 2.5	E4	...	...	...	...	240	80
4387	32	13.42	13.00	...	...	1	13.2	...	...	0.8 0.6	E3	...	...	...	...	252	75
4406	32, 35	11.92	11.42	10.86	10.71	3	10.9	10.9	...	3.8 2.9	E2	...	+ .08	0.01	3	251	75
4414	34	...	...	11.2	...	1	11.3	11.1	...	3.0 1.5	Sc	...	−0.05	...	1	135	85
4417	35a	...	...	12.11	12.04	1	12.2	12.3	− .1	2.7 1.1	SBa	...	...	...	...	255	71
4424	35a	...	...	12.44	12.35	1	12.5	12.6	−0.1	2.7 1.6	SBa	...	...	...	...	255	+71

TABLE 4—*Continued*

NGC (1)	Yr. (2)	*Pe* Magnitude 42″ (3)	64″ (4)	128″ (5)	163″ (6)	No. (7)	Pg_p (8)	HPg (9)	Pg_p-HPg (10)	Diam. (11)	Type (12)	Spec. (13)	C_2 (14)	A.D. (15)	No. (16)	l (17)	b (18)
4425	32		13.14			1	13.3	13.1		2′.2 0′.5	Sa					255°	+74°
4429	35a		11.64*	11.17*		1	11.3	11.7	−0$^{\mathrm{M}}$4	3.0 1.0	Sa					255	72
4435	32	12.29	11.96	11.61	11.55	2	11.7	11.8	− .1	1.6 1.0	E6	G3	+0$^{\mathrm{M}}$08	±0$^{\mathrm{M}}$04	2	252	75
4438	32	12.59	12.09	11.76	11.74	2	11.9	11.9		8.0 3.0	Sb	G5	+ .04	.03	2	252	75
4442	35a			11.28*	11.34*	1	11.5	11.4	+ .1	3.2 1.0	SBa					256	71
4445	35a			13.7	13.5	1	13.6			2.0 0.5	Sb					257	72
4450	35a				10.99*	1	11.1	11.4	− .3	4.4 3.5	Sb					249	80
4451	35a		13.50	13.26		1	13.4			1.0 0.5	Sb					257	71
4458	35a		13.10			2	13.2			0.7 0.7	Eo	G5				254	75
4459	35		12.22			1	12.4			2.0 1.0	So					255	76
4459	35a		11.70*	11.38*		1, 2	11.5	11.9	− .4	2.0 1.0	So					255	76
4461	35a			12.17	12.07	1	12.2	12.4		3.0 1.0	E7 to Sa					255	75
4472	35	11.22		10.40	9.92	1, 1	10.1	10.1	.0	4.5 4.0	E1		+ .10		1	258	70
4473	35, 35a			11.37	11.29	2, 1	11.4	11.7		3.0 1.5	E4	G8	+ .03		1	255	75
4477	35, 35a			11.66	11.52	2, 2	11.7	11.8	− .1	2.5 1.8	SBa	G5	+ .08		1	256	75
4478	35a		12.37	12.26		1, 1	12.4	12.5	− .1	1.2 1.0	E2		+ .09		1	256	74
4479	35		13.81	13.48		1, 2	13.6			1.0 0.6	SBa	G3	+ .10		1	255	76
4486	35	11.59		10.64	10.06*	1, 1	10.2	10.7	−0.5	3.3 3.3	Eo		+ .15		1	255	75
4490	34			10.7		1	10.8	10.5		4.0 1.8	Sc		− .01		1	102	76
4501	34, 35	12.54		11.0	11.06	1, 1, 1	11.2	10.9		6.0 3.0	Sc		+ .02	±0.02	2	255	75
4501	35a				10.47*	1	10.6	10.9		6.0 3.0	Sc					255	75
4535	35	13.72		11.86	10.94*	1, 1	11.0	11.1		6.4 5.0	Sc		− .03		1	261	70
4536	34			11.9		1	11.9	11.2		7.0 1.8	Sc		− .17		1	265	65
4550	32		12.70			1	12.8	12.7		2.7 0.8	E7		+0.06		1	260	75
4551	32		13.02			1	13.2			0.8 0.6	E3	G5				261	+75

TABLE 4—*Continued*

NGC (1)	Yr. (2)	*Pe* Magnitude 42″ (3)	64″ (4)	128″ (5)	163″ (6)	No. (7)	Pg_p (8)	HPg (9)	Pg_p-HPg (10)	Diam. (11)	Type (12)	Spec. (13)	C_2 (14)	A.D. (15)	No. (16)	l (17)	b (18)
4552	32		11.52			1	11.7	11.3		2′.2 2′.2	E0		+0^{M}15		1	261°	+75°
4559	34			12.0		1	12.0	10.7		8.0 2.0	Sc		− .18		1	160	87
4569	34			11.2		2	11.3	11.2		6.0 3.0	Sbc	F0	− .05	±0^{M}01	2	260	75
4579	34, 35	12.20		11.04	10.64*	1, 2, 1	10.8	11.0	−0^{M}2	3.6 3.2	Sb		+ .05	.01	2	263	74
4621	32		11.65			1	11.8	11.4		2.7 1.6	E5	G6	+ .13		1	266	73
4631	34			11.6		2	11.6	9.6		12.0 1.2	Sc		− .21	.02	2	98	84
4638	32		12.29			1	12.4	12.2	+ .2	1.0 0.5	E5		+ .10		1	268	74
4647	32		12.62			1	12.7	12.0		2.5 2.2	Sc		+ .03		1	268	74
4649	32		11.02			2	11.2	10.6		3.9 3.1	E2		+ .16	.00	2	269	74
4660	32		12.26			1	12.4	12.3	+ .1	1.0 0.5	E5		+ .12		1	270	74
4666	34			11.7		1	11.8	11.3		4.0 0.6	Sc		− .10		1	270	62
4710	35*a*			11.87*		1	12.0	12.0	.0	3.5 0.5	Sa					275	78
4874	35*a*	13.8:	13.5:			1	13.6			0.5 0.5	E0					10	87
4884	35*a*	13.5:	13.0:			1	13.1			0.7 0.5	E2					10	87
5005	34			11.2		1	11.3	11.3		5.0 1.5	Sc		+ .04		1	64	78
5033	34			11.7		1	11.8	11.6		6.0 3.0	Sc		− .05		1	58	78
5248	34			11.4		1	11.5			3.2 1.4	Sc		− .02	.02	2	306	67
5248	35*a*			10.96*		1	11.1	11.0	+ .1	3.2 1.4	Sc					306	67
5363	34		11.9			1	12.1			1.2 1.0	I		+ .14	±0.06	2	310	62
5363	35*a*		11.38*	10.94*		1	11.1	11.1	.0	1.2 1.0	I					310	62
5364	34, 35*a*			12.0	11.34*	1, 1	11.4	11.8	− .4	4.0 3.0	Sc		− .02		1	310	62
5645	35*a*			12.85		1	13.0	12.9	+ .1	1.4 1.0	Sab					327	58
5690	35*a*				12.47	1	12.6	12.9	− .3	2.6 0.5	Sbc					323	53
5701	35*a*			12.30		1	12.4	12.8	−0.4	1.5 ...	SBa					325	56
5728	35*a*		12.5			1	12.6	12.4		2.0 1.0	Sbc		−0.03		1	306	+37

TABLE 4—*Continued*

NGC	Yr.	*Pe* Magnitude 42″	64″	128″	163″	No.	Pg_p	HPg	Pg_p-HPg	Diam.	Type	Spec.	C_2	A.D.	No.	l	b
(1)	(2)	(3)	(4)	(5)	(6)	(7)	(8)	(9)	(10)	(11)	(12)	(13)	(14)	(15)	(16)	(17)	(18)
5740	35*a*	...	...	...	12.65	1	12.8	12.8	...	3′.0 2′.0	Sb	...	...	...	...	323°	+52°
5757	35*a*	13.36	...	...	...	1	13.5	12.6	...	1.2 0.9	SBb	...	$+0^M10$	...	1	306	+34
5791	35*a*	13.06	...	...	...	1	13.2	13.0	...	0.8 0.4	E6	...	+ .10	...	1	308	+33
5839	33	13.87	...	...	...	1	14.0	...	...	0.7 0.7	So	...	...	...	...	328	+48
5845	33	13.39	...	...	...	1	13.5	...	...	0.7 0.5	E3	...	+ .02	...	1	329	+48
5846	33, 35*a*	12.57	11.67*	11.50*	...	1, 1	11.6	11.6	0^M0	1.0 1.0	Eo	G5	− .03	...	1	328	+47
5898	35*a*	...	12.57	...	...	1	12.7	12.6	+ .1	0.5 0.5	Eo	...	+ .07	...	1	309	+26
5903	35*a*	...	12.67	...	...	1	12.8	12.9	− .1	0.7 0.7	E2	...	+ .14	...	1	309	+26
5936	35*a*	...	13.45	12.87	...	1	13.0	12.9	+ .1	1.0 0.8	Sc	...	...	...	...	348	+49
6106	35*a*	...	13.42	12.69	...	2, 1	12.8	12.9	− .1	1.7 0.8	Sc	...	.00	$\pm0^M08$	2	349	+36
6118	35*a*	...	13.56	...	...	1	13.7	12.3	...	4.0 1.2	Sc	...	+ .05	...	1	340	+31
6359	35*a*	13.40*	...	...	...	1	13.6	...	...	0.6 0.4	E2	G3	...	...	...	46	+34
6384	35*a*	...	12.96	...	...	2	13.1	12.7	...	3.0: 3.0:	SBb	G8	+ .07	.00	2	358	+20
6482	35*a*	...	12.38	...	...	2	12.5	12.2	+ .3	0.3 0.3	E2	...	+ .05	.02	2	15	+22
6574	35*a*	13.10	12.77	...	...	1, 3	12.9	12.7	+0.2	1.0 0.6	Sbc	Go	+ .02	.04	4	10	+14
6814	35*a*	13.49	12.95	...	...	2, 1	13.1	12.2	...	2.0 2.0	SBb	...	+ .05	.02	2	357	−17
6835	35*a*	...	13.48	...	...	2	13.6	13.0	...	1.8 0.3	Sab	...	+ .03	.07	2	356	−22
6907	35*a*	...	12.73	...	...	2	12.8	12.1	...	2.0 1.8	Sbc	...	− .08	.02	2	346	−32
6946	35*a*	...	...	11.00*	...	1	11.1	11.1	...	8.0 8.0	Sc	Pd	+ .03	...	1	64	+11
6951	35*a*	13.05*	...	...	...	1	13.2	12.4	...	3.5 3.5	SBbc	...	+ .13	...	1	67	+15
7177	35*a*	...	12.24	...	...	1	12.3	12.1	...	2.5 1.5	Sbc	G2	.00	...	1	43	−30
7217	35*a*	...	12.06	...	...	1	12.2	11.6	...	3.0 2.5	Sa*	G4	+ .11	...	1	55	−20
7448	35*a*	...	12.45	...	...	2	12.5	11.8	...	2.0 0.8	Sc	G3	− .13	.04	2	56	−40
7457	35*a*	...	12.70	...	...	2	12.8	12.3	...	2.0 0.5	Sa	G2	+0.05	±0.02	2	65	−27
7469	35*a*	...	12.91	...	...	1	13.1	13.0	...	1.5 1.2	Sab	...	...	...	...	52	−46

* listed Sb in ApJ 115, p 288

TABLE 4—*Continued*

NGC	Yr.	*Pe* Magnitude				No.	Pg_p	HPg	Pg_p-HPg	Diam.	Type	Spec.	C_2	A.D.	No.	l	b
		42″ (3)	64″ (4)	128″ (5)	163″ (6)												
(1)	(2)					(7)	(8)	(9)	(10)	(11)	(12)	(13)	(14)	(15)	(16)	(17)	(18)
7479......	35*a*	......	......	12.22	......	1	12.3	11.9	....	3′.0 2′.5	SBc	....	....	....	....	55°	−44°
7541......	35*a*	......	......	12.64	......	1	12.8	12.8	....	2.6 0.6	Sbc	....	....	....	....	52	51
7619......	32	13.10	12.68	12.22	12.12	1	12.3	12.8	$-0^{M}5$	0.7 0.5	E3	G3	$+0^{M}13$	....	1	56	49
7626......	32	13.04	12.69	12.26	12.09	1	12.2	12.8	− .6	0.7 0.7	E1	G3	+ .07	....	1	56	49
7679......	35*a*	......	13.38	......	......	1	13.5	13.1	+ .4	0.7 ...	E1	....	....	....	....	56	54
7716......	35*a*	......	......	13.00	......	1	13.1	13.0	....	2.3 1.7	Sbc	....	....	....	....	57	58
7723......	35*a*	......	12.48	......	......	2	12.6	12.1	....	3.0 2.0	SBb	....	− .03	$\pm\ 0^{M}02$	2	41	68
7727......	35*a*	......	12.10	......	......	1	12.3	12.0	....	2.7 2.7	Sa	G5	+ .11	....	1	41	68
7743......	35*a*	......	......	12.48	......	1	12.6	12.8	− .2	1.8 1.3	SBab	....	....	....	....	66	50
7782......	35*a*	......	......	13.12	......	1	13.2	13.1	+0.1	1.8 1.2	Sb	....	....	....	....	68	54
7785......	35*a*	......	13.10	......	......	2	13.3	12.9	....	1.2 0.5	E5	....	....	....	....	66	55
7793......	35*a*	......	......	11.25	......	2	11.3	9.7	....	8.0 6.0	Sc	....	− .08	.02	2	330	78
7814......	33	......	12.51	11.82	......	1, 1	11.9	12.4	....	3.0 0.8	Sa	G3	+0.02	±0.05	2	76	−45

puted photographic magnitude Pg_p was derived from the Pe magnitude for the largest diaphragm by equation (5). In cases where the color C_2 had not been observed, the mean C_2 for the type of nebula was used.

In column (9) is the Harvard photographic magnitude by Shapley and Ames.[7] Where our diaphragm was clearly large enough to include all of the nebula indicated by the recorded diameter, the difference $Pg_p - HPg$ is entered in column (10). The diameters in column (11) were taken from the Harvard Survey, with some additions or changes furnished by Hubble from Mount Wilson plates. The types of the nebulae in column (12), as well as the spectra in (13), were also furnished by Hubble from plates usually taken by Humason.

In column (14) the measured color index C_2 refers to the diaphragm 64″, or to the smallest of the other diaphragms if 64″ was not used. The seasonal corrections which have already been applied to C_2 in Table 4 are: 1932, 0.00 mag.; 1933, −0.01 mag.; 1934, −0.05 mag.; 1935, −0.05 mag.; 1935*a*, +0.05 mag. The jump between 1935 and 1935*a* was due to the aluminizing of the mirrors of the telescopes.

The average deviation and the number of nights are in columns (15) and (16), while in (17) and (18) are the approximate galactic coordinates taken from the Harvard Survey or the Lund Tables. The galactic pole is at R.A. 12^h40^m, Decl. $+28°$ (1900).

In the summer of 1936 we measured a dozen nebulae in low latitudes near the edge of the zone of avoidance. These nebulae are faint, of magnitude 14 or 15, and are likely to be involved in rich star fields; hence small diaphragms were used to avoid including stars and to reduce the light of the sky. Measures were not attempted if there were superimposed stars. The rate-of-drift method of measurement was used, with photographic registration of the galvanometer record. The recording drum was driven at the rate of about 50 mm per minute, and the slope of the traced line was determined for an interval of 30 or 45 seconds. The results are in Table 5.

Magnitudes.—The magnitudes for the different areas of the nebulae in Table 4 indicate both the advantages and the disadvantages of measures with the photocell. The limited diaphragms tell exactly

[7] *Harvard Ann.*, **88**, No. 2, 1932.

which part of a nebula was measured, but for large nebulae the magnitude of a central area may not be of much significance. For instance, for a diaphragm of 42″ the photoelectric magnitudes of the Andromeda nebula and its brighter companion, NGC 224 and 221, are 9.33 and 10.03, respectively. The total magnitude of the companion is reached at about 9.33 for 163″, but it is necessary to open to a diameter of several degrees to get most of the main nebula, which, with allowance for the many superimposed stars, turns out to be of magnitude about 4.5. It was not feasible to make a special

TABLE 5

MEASURES OF FAINT NEBULAE, 1936

NGC	Pe	Pg_p	Diaph.	Diameters	Type	Spec.	C_2	l	b	Remarks
1275	13.41	13.5	32″	80″×40″	Ir	G pec.	$+0^{M}.05$	119°	−12°	
1277	14.74	14.9	32	25 ×..	E3	G3	.17	119	−12	
1278	14.42	14.6	32	30 ×..	E0	......	.11	119	−12	
1281	14.96	15.2	32	25 ×..	E2	......	.19	119	−12	
6615	14.74	14.9	15	20 ×10	SBa	......	.09	9	+12	
6627	15.51	15.7	15	70 ×50	SBbc	......	.18	11	+12	2 obs.
6635	14.88	15.1	24	15 ×..	E0	......	.12	12	+11	2 obs.
6658	14.36	14.5	24	90 ×20	Sa	G3	.14	19	+12	
6661	14.01	14.2	24	95 ×65	Sa	G5	.09	19	+12	
IC 1303	15.51	15.6	42	90 ×60	Sc	......	.05	36	+ 7	
6921	14.29	14.4	42	55 ×20	Sb	......	.05	34	− 9	
7013	13.22	13.4	42	80 ×35	Sa	......	+0.10	43	−12	

study of every nebula on the list and be sure that we had all the outer regions. The magnitudes, as given, furnish a series of standards which can be used for a further study of photographs to get over-all magnitudes if desired.

While the magnitudes depending upon the comparison stars may have probable errors up to about ±0.1 mag., the values for the four diaphragms in Table 4 are given to hundredths because their differences are significant to two decimals. There are numerous cases where the difference between, say, 128″ and 163″ indicates faint outer extensions which are not always shown on photographs. The cases where these extensions are real seem to run from about magnitude 24 to 25 per square second of arc. The light of the dark non-

galactic sky at Mount Wilson is something like magnitude 22 per square second. Most of the measures with different diaphragms on the same nebula were made in the early years with the electrometer; the later measures with the amplifier were on fainter and smaller objects. Under the most favorable conditions the limit of detection of faint nebulosity is from magnitude 26 to 27 per square second, or about 4–5 mag. fainter than the surface brightness of the sky. Such a limit would be independent of the size of the telescope were it not for the interference of the stars. However, with a large telescope the number of faint stars brought into view is not sufficient to compensate for the reduction of the field, and it is therefore easier to find a blank field with the 100-inch than with a smaller telescope of the same focal ratio.

The photographic magnitudes Pg_p in column (8) of Table 4 are directly comparable with the Harvard magnitudes in (9) when the diaphragm used was as large as the major diameter in (11). In these cases, where our measure took in all the nebula, the difference $Pg_p - HPg$ is given in column (10). The mean value of the difference $Pg_p - HPg$ for 59 nebulae is -0.08 ± 0.02 (P.E.), which happens to agree exactly with the difference Yerkes *minus* Harvard found by Keenan[8] from photographic magnitudes of about fifty nebulae between the eleventh and thirteenth magnitude and north of declination $+50°$. Seyfert[9] had also found -0.05 for the correction to the Harvard magnitudes fainter than 11.0. Since our magnitudes were connected with the Polar Sequence by way of the Harvard visual system, the close agreement of the three results must be accidental. From our determination Hubble has applied a correction of -0.1 to the Harvard magnitudes at magnitude 13.

The mean error of a single difference $Pg_p - HPg$ is ± 0.25, which is about the same as the ± 0.26 found by Keenan for Yerkes *minus* Harvard. The internal accidental error of Pg_p is small compared with the errors of the Harvard visual magnitudes, and it seems fair to assume a mean error of ± 0.15 for Pg_p and ± 0.20 for HPg. Our measures show that the Harvard magnitudes of nebulae from 11 to 13 are better than the ordinary *Durchmusterung* magnitudes of

[8] *Ap. J.*, **85**, 326, 1937.

[9] *Harvard Circ.*, No. 403, p. 10, 1935.

stars, and that they make a reliable basis for magnitudes of fainter nebulae.

Colors.—The color indices in Tables 3 and 4 are independent of the magnitudes. With C_1 referring to our heavy filters and C_2 to the light filters used for the nebulae, the relation between C_1 and C_2 is

$$C_1 + 0.10 = 1.68(C_2 + 0.27) , \tag{6}$$

where the zero point for each system is fixed by the average color index of an unobscured A0 star. The relation between the color excesses in the two systems is, therefore,

$$E_1 = 1.68E_2 . \tag{7}$$

The colors of some nebulae were not measured because they were too faint and difficult or because they would have taken more time than we could afford to spend on the observing program. The magnitude of a nebula from a couple of galvanometer deflections is easily determined as accurately as the magnitudes of the comparison stars; but the colors must be more precise, and hence are more difficult. The errors of the colors increase, of course, with the faintness of the nebulae. From observations of the same nebulae on different nights the mean error of one observation of C_2 for different magnitudes is as follows:

Brighter than magnitude 12.0	$\pm 0^{M}044$
Fainter than magnitude 12.0	.070
All	± 0.053

The light of even the darkest sky adds up to about magnitude 13 for a 64″ circle; and when the superimposed sky is as bright as the nebula, the observations are difficult by any method. With the amplifier and with alternate readings on nebulae and blank sky through small diaphragms, colors can be measured down to magnitude 15, as in Table 5; but the observations are tedious and require about an hour for each object.

The study of the colors of extragalactic nebulae was originally undertaken to determine how much selective absorption there might be either within our own galaxy or outside in intergalactic space. Perhaps the first test is to compare, for each type of nebula, the observed mean color with the corresponding color for the mean spec-

tral class, as in Table 6. The mean spectral classes for the different types of nebulae are given by Hubble.[10] For each type the mean color index C_2 for dwarf stars of the same spectrum is taken from our Table 2, and the difference E_2 is the mean color excess. The mean

TABLE 6

MEAN COLORS OF NEBULAE

Type	Spectral Class	Mean C_2 Stars	Observed C_2 Nebulae	E_2	M.E. 1 Neb.	No.
E	G4	$+0^{M}02$	$+0^{M}09$	$+0^{M}07$	$\pm 0^{M}053$	30
Sa, SBa	G3	+ .01	+ .07	+ .06	.046	13
Sb, SBb	G2	.00	+ .06	+ .06	.053	12
Sc, SBc	F9	−0.04	−0.06	−0.02	±0.078	36

error for a nebula is computed from the observed deviations of C_2 from the mean for each type. For this test, nebulae in latitudes less than 20° were excluded.

One defect of the material in Table 6 is that the mean spectral classes and the observed colors refer only in part to the same nebulae.

TABLE 7

MEAN COLOR EXCESSES OF NEBULAE WITH KNOWN SPECTRA

Type	E_2	M.E. 1 Neb.	No.
E	$+0^{M}06$	$\pm 0^{M}051$	13
Sa	+ .07	.043	8
Sb	+ .06	.058	7
Sc	−0.04	±0.099	7

In Table 7 are the mean color excesses of those nebulae for which we have both the individual spectra and the colors. These data are included in Table 6; but on any basis of computation the three types E, Sa, and Sb show a color excess E_2 of +0.06 mag. or +0.07 mag., with a probable error of ±0.01 mag. to ±0.02 mag. for each mean. The Sc nebulae have earlier spectra and are bluer in color. Seares[11] found in a number of late-type spirals that the outer arms are distinctly bluer than the central regions, but even in the central

[10] *The Realm of the Nebulae*, p. 53, 1936.

[11] *Mt. W. Comm.*, No. 36; *Proc. Nat. Acad. Sci.*, **2**, 553, 1916.

regions the presence of a few white or blue giant stars would cause these nebulae to appear bluer than the other types of nebulae whose spectra seem to be predominantly dwarflike. Presumably, there could not be a large proportion of white or blue giant stars in a nebula without their showing up in the spectrum, but we must have some leeway in interpreting the integrated spectrum and color of a million stars.

The mean error of one observed C_2 from the measures of the same nebulae on different nights was ± 0.053 mag., which, compared with

TABLE 8

COLOR EXCESS AT DIFFERENT LATITUDES

	b (1)	csc b (2)	E_1 (Obs.) (3)	E_1 (Comp.) (4)	O−C (5)	No. (6)
Nebulae.....	$9^\circ-17^\circ$	4.7	$+0^M.17$	$+0^M.17$	$0^M.00$	11
	20 −27	2.6	.13	.13	.00	10
	32 −49	1.5	.10	.11	− .01	15
	54 −69	1.1	.08	.11	− .03	12
	73 −76	1.0	.13	.10	+ .03	18
Globular clusters.......	20 −23	2.8	.05	.04	+ .01	3
	28 −34	2.0	.02	.03	− .01	5
	37 −50	1.5	.03	.03	.00	6
	73 −89	1.0	.02	.02	.00	5
B stars......	8 −14	5.3	.04	.04	.00	10
	15 −19	3.3	.02	.03	− .01	15
	20 −27	2.6	.02	.02	.00	18
	30 −37	1.8	.03	.02	+ .01	14
	40 −62	1.3	+0.00	+0.01	−0.01	13

the mean errors or standard deviations in the next to the last columns of Tables 6 and 7, shows that for the types E, Sa, and Sb the dispersion in color is practically accounted for by errors of observation. The greater dispersion for the Sc nebulae is probably a real effect, caused by varying proportions of giant stars.

The colors of all the observed nebulae of types E, Sa, and Sb are grouped according to galactic latitude in Table 8.[12] The respective columns contain: (1) the limiting latitudes; (2) the mean csc b

[12] The single nebula with a large color excess, IC 356, $E_2 = +0.39$ mag. for $b = 14^\circ$, is not included in the mean. This nebula was difficult with the 60-inch, but the reddening seems to be real. The near-by nebula, IC 342, in lower latitude has $E_2 = +0.12$ mag.

The globular clusters NGC 2419 and 7492 were also omitted as being anomalous; and NGC 6779, as being on the border of the zone.

for the group; (3) the mean color excess on the scale of E_1 for comparison with globular clusters and B stars, $E_1 = 1.68E_2$; (4) the computed E_1 from equations (8); column (5) gives the residual, and (6) the number of objects. Since the observed E_1 is derived by subtracting the color for the mean spectral class from the measured color of each nebula, the difference is not necessarily zero for high latitude.

GLOBULAR CLUSTERS AND B STARS

The nebulae can be compared with the globular clusters and B stars outside the nebular zone of avoidance. The clusters are probably all far enough from the galactic plane to be well outside the hypothetical absorbing layer, while the B stars are those with computed distances from the plane, $r \sin b$, > 100 parsecs. The mean color excesses of these clusters and B stars are also given in Table 8; and the solutions for their variation according to the cosecant law give equations (8), with probable errors.

$$\left.\begin{array}{lll}
\text{Nebulae,} & E_1 = +0^{\mathrm{M}}.088 + 0^{\mathrm{M}}.017 \csc b \\
& \qquad\quad \pm 7 \qquad\quad \pm 5 \\
\text{Clusters,} & E_1 = +0.009 + 0.013 \csc b \\
& \qquad\quad \pm 16 \qquad\ \pm 9 \\
\text{B stars,} & E_1 = +0.004 + 0.007 \csc b \\
& \qquad\quad \pm 6 \qquad\quad \pm 2
\end{array}\right\} \qquad (8)$$

In these equations the three constant terms give the computed color excess for zero absorption. For the nebulae the term may be real. For the clusters and B stars E_1 should equal 0.00 mag. for $\csc b = 1$; the small discrepancies are due to the choice of the zero points. The three coefficients of $\csc b$ indicate a small but probably real variation with the latitude in each case. Some of the B stars may still be in the absorbing layer, and hence show a smaller latitude effect.

We can adopt the mean from the nebulae and clusters as the selective absorption at the pole, $E_1 = +0.015$ mag. ± 0.005 mag. (P.E.), which is in contrast with Hubble's value of 0.25 mag. for the total photographic absorption.

These figures indicate that in high latitudes the selective absorption is a small fraction of the total. If we assume the same propor-

tion of selective absorption in the zone of avoidance, we run into difficulties. There are five strongly colored globular clusters which average $E_1 = +0.72$ mag.; the total absorption would then be 0.72 mag. $\times$ 0.25/(0.015$\pm$0.005), or 12 mag., with a probable error of $\pm$4 mag. Similarly, the many B stars with values of E_1 between +0.4 mag. and +0.6 mag. would require an impossibly large total absorption. Despite the uncertainty of the numerical results, there seems to be no way of reconciling the small selective absorption in high latitude and the large selective absorption in low latitude without abandoning the assumption of a constant ratio of the selective to the total absorption. In the course of various discussions with Dr. Hubble he has suggested that the space absorption in the Galaxy may involve a tenuous layer of small selectivity, condensed clouds of large selectivity, and the source of stationary spectral lines. Our material can be made to agree with this view by assuming that the sun is in a region of small selectivity. The absorbing stratum obscures the nebulae roughly according to the cosecant law; and when the line of sight approaches the galactic circle, it passes through the clouds of large selectivity, but the nebulae are then lost to view. The nebulae, clusters, and B stars all agree in showing that both the selective and the total absorption are spotted in latitude and longitude. The cosecant law can be only a rough approximation, as is shown by the irregular outlines of the zone of avoidance. Even the naked-eye appearance of the Milky Way contradicts a simple geometrical conception of the Galaxy.

INTRINSIC COLORS OF NEBULAE

If the selective absorption within our Galaxy has little effect upon the color of the visible nebulae, we can study the intrinsic colors of the nebulae themselves. The constant term in the first equation (8), $E_1 = +0.088 \pm 0.007$ mag., is the unexplained color excess in the nebulae. The natural interpretation of such a result is that it can be due to some systematic error. In terms of spectral class and color the discrepancy means that nebulae of estimated spectrum G3 have the color g9. If the nebulae of types E, Sa, and Sb contained giants and dwarfs intermixed, instead of dwarfs only, as assumed, the difference would be less but would not vanish. However, the

giant stars are not found in near-by nebulae like M32, whose spectrum is certainly dwarflike.

The color excess does not seem to be a function of the nebular distance, but we have only a small range of magnitude for the test. In Table 9 the 30 type-E nebulae are divided into three groups, according to apparent magnitude. There is no indication of increasing color index with increasing distance; the small reverse effect must be accidental. The nebulae of magnitude 12.7 are probably ten times as far away as M32, but their average color is about the same. This test of the transparency of space can be continued outward until the red shift begins to affect the colors of the nebulae.

TABLE 9

m	E_1	P.E.	No.
10.7..........	$+0^{M}.13$	$\pm 0^{M}.016$	10
11.7..........	.11	.024	10
12.7..........	+0.08	±0.017	10

We are left with the residual color excess, $E_1 = +0.09$ mag., as a possible measure of selective absorption within the nebulae themselves. It is simple to assume an arrangement of scattering material within a nebula sufficient to produce this effect for an external observer. A thin layer of dark stuff near the main plane would redden all the stars on the far side of a nebula. Our own Galaxy may well have something of the sort near the nucleus, but near the sun the effect at right angles to the main plane would be small. Because of the manner of finding the color excess of the nebulae, we attach little weight to the numerical value; but the discrepancy between estimated spectrum and measured color is in the right direction, to be accounted for by selective absorption within the nebulae.

SUMMARY

We summarize the main conclusions from the colors of B stars, globular clusters, and nebulae. In addition to the published results,[4, 6] we have the colors of more than four hundred B stars, including most of those in classes B0 to B2 north of declination $-40°$ and down to the limit of the *Draper Catalogue*. For uniformity the

colors are all expressed in terms of E_1; the relation to the international scale is $IE = 1.55E_1$.

The brightest, and hence the nearest, B stars are all about normal in color, $E_1 = 0$ for all latitudes. The fainter B stars in the flattened system are near the galactic circle. They show increasing color index with increasing distance from the sun, and practically all stars with $E_1 > +0.10$ are located within the zone of avoidance of the nebulae. Outside this zone the B stars show a small latitude effect, represented roughly by $E_1 = (+0.007 \pm 0.002) \csc b$, from stars more than 100 parsecs from the galactic plane. The reddest B stars are usually within 3° or 4° of the galactic circle; they have color excesses up to $E_1 = +0.30$ in all longitudes from 300° through 360° to 200°. The reddening is rather spotted along the Milky Way, but in general it is greatest near the galactic center and least toward the anticenter. Color excesses of $E_1 = +0.63$ and $+0.68$ have been found for two eighth-magnitude B0 stars in longitude 345°, with a dozen others near by with $E_1 = +0.40$ to $+0.55$, but we have not found a single B star with $E_1 > +0.30$ in the range of longitude from 115° to 190°. There are, however, not many B stars of magnitude 8.0 and fainter in this region of the anticenter. The coefficient of selective absorption—color excess per kiloparsec—is perhaps twice as great toward the center of the Galaxy as toward the anticenter. The reddening of the B stars is not primarily connected with obviously obscured areas; in fact, the brightest star clouds in Sagittarius contain many reddened B stars. Their colors are likewise not directly connected with the interstellar absorption of calcium and sodium. However, with Dr. Merrill, we have a suspicion of a closer connection between our color excess and the strength of the new unknown interstellar lines he has found in the spectra of early-type stars.

The colors of the globular clusters are as strikingly related to the galactic center as are the positions of the clusters themselves. A circle with about 35° radius and its center at longitude 330° includes some 54 globular clusters, more than half of those known. Within this circle, which also contains the great bulge of the zone of avoidance of the nebulae, are all the clusters with marked reddening. The 5 reddest clusters, $E_1 = +0.64$ to $+0.82$, are on the edges of the middle zone, 7° wide, where no globular clusters can be seen. The

22 clusters outside the central group, which we have measured, are widely scattered over the sky and are all nearly of the same color. The small latitude effect is represented by $E_1 = (+0.013 \pm 0.009) \times$ csc b. The boundaries of the nebular zone of avoidance are not sharp. The globular clusters are the redder the fewer the nebulae in the field, until, when $E_1 > +0.20$ for a cluster, the nebulae are blotted out. This limit seems to be about the same for B stars.

The nebulae of types E, Sa, and Sb are nearly uniform in color; those of type Sc are more varied, owing presumably to the presence of giant stars. The colors of the first three types indicate an excess of $E_1 = +0.09$, possibly because of selective absorption within the nebulae. There is no indication of selective absorption in inter-nebular space. The latitude effect for the nebulae is represented by $E_1 = (+0.017 \pm 0.005)$ csc b. Thus the nebulae, like the B stars and the globular clusters outside the zone of avoidance, show little variation in color. Despite the paradox, what we need are colors of nebulae within that zone. There are a few "holes" in low latitude where very faint nebulae are detected, and we hope to observe some of these if any as bright as the fifteenth or sixteenth magnitude can be found.

In order to reconcile the small selective absorption in high latitude with the large selective absorption in low latitude, we assume that the sun is immersed in a layer of small selectivity near the plane of the Galaxy. This layer would account for the total photographic absorption shown by the nebulae, which varies roughly according to the cosecant law and amounts to 0.25 mag. at the pole. The clouds of large selectivity which produce the strong reddening in low apparent latitude are also near the plane of the Galaxy but not immediately about the sun. They cannot be far distant along the main plane since some of the B stars are strongly colored at only a few hundred parsecs.

In the study of the nebulae the color effects we were looking for have all turned out to be very small; but the side results of conspicuous reddening of B stars and globular clusters toward the galactic center, and the lesser reddening of B stars along the galactic circle in all longitudes, have indicated where and how much the nebulae may contribute to the problem. Because of the uniform intrinsic

colors of the nebulae, particularly of type E, it is hoped that an extension to fainter objects will produce results barely hinted at in the present investigation.

We are indebted to Dr. Edwin Hubble for constant collaboration and advice. This investigation has been supported by grants from the Alumni Research Fund of the University of Wisconsin, the National Research Council, and the California Institute of Technology, the last in connection with plans for the 200-inch reflector.

CARNEGIE INSTITUTION OF WASHINGTON
MOUNT WILSON OBSERVATORY,
UNIVERSITY OF WISCONSIN
WASHBURN OBSERVATORY
July 1937

INTERSTELLAR LINES*

INTENSITIES AND DISPLACEMENTS OF INTERSTELLAR LINES*

PAUL W. MERRILL, ROSCOE F. SANFORD, O. C. WILSON,
AND CORA G. BURWELL

ABSTRACT

The main purpose of this *Contribution* is to record measurements of the intensities and displacements of the interstellar lines D1, D2, H, and K in the spectra of numerous early-type stars. Intensities of the unidentified lines λλ 5780, 5797, and 6284 are included. Observational methods and the technique of measurement are fully described, and the accuracy of the results is discussed.

Comparison of the Mount Wilson values of the intensities of the D lines with those of Beals (Table 3, Fig. 1) indicates a fairly small accidental error in both series but a considerable systematic difference between them. Displacements of the D lines measured at various observatories (Table 7) are in good agreement.

The Catalogue, Table 6, includes 254 stars brighter than apparent magnitude 7.0, 147 fainter stars, and, in addition, 3 novae. The numbers of objects with the various kinds of data are as follows:

		Ca	*Na*	λ 6284
Displacement		174	264	...
Intensity	measured	114	213	129
	estimated	89	107	...

Table 8 lists stars with especially strong interstellar lines.

PROGRAM

When observations of interstellar lines were begun at Mount Wilson many years ago, the plan was to concentrate on a few small regions of the sky in which spectra of all B-type stars down to the lowest practicable limit of magnitude were to be examined. It was hoped in this way to determine the behavior of detached lines as a function of distance from the sun.

As the general complexity of the whole problem of the intensities and displacements of these lines became increasingly evident, however, the program was enlarged to include numerous stars in other regions. One important consideration was the desire to provide adequate material for a systematic investigation of interstellar lines in relationship to galactic rotation. This necessitated including stars

* *Contributions from the Mount Wilson Observatory, Carnegie Institution of Washington,* No. 576.

near the galactic plane at all longitudes within reach from Mount Wilson. Another extension of the program arose from the emphasis placed, in the latter part of the work, on stars of high luminosity. Stars of types earlier than B2, and especially c stars of types B0 to A2, offer substantial strategic advantages in extending the observational limits outward into space. A c star (type B0 to A2) of the seventh apparent magnitude is probably as distant as one of type B8n of the twelfth magnitude.

The distribution in longitude and latitude of the stars finally observed resembles roughly that of B-type stars in general, except for decided concentration in two small areas, one in Cygnus, $l = 40°$, $b = +1°$, the other surrounding the h and χ clusters in Perseus, $l = 102°$, $b = -3°$, and less conspicuous concentration in a larger area in Cepheus, $l = 70°$, $b = +5°$, and another in Cassiopeia, $l = 85°$, $b = 0°$.

OBSERVATIONS OF LINES IN THE YELLOW AND RED

Spectrograms for the D lines and $\lambda\lambda$ 5780, 5797, and 6284, taken with a plane-grating spectrograph[1] at the Cassegrain focus of the 100-inch telescope, number approximately 720. Of these, about 660 were taken between May, 1928, and August, 1936, with the instrument in its specially designed mounting; the remainder were taken between September, 1924, and March, 1926, with the grating in a preliminary mounting.

The majority of the spectrograms were taken with an 18-inch camera, dispersion 34 A/mm; the remainder with a 10-inch camera, 66 A/mm. Most of the spectra were widened. Comparison lines of neon have been employed throughout, while the D3 line of helium has been included since October, 1932, and the yellow mercury lines since May, 1936.

Since 1930, the III C emulsion supplied by the Eastman Kodak Company has been regularly used. This fine-grained, contrasty emulsion is very rapid when hypersensitized by bathing in dilute ammonia, and has given excellent results. Most of the earlier spectrograms were taken on the Eastman 33 plate sensitized with pinacyanol, or on the Ilford Special Rapid Panchromatic emulsion.

[1] *Mt. W. Contr.*, No. 432; *Ap. J.*, **74**, 188, 1931.

All the grating plates on which the D lines are visible were measured for line displacements by Miss Burwell, and most of them were remeasured by her after the lapse of three months or more. On the remaining plates the second measure was by Mr. Merrill. The probable error of the mean displacement of the D lines derived from a single spectrogram appears to be about 2.2 km/sec for the 18-inch camera and 3.0 km/sec for the 10-inch.

Photometric tracings were made of all plates from which it appeared beforehand that a reliable result should be obtained. The principal material rejected may be classified as follows: (1) poor spectrograms; (2) lines of extremely low intensity; (3) early spectrograms without photometric calibration; (4) dense exposures, poor for intensity measurements, although often excellent for displacements. As a result of this selection practically all the tracings were measured, and very few data were later rejected. Four-fifths of the spectrograms used for intensity measurements were taken with the 18-inch camera, dispersion 34 A/mm.

A set of standard circles for photometric calibration was impressed on each plate immediately after the star exposure, by means of a tube sensitometer having seven apertures of known area. The exposure in the sensitometer was in two parts: first for about 5 seconds; then, after the plate had been shifted half the diameter of one of the circles, a second exposure for about 12 seconds. This method[2] produced 21 standard densities in 3 overlapping groups of 7 points each, which define the calibration-curve with sufficient accuracy. The source of the calibrating light was a Mazda lamp shielded by an orange filter, which shuts out light of wave-length shorter than 5535 A. Trials with a spectrum sensitometer showed that the III C emulsion yielded calibration-curves having sensibly the same slope from 5535 A to the effective limit of sensitivity of the plate at or beyond 6400 A.

The line intensities were determined in the usual way by measuring the widths of the lines at selected points below the level of the continuous spectrum and computing the equivalent widths by a simple process of numerical integration. Partially independent values were obtained also from the measured central intensities by an

[2] Suggested by Mr. Wilson.

empirical method employed by M. Minnaert and B. van Assenbergh[3] for Fraunhofer lines, and by E. G. Williams[4] for interstellar K. For each line[5] a smooth curve was drawn through the points obtained by plotting the observed central intensities against the equivalent widths found directly from the areas. The equivalent width corresponding to each measured central intensity was then read from the curve and combined with that obtained directly.

A weight of from 1 to 3 was assigned each line at the time of measurement, in accordance with the observer's judgment of the reliability of the resulting value. Since all the measuring and weighting were done by one person (Mr. Wilson), the system should be fairly homogeneous.

One of the chief sources of error in measurements of equivalent line-widths usually lies in the difficulty of determining from the tracing the exact position of the continuous spectrum near the line. In the present investigation this difficulty was minimized by the use of the fine-grained III C emulsion and by the fact that few of the spectra are very narrow. Moreover, in these early-type spectra relatively little uncertainty is caused by neighboring lines. The presence of the alpha band due to oxygen in the earth's atmosphere did, however, cause some difficulty in the measurement of the interstellar line λ 6284, especially on spectrograms taken at a considerable zenith distance. The violet wing of λ 6284 overlaps the head of the alpha band. Attempts to measure the total intensity of the blended features, and then to subtract a correction for the α head, determined as a function of zenith distance, did not yield satisfactory results. The method adopted was to measure the intensity of λ 6284 by itself on the assumption that the blended violet wing has the same shape as the red wing. In a few stars with very weak interstellar lines the *C* II pair at λ 5889.97 and λ 5891.65 interferes with the measurement of D2; attention is called to several instances in the notes following the Catalogue (Table 6).

In the measurements of the D lines we have, in general, assumed the contribution made by stellar D lines to be negligible. In types

[3] *Zs. f. Phys.*, **53**, 248, 1929.

[4] *Mt. W. Contr.*, No. 487; *Ap. J.*, **79**, 280, 1934.

[5] D2 and D1 were taken together.

A0 and later, and in a few stars of earlier type, this assumption may not be precisely true; but we think the errors caused by the inclusion of stellar components are usually smaller than the accidental errors of observation, and of minor consequence. The question of the intensity of the stellar D lines in c stars, particularly those of classes B8 to A2, needs especial consideration. Most of these stars are so distant that the interstellar lines are strongly predominant and no direct measure can be obtained of the stellar lines. The indirect evidence from displacements and from correlations with other interstellar lines is that the stellar D lines are very weak. Some data are available for β Orionis cB8 and for α Cygni cA2, the brightest c stars of early type. The measured equivalent widths of D2 and D1 in β Orionis are 0.14 and 0.04 A, respectively. The D2 line is abnormally intense compared to D1, probably because blended with lines of *C* II. If β Orionis is a typical c star, its distance should be about 100 parsecs; hence the interstellar D lines might be expected to have intensities of a few hundredths of an angstrom. In any event, the intensities of the stellar D lines are very low. In α Cygni the mean equivalent width of the D lines is about 0.5 A, but these lines appear to be chiefly interstellar. High-dispersion coudé spectrograms reveal clearly that the lines are composite, one component being deep and narrow and typically interstellar in appearance, and the other, shallow and slightly diffuse, resembling the other stellar lines. The two components always overlap, but at times the relative displacement of the lines is sufficient to show that the stellar lines are not of great intensity. A rough estimate is that they do not contribute more than 20 per cent of the total intensity. A more detailed investigation is desirable.

From the results of nine plates of HD 224151 (Boss 6142), Table 1, it appears that the probable error of the measurement of a line of moderate intensity on a single good plate with a dispersion of 34 A/mm is about 8 per cent of the intensity for the D lines and about 14 per cent for λ 5780 and λ 6284. For weak lines, as well as those on spectrograms below standard quality, errors of 20 per cent are probably not uncommon.

As a check on systematic error we have measured the intensities of the D lines on a few spectrograms of skylight. The appearance

of the solar D lines on our spectrograms does not differ very greatly from that of interstellar lines of comparable intensity. The standard method was used, of course, in the measurement of the control plates. The results from plates with the 18-inch camera, with which

TABLE 1

EQUIVALENT WIDTHS FROM INDIVIDUAL PLATES; HD 224151

D2	D1	λ 5780	λ 6284
0.56 A	0.44 A	0.19 A	0.42 A
.64	.52	.12	.58
.71	.58	.22	.70
.60	.51	.26	.48
.58	.46	.22	.50
.66	.53	.16	.48
.57	.36	.26	.60
.62	.53	.26	.54
0.65	0.53	0.18	0.43
Mean 0.62 ± .011	0.50 ± .015	0.21 ± .011	0.52 ± .020
PE single plate ± .033	± .044	± .033	± .060

TABLE 2

MEASUREMENTS OF SOLAR D LINES

Observer	D2	D1	Remarks
Unsöld	0.66 A	0.46 A	High dispersion
Korff	.58	.44	High dispersion
Allen	.75	.54	High dispersion
Thackeray	.63	.57	High dispersion
Thackeray	.65	.53	High dispersion
Mulders	0.70	0.56	High dispersion
Mean	0.66	0.52	High dispersion
Mt. Wilson	.73	.52	34 A/mm, 7 plates
Mt. Wilson	0.80	0.60	66 A/mm, 4 plates

most of our stellar spectrograms were made, are in good accord with those obtained by observers using high dispersion, while those from the 10-inch camera plates are somewhat higher (Table 2).

The only measurements of interstellar D lines with which we may compare ours are those of Beals[6] for the 15 stars listed in Table 3. The Mount Wilson values are systematically smaller by about 30

[6] *M.N.*, **96**, 661, 1936.

per cent, although the nearly linear grouping of the points in the correlation diagram (Fig. 1) indicates that in both series the accidental

TABLE 3

COMPARISON WITH MEASUREMENTS BY BEALS
EQUIVALENT WIDTHS IN ANGSTROMS

STAR	BEALS		MOUNT WILSON	
	D2	D1	D2	D1
HD 14143	1.51	1.30	1.18	1.01
14818	1.13	0.86	0.76	0.60
24912	0.34	0.29	0.24	0.22
33656	0.82	0.61	0.50	0.38
36861	0.35	0.26	0.42	0.24
37043	0.19	0.14	0.14	0.07
37128	0.41	0.24	0.21	0.13
91316	0.21	0.10	0.17	0.08
149757	0.24	0.16	0.26	0.18
166182	0.24	0.12	0.16	0.06
190918	1.08	0.86	0.77	0.57
193237	0.48	0.52	0.36	0.34
193793	1.19	1.01	0.74	0.66
203064	0.54	0.43	0.30	0.26
209975	0.71	0.59	0.41	0.38

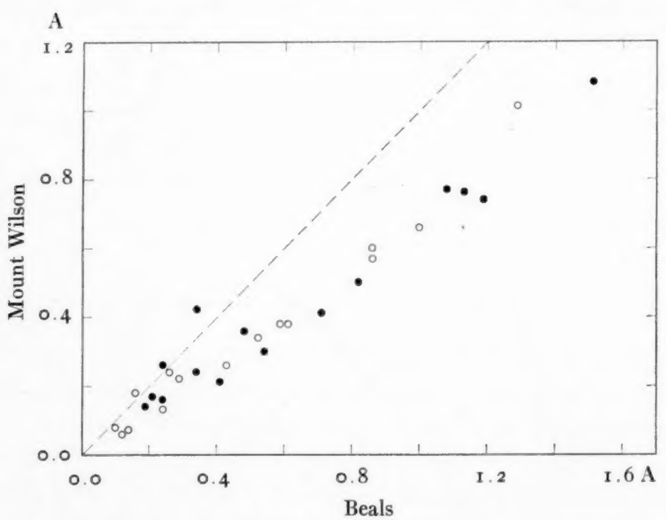

FIG. 1.—Equivalent widths of D lines measured at Mount Wilson and by Beals. Dots D2, open circles D1.

PLATE VI

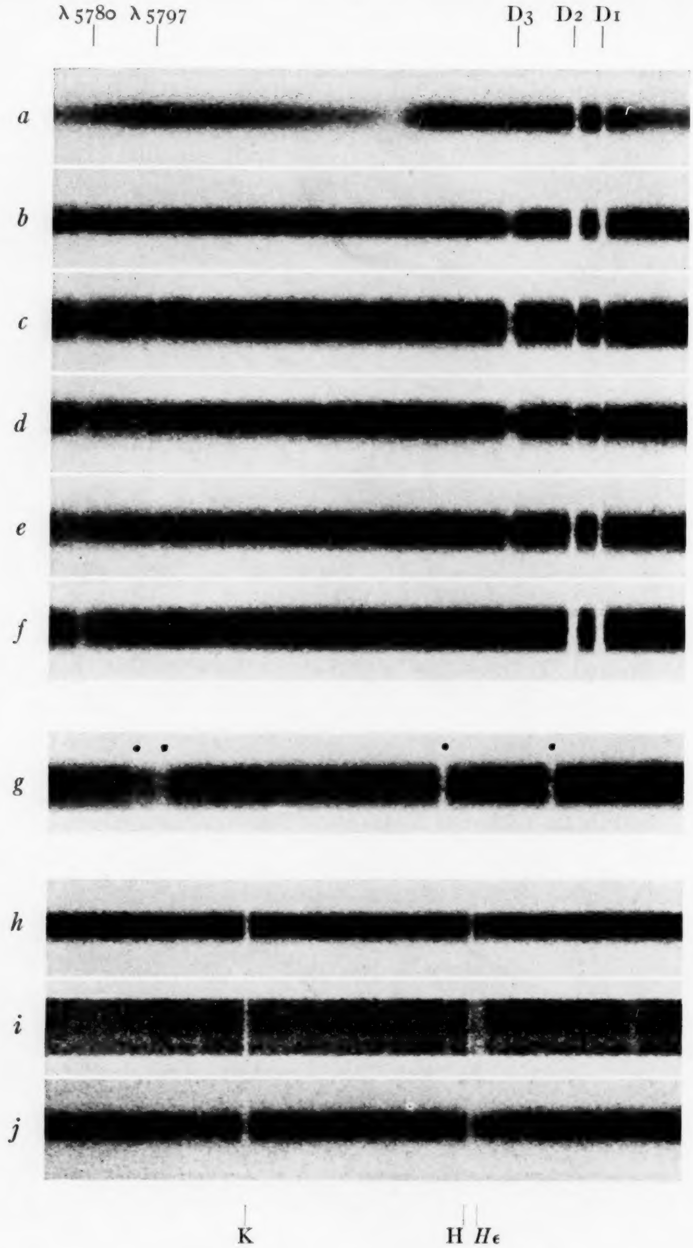

SPECTROGRAMS OF INTERSTELLAR LINES

(*a*) HD 192163: mag. 7.4, sp. Ob; (*b*) HD 14143: 6.7, cB1; (*c*) χ Aurigae, HD 36371: 4.9, cB3; (*d*) ω^1 Scorpii, HD 144470: 4.1, B2n; (*e*) HD 21291: 4.4, cB9; (*f*) (*g*) HD 223385, Boss 6111: 5.6, cA2eα; (*h*) HD 193793: 6.8, Oa; (*i*) χ^2 Orionis, HD 41117: 4.7, cB1eα; (*j*) HD 223987: 7.6, Bo.

In (*g*) dots, left to right, indicate: λ 6278, head of the terrestrial alpha band; λ 6284; λ 6347 *Si* II, stellar; λ 6371 *Si* II, stellar.

errors are satisfactorily small. The source of the systematic error is not clear. The grating with which our spectrograms were taken is known to be particularly free from scattered light, while Beals's spectrograms were obtained by means of a prism. Hence it is not probable that scattered light can account for the difference in the results.

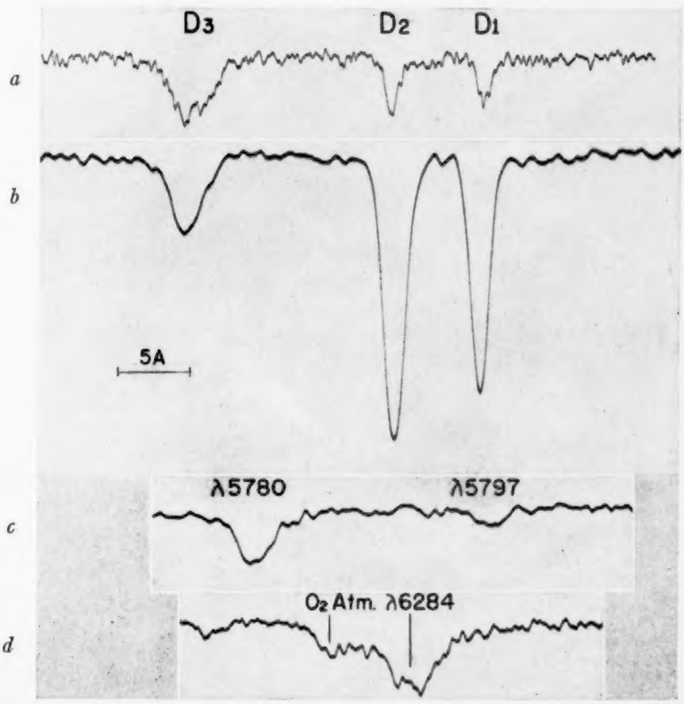

FIG. 2.—Tracings of interstellar lines in the yellow and red. (*a*) and (*b*) also show the stellar line D3. (*a*) ω^1 Scorpii, HD 144470: mag. 4.1, sp. B2n; (*b*) HD 14143: 6.7, cB1; (*c*) (*d*) HD 223385, Boss 6111: 5.6, cA2e*a*. In (*d*) the feature marked O_2 Atm is the head of the alpha band due to molecular oxygen in the earth's atmosphere. Spectrograms showing these lines are reproduced in Plate VI.

OBSERVATIONS OF H AND K

Most of the photographs of the H and K lines were made with a three-prism ultraviolet spectrograph having a camera of 10 inches focal length, dispersion at K, 24 A/mm. A 15-inch camera, dispersion 17 A/mm, was employed for a few bright stars. A few early observations were made with a one-prism spectrograph, dispersion

about 24 A/mm. More than three hundred spectrograms of two hundred stars were obtained, largely during the interval 1931–36. Most of the plates were taken with the aid of the 60-inch telescope; but for a number of the fainter stars, the 100-inch was employed. The Imperial Eclipse Soft emulsion HD 850 was used throughout

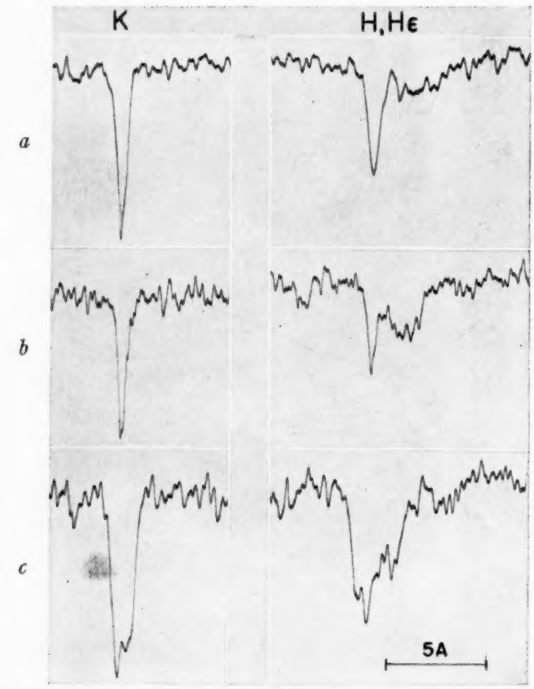

FIG. 3.—Tracings of interstellar H and K lines. (*a*) HD 193793: mag. 6.8, sp. Oa; (*b*) χ^2 Orionis, HD 41117: 4.7, cB1ea; (*c*) HD 223987: 7.6, B0. Spectrograms showing these lines are reproduced in Plate VI.

except for a few exposures on bright stars with the Eastman 33 or Eastman 40 emulsion. Most of the spectra were widened.

The H line, as well as the K, was measured for radial velocity whenever possible, although the result was often given low weight because of the unfavorable influence of the neighboring $H\epsilon$ line. Nearly all the velocities depend on two measures of each plate by Mr. Sanford.

The probable error of the velocity from a single plate, as deter-

mined from stars with numerous plates, appears to be somewhat less than 3 km/sec. For stars with two plates the mean arithmetic difference of the measured velocities is 4.5 km/sec. The mean arithmetic difference between a velocity determined at Victoria and the result from a single Mount Wilson plate of the same star is 4.2 km/sec. The mean arithmetic difference between the first and second measure of the same plate for the first 50 entries in the Catalogue (Table 6) is 2.5 km/sec. These last three comparisons make it probable that 3 km/sec is a liberal estimate of the probable error of a single plate.

TABLE 4

WEIGHTS OF RADIAL VELOCITIES

Weight	Average PE (Km/Sec)		Typical Number of Plates
	Ca	*Na*	
A	1.8	1.1	3 or more good
B	2.5	1.5	2 good
C	3.0	2.2	1 good or 2 fair
D	4.0	3.0	1 fair
E	....	....	1 poor, unreliable

The intensity of the K line was measured by the same method as that employed for the D lines. Miss Grace Wilson made the tracings and drew the characteristic curves, while Mr. Sanford made the actual measures. The standardizing exposures were impressed on each plate either with a tube sensitometer or by the spectroscopic method described by E. G. Williams.[4] The accuracy of the determinations of equivalent width may be inferred from the fact that the mean arithmetic difference between two plates of the same star ranges from 11 per cent of the value for the strongest lines measured to 20 per cent for the weakest.

DESCRIPTION OF THE CATALOGUE

The accuracy of the velocities recorded in the Catalogue (Table 6) varies so widely from star to star that it seems desirable to indicate the approximate weight of each entry. This has been done by use of the letters "A" to "E," whose significance is explained in Table 4.

A number of values of the calcium velocity in column 8 of the Catalogue (Table 6), not accompanied by weight symbols, are measurements at other observatories, taken from Moore's *Catalogue of Radial Velocities*.[7]

Similarly in the data for intensity, "A" indicates a weight greater than 4; "B," weights 2 to 4; and "C," weight 1, the weight assigned to a single spectrogram varying from 1 to 3. On those plates which, for various reasons,[8] were not run on the microphotometer, the line intensities were estimated by visual inspection under the microscope. These estimates do not lead to reliable numerical values but are useful for giving an approximate idea of the intensity, especially to indicate the spectra in which the lines are very weak. As nearly as can be specified, the equivalent widths for the K line or for 0.5 (D2 + D1),[9] corresponding to the Roman numerals, are

TABLE 5

NUMBERS OF STARS OF VARIOUS SPECTRAL TYPES IN THE CATALOGUE, TABLE 6

Type	No Additional Symbol	c	n
Novae	3	.....	.....
Wolf-Rayet	9	.....	.....
O5–9	44	.....	9
B0, 1	53	17	18
B2, 3	73	14	63
B5–9	22	21	16
A0–2	7	21	3
A3–5	.....	3	.....
Misc.	4	.....	.....
	215	76	109

I . . <0.04 A	Line either not seen or a barely perceptible trace
II . . . . 0.06 ± A	Definitely present
III . . . . 0.1 to 0.3 A	Well marked
IV . . >0.3 A	Strong

[7] *Pub. Lick Obs.*, **18**, 1932.

[8] Mainly very low intensity of the lines.

[9] The estimates in the column headed "D2" are for the mean of the D lines.

Except where otherwise indicated, stellar components are believed to add little to the observed intensities, and no corrections have been applied to the estimates. Thus an estimate of I or II means that both stellar and interstellar components are of low intensity.

Of 400 stars in the Catalogue (Table 6), 254 are brighter than apparent magnitude 7.0, 124 are between 7.0 and 9.0, and 19 are fainter than 9.0. The distribution of types is indicated in Table 5.

Displacements of the sodium lines are recorded for 264 stars, measured intensities for 213, and estimated intensities for 107. For the calcium lines the corresponding numbers are 174 (Mount Wilson values), 114, and 89, respectively. The intensity of λ 6284 is recorded for 129 stars; of λ 5780, for 117 stars.

TABLE 6

CATALOGUE OF MOUNT WILSON OBSERVATIONS OF INTERSTELLAR LINES

HD	R.A. 1900	Dec. 1900	Mag.	Spec.	l	b	Velocity (Km/Sec)		Intensity Equivalent Width (Angstroms)					
							Ca	*Na*	K	D2	D1	λ 5780	λ 5797	λ 6284
593	$0^h\ 5^m.3$	+59° 6′	6.7	B2	85°	− 3°	− 3C	− 7E	I	...	...	...	...	...
698	6.3	+57 39	7.1	cB8ea*	85	− 4	...	−16C	...	0.36C	0.31C	0.17B	...	0.29B
886*	8.1	+14 38	2.9	B2	79	−46	...	...	...	I	...	...	...	...
1383	12.9	+61 10	7.9	B0	87	− 1	−24B	...	0.47A	...	...	...	...	...
1544	14.6	+61 31	8.0	B2n	87	0	−20C	...	.39B	...	...	...	...	...
1743	16.6	+61 38	8.4	B0	87	0	−19B	...	.48B	...	...	...	...	...
1810	17.4	+61 41	8.2	B3n	87	0	−17C	...	.41B	...	...	...	...	...
2451	23.2	+61 57	8.6	B1	88	0	−20D	...	III	...	...	...	...	...
2626	24.8	+59 25	5.9	B9n	88	− 3	...	−17D*	II	III*	...	...	...	...
2654	25.1	+61 48	7.3	B3	88	0	...	− 9D	...	III	...	...	...	...
2905*	27.3	+62 23	4.2	cB0ea	89	0	−20B	−14A	.31B	0.54A	.51A	.30B	0.07B	0.49A
3191	30.1	+60 55	8.6	B3n	89	− 1	−14D	...	.38C	...	...	...	...	...
3940	36.9	+63 45	7.4	cB8	90	+ 2	...	−15D	...	0.56B	.43B	.66B	.14B	0.94B
3950	37.0	+51 48	6.9	B0	90	−10	−17	−10C	...	0.62B	.53B	...	...	0.31C
4142	38.8	+47 19	5.6	B5n	90	−15	...	−14D	(I)	0.14C	.10C	...	...	...
4717	44.2	+62 37	8.8	cA1	90	+ 1	...	−24D	...	1.04B	.91B	.60B	.14C	1.16B
4768	44.6	+59 7	8.0	cB3	91	− 3	−26D*	−11D	IV*	0.86B	.78B	.24C	...	0.78B
4841	45.4	+63 14	7.1	cB5	90	+ 1	...	−15B	...	0.75A	.60A	0.38B	0.17B	0.97B
5394*	50.7	+60 11	2.2	B0ne	91	− 2	...	− 3B*	...	0.05C	0.02C	...	...	...
5458	51.3	+62 1	8.6	B2n	91	0	−13B	...	0.39B	...	...	...	...	...

* Refers to notes at end of table.

5551	0^h52^m2	+63°11′	7.7	B1	91°	+ 1°	−18C	......	0.57B	......	......	......	......	......
5689	53.5	+63 5	9.2	B0n	91	+ 1	−18D	......	.58B	......	......	......	......	......
6182	57.8	+61 18	8.6	B1	92	− 1	−17B	......	.62B	......	......	......	......	......
6226	58.2	+47 6	6.7	B5	94	−15	......	−19B	......	0.55A	0.45A	......	......	0.16B
7252	1 7.7	+60 21	7.3	B2	94	− 2	−16C	−16D	.26B	III	......	......	......	......
7636	11.2	+57 6	7.6	B2ne	94	− 5	−12C	......	.28B	......	......			......
7902	13.6	+57 40	7.9	cB5eα	95	− 4	......	−26C	......	IV	......			......
8065	15.0	+78 12	6.1	cA2	92	+16	− 8B*	......	.18C*	......	......			......
9105	24.6	+62 51	7.5	cB5(e)	95	+ 1	......	−20D	......	0.98B	0.80B	0.28B	0.08C	1.00C
12301	55.6	+63 54	5.6	cB8	98	+ 3	......	− 9B	......	0.41A	0.34A	.22A	.08B	0.44B
12953	2 1.7	+57 57	5.9	cA2eα*	101	− 2	......	−22A	......	0.94A	0.75A	.33A	.06B	0.65A
12981	2.0	+55 36	9.5	B3	101	− 5	−17E	......	III	......	......	......	......	......
13267	4.6	+57 11	6.4	cB8	101	− 3	......	−19B	......	0.70A	0.56A	.22B	.09B	0.50B
13476	6.6	+58 6	6.5	cA0	101	− 2	......	−22B	......	1.12A	0.88A	.64A	.20B	0.81B
13744	8.9	+57 50	7.8	cA0	102	− 2	......	−25C	......	0.95B	0.84B	.32B	.09B	0.78B
13745	8.9	+55 32	8.0	B1n	102	− 4	......	−19D	......	0.88B	0.73B	.24B	......	0.65B
13841	9.8	+56 34	7.2	cB2	102	− 3	−28	−29D	......	1.08B	0.84B	......	......	0.60B
13854	9.9	+56 36	6.4	cB1eα	102	− 3	−22E	−23B	IV	0.90A	0.74A	.23B	.08B	0.62B
13866	10.0	+56 15	7.7	cB2	102	− 4	−21C	− 7D	0.70B	IV	......	......	......	......
14010	11.1	+63 58	7.0	cB8	100	+ 4	......	−13C	......	0.98B	0.75B	.45B	.10C	0.85B
14134	12.1	+56 40	6.7	cB3eα	102	− 3	−31	−28B	......	0.98A	0.76A	.27B	.11C	0.58A
14143	12.2	+56 43	6.7	cB1	102	− 3	−26	−31B	......	1.18A	1.01A	.38B	.10C	0.94A
14322	13.8	+55 27	6.8	cB9	103	− 4	......	−16C	......	0.78B	0.65B	.26B	......	0.78B
14422	14.7	+56 56	9.4	B1e	103	− 3	−25E	......	IV	......	......	......	......	......
14433	14.8	+56 47	6.5	cA2	103	− 3	......	−20B	......	0.89A	0.72A	.31B	......	0.88B
14489*	15.3	+55 23	5.2	cA2	103	− 4	......	−14B	......	0.62B	0.54B	.23B	......	0.69B
14535	15.8	+56 47	7.5	cA2	103	− 3	......	−18D	......	1.08B	0.86B	.31C	.08C	0.99B
14542	15.9	+56 56	7.0	cB9	103	− 3	−11C*	−17B	......	1.06A	0.90A	.44A	0.12B	0.78A
14633	16.7	+41 2	7.7	O8	109	−18	−15E	......	IV	......	......	......	......	......
14818	18.2	+56 10	6.2	cB1eα	103	− 3	−24	−17B	IV	0.76A	0.60A	0.28B	......	0.61A

TABLE 6—*Continued*

HD	R.A. 1900	Dec. 1900	Mag.	Spec.	l	b	Velocity (Km/Sec)		Intensity Equivalent Width (Angstroms)					
							Ca	*Na*	K	D2	D1	λ 5780	λ 5797	λ 6284
14947	2h19m.5	+58°25′	8.0	O5f	103°	− 1°	−26	−27E	...	0.64C	0.68C	0.39C	...	0.84C
14956	19.6	+57 14	7.3	cB1	103	− 3	−20	−16E	...	IV	...	...	...	...
15316	22.8	+57 22	7.3	cA2	104	− 2	...	−24B	...	1.15A	1.00A	.42A	0.10B	0.96A
15497	24.6	+57 15	7.2	cB7	104	− 2	...	−23D	...	1.49B	1.39B	.73B	...	1.38B
15785	27.2	+60 6	8.4	B2±	103	+ 1	...	−10E	...	0.81B	0.68B	.58B	.19C	0.82B
16778	36.3	+59 24	7.7	cB9	104	+ 1	...	−22D	...	0.99B	0.71B	.38C	.08C	0.88C
17088	39.5	+57 19	7.5	B6	106	− 1	...	−16E	...	IV	...	...	...	...
18326	51.6	+60 10	7.9	B0n	106	+ 2	−16B	−17D	0.35A	0.72B	0.64B	.24C	.13C	0.61B
18978*	58.0	−24 1	4.2	(A0n)	181	−59	...	...	...	I	...	...	...	...
19243	3 0.7	+62 0	6.5	B2ne	106	+ 4	− 8	−10D	...	0.57B	0.46B	.12C	...	0.38C
19356*	1.7	+40 34	var.	B9	117	−14	...	...	...	I	...	...	...	...
20041	8.2	+56 45	5.9	cA0	109	+ 1	...	− 9A	...	0.66A	0.56A	.62A	.14B	0.87A
20756*	15.5	+20 47	5.2	B8	132	−28	...	+10E*	...	(III)*	...	...	...	...
21291	21.0	+59 36	4.4	cB9	109	+ 4	...	− 7A	...	0.60A	0.47A	.20B	.06B	0.48B
21389	21.9	+58 32	4.8	cA0eα	110	+ 3	...	− 9A	...	0.74B	0.66B	.46B	.08B	1.00C
22192*	29.4	+47 51	4.3	B5ne	117	− 5	...	+ 3B	...	0.28B	0.22B	...	...	0.18C
22253	29.9	+56 23	6.8	B1n	112	+ 2	+ 3C	− 2C	.19C	III	...	...	...	...
22928*	35.8	+47 28	3.1	B8n	118	− 5	...	...	...	I	...	...	...	...
23180*	38.0	+31 58	3.9	B2	128	−17	+12B	*	...	...	...	...	...	...
23675	41.9	+52 21	6.8	B0	116	0	− 5C	− 1C	.30B	0.52B	0.46B	0.24B	0.07B	0.62B
23800	42.9	+52 11	6.9	B2n	116	0	− 3C	− 5C	.40B	IV	...	...	...	...
24398*	47.8	+31 35	2.9	cB1	130	−15	+15E	+12A*	.15B	0.22C	0.16C	...	...	...
24431	48.1	+52 21	6.7	O8	117	0	− 2	− 4C	...	III	...	...	...	...
24534*	49.1	+30 45	var.*	B0ne*	131	−16	+11C*	+11C	0.12C*	0.18C	0.12C	...	...	...
24760*	51.1	+39 43	3.0	B2	125	− 9	+12E	+12B	II	0.11B	0.06B	...	...	0.13B

24912*	3^h52^m5	+35°30′	4.0	O7n	128°	−12°	+10A	+10A*	III	0.24B	0.22B	0.18B		0.36B
25914	4 1.2	+56 50	8.1	cB3	115	+ 5	−27C		0.64B					
25940*	1.4	+47 27	4.0	B3ne	122	− 2		+ 2B		.16C	.11C			
27795	18.2	+45 56	7.2	B3	125	− 1	+ 9	+13E		III				
28446*	24.1	+53 42	5.9	B1n	119	+ 5	0B	− 1B	.24B	.36B	.34B	.12C	0.05C	.18B
28446*	24.1	+53 42	6.6	B0	119	+ 5	+ 4	0B		.36C	.36C			
28497	24.5	−13 17	5.5	B3ne	176	−36				I				
29248*	31.3	− 3 33	4.1	B2	168	−30			II					
30614*	44.1	+66 10	4.4	O9eα	112	+15	− 9D	*	III					
30836*	45.9	+ 5 26	3.8	B2	161	−22	+24C	+21C*	.20B	II*				
31293*	49.4	+30 24	7.5	A0ep*	140	− 7				I				
31327	49.7	+36 1	6.2	B2	136	− 3	+ 6	+13C		.36B	.33B	.16B		.42B
31617	52.2	+43 11	7.3	B2	131	+ 2	+ 4C	+ 2D	.27B	.51B	.40B			
32991	5 2.0	+21 34	6.0	B3ne	149	− 9	+ 9	+17C		.28C	.24C			.22C
34078*	9.7	+34 12	5.8	O9	140	− 1	+17C	+13B	III	.42B	.38B			.50C
34452	12.4	+33 39	5.4	A0p	141	− 1				I				
34578	13.4	+33 52	5.2	cA5	141	− 1		(+ 3)A*		(.50)A*	(.43)A	.16A	.03C	.45A
34656	14.0	+37 20	6.7	O6f	138	+ 2	+ 5	+ 4D		.50B	.38B	.19B		.42B
34989	16.4	+ 8 20	5.7	B2	163	−14	+19E	+20C	II	.24B	.18B			
35411*	19.4	− 2 29	3.4	B0	172	−19	+15E	+17E	I	II				
35439*	19.6	+ 1 45	4.7	B3ne	169	−17				I				
35468*	19.8	+ 6 16	1.7	B2	165	−14			I	I				
35497*	20.0	+28 31	1.8	B8	146	− 2				I				
35600	20.8	+30 7	5.7	cB9	144	− 1		+14B		.44A	.40A	.28B	.07C	.28B
35708*	21.6	+21 51	4.8	B3	152	− 6	+21D		III					
36371*	26.2	+32 7	4.9	cB3	144	+ 1	+ 9B	+ 8B	.46B	.43A	.36A	.40A	0.12A	.64A
36486*	26.9	− 0 22	2.5	B0	172	−16	+17A	*	II					
36576	27.6	+18 29	5.5	B3ne	155	− 7	+21	+19C		.47B	.36B	0.24B		0.36B
36822*	29.3	+ 9 25	4.5	B0	163	−11	+16C	+20C	0.18B	.29B	.20B			
36861*	29.6	+ 9 52	3.7	O8	163	−11	+13	+20C*		0.42B	0.24B			

TABLE 6—*Continued*

HD	R.A. 1900	Dec. 1900	Mag.	Spec.	l	b	Velocity (Km/Sec) *Ca*	Velocity (Km/Sec) *Na*	Intensity Equivalent Width (Angstroms) K	D2	D1	λ 5780	λ 5797	λ 6284
36862*....	5^h29^m6	$+ 9°52'$	5.6	B1	163°	−11°	+13A	+22C	III	0.40B	0.23B	......	......	......
37022*....	30.4	− 5 27	5.4	O7	177	−18	+21	+22B	......	.26B	.16B	......	......	0.26B
37041*....	30.5	− 5 29	5.2	O9	177	−18	+13	+22C	......	.32B	.17B	......	......	......
37042*....	30.5	− 5 29	6.5	B1	177	−18	+11	+15C	......	.26B	.12B	......	......	......
37043*....	30.5	− 5 59	2.9	O8	177	−18	+31A	*	II	.14B*	.07B	......	......	......
37128*....	31.1	− 1 16	1.8	B0	173	−16	+17B*	+20A*	II	.21A	.13A	......	......	......
37468*....	33.7	− 2 39	3.8	B2	174	−16	+16	......	II	......	......	......	......	......
37490*....	33.9	+ 4 4	4.5	B3ne	168	−13	+25	+28C	......	.35B	.28B	......	......	......
37742*....	35.7	− 2 0	2.0	B0n	174	−15	+17A	+18B*	II	.27A	.17A	......	......	......
37743*....	35.7	− 2 0	4.2	B3n	174	−15	......	+17C	......	.28C	.16C	......	......	......
37795*....	36.0	−34 8	2.8	B8ne	206	−28	......	......	......	I	......	......	......	......
37903.....	36.7	− 2 18	8.6	B2	175	−15	......	......	II	......	......	......	......	......
37967.....	37.2	+23 10	6.1	B3ne	152	− 2	+21D	+30D	0.12B	.18C	.10C	......	......	......
38010.....	37.5	+25 24	6.9	B3ne	150	− 1	+ 8	+ 9E	......	III	......	......	......	......
38771*....	43.0	− 9 42	2.2	cB0	182	−17	*	+12B	......	.20B	.12B	......	......	......
39698.....	49.1	+19 44	5.9	B3	157	− 1	......	+19D	......	.20B	.12B	......	......	......
39970.....	50.9	+24 14	6.0	cB9	153	+ 1	......	+11B	......	.50B	.41B	0.45B	0.07C	.92C
41117*....	58.0	+20 8	4.7	cB1ea	157	+ 1	+11A	+13A	.42A	.43B	.38B	.31A	.08B	.62B
41689.....	6 1.6	+62 21	8.6	B2n	119	+20	− 8B	......	.14C	......	......	......	......	......
42087.....	3.7	+23 8	5.8	B2	155	+ 3	+ 6	+ 7C	......	.43B	.37B	.20C	.06C	.46C
42088.....	3.7	+20 31	7.4	O6	158	+ 2	+10	+21D	......	.38C	.36C	......	......	......
42745.....	7.3	−14 25	8.1	B2	189	−14	......	......	III	......	......	......	......	......
43384.....	10.8	+23 46	6.3	cB3	156	+ 5	+12B	+13B	.50B	.58B	.50B	.41B	.11C	.88C
43836.....	13.3	+23 19	7.0	B9	156	+ 5	......	+17C	......	0.50B	0.43B	0.54B	0.20B	0.86B
44112.....	14.9	− 7 47	5.1	B3	184	− 9	+23B	......	0.15C	......	......	......	......	......

44458	$6^h16^m.8$	−11°44′	5.5	B2ne	188°	−11°	+24C		0.21B					
44743*	18.3	−17 54	2.0	cB1	194	−13				I				
45314	21.6	+14 57	7.1	B2ne	164	+ 3	+20	+15C		0.40B	0.36B			
45677	23.7	−13 0	7.5	Bep	190	−10		+ 7E		(II)				
45725*	24.0	− 6 58	4.7	B3ne	184	− 7	+24E	+18C*	II	.20B*	.14B*			
45726*	24.0	− 6 58	5.2	B3	184	− 7			II	.12C	.07C			
45727*	24.0	− 6 58	5.6	B3ne	184	− 7			II	I				
45827	24.6	+ 9 6	6.5	B8±	170	+ 1		+22D		.34B	.24B			
46106	26.3	+ 5 5	8.1	B0	174	− 1		+23D		.39B	.38B	0.42B	0.08C	
46149	26.6	+ 5 6	7.7	O8	174	0	+26C		.30B					
46300	27.5	+ 7 24	4.5	cA0	172	+ 1		+ 8B		.48A	.39A			
46966	31.1	+ 6 10	7.3	O8	174	+ 1	+15	+26D		.56B	.40B			
47129*	32.0	+ 6 13	6.1	O8	174	+ 1	+16	+19B		.49B	.45B	.12B		0.30B
47432	33.5	+ 1 42	6.1	B0	178	− 1	+14C		.40B					
47839*	35.5	+ 9 59	4.7	O7	171	+ 4	+16	+16A*	III	.15A	.06B			
48099	36.6	+ 6 27	6.2	O7	174	+ 2	+12D	+23C	IV	.53B	.44B	.10C		.32B
48279	37.5	+ 1 49	7.8	O8	178	0	+20B	+26D	.30B	III				
48434	38.3	+ 4 2	5.8	B0	176	+ 2	+20	+19A		.52A	.45A	.14B		.28B
50013*	46.1	−32 23	3.8	B2ne	210	−13				I				
50896	50.0	−23 48	6.6	Ob	202	− 9		+44C		.36B	.26B			
52266	55.4	− 5 40	7.0	B2n	187	+ 1	+18C		.18B					
52382	55.9	− 9 4	6.4	B2	190	− 1	+30C	+39C	III	.37B	.35B	.22B		.38B
53138*	58.8	−23 41	3.1	cB3	203	− 7				I				
53367	59.7	−10 18	7.0	B1ne	191	− 1	+26D*	+26C	0.14B*	.38B	.29B	0.14B		0.22B
53456	7 0.0	−11 23	7.8	B5	192	− 1		+26D		.38C	.26C			
53975	2.0	−12 14	6.4	B5	193	− 1		+27E		(III)				
54662	4.6	−10 11	6.2	O7	192	+ 1	+31	+18E		III				
55879	9.7	−10 8	6.0	O9	192	+ 2	+30	+24C		.26B	.18B			
57060*	14.5	−24 23	4.9	O7f	205	− 4	+30	+31C		.30B	.21B			
57061*	14.5	−24 47	4.4	O9	206	− 4	+28	+28C		0.24B	0.13B			

TABLE 6—*Continued*

HD	R.A. 1900	Dec. 1900	Mag.	Spec.	l	b	Velocity (Km/Sec) *Ca*	Velocity (Km/Sec) *Na*	Intensity Equivalent Width (Angstroms) K	D2	D1	λ 5780	λ 5797	λ 6284
57682	$7^h17^m.2$	− 8°48′	6.2	O9	192°	+ 4°	+13D	+22D	0.17B	0.25B	0.14B	...	...	...
58343	20.1	−16 0	5.2	B3e	199	+ 1	+11E	+19C	.07C*	.20B	.12B	...	...	...
58350*	20.1	−29 6	2.4	cB7	210	− 5	...	+21C	...	.31B*	.14B	...	...	...
58715*	21.7	+ 8 29	3.1	B8ne	178	+13	...	...	...	I	...	...	...	...
60848	31.4	+17 7	7.7	O7ne	170	+19	+ 4C	+21D	III	.22B	.18B	...	...	...
62623*	39.8	−28 43	4.1	cA2ep	212	− 1	...	+32A	...	.42A	.32A	0.13B	...	0.44A
63462*	43.9	−25 42	4.6	B3e	210	+ 1	...	...	...	(I)	...	...	...	...
65875	55.8	− 2 36	6.4	B2e	192	+15	...	...	...	I	...	...	...	...
66665	59.5	+ 6 29	8.1	B3	184	+21	...	...	I	I	...	...	...	...
66811*	8 0.1	−39 43	2.3	O8nf	224	− 4	...	...	I	(I)	...	...	...	...
66824	0.2	+43 34	6.2	(A0)	144	+33	...	...	...	I	...	...	...	...
67880	4.9	−15 57	5.5	B3	204	+10	...	...	...	I	...	...	...	...
68980*	9.7	−35 35	4.8	B3ne	221	0	...	...	...	I	...	...	...	...
72968	30.6	− 7 38	5.6	A2p	201	+20	...	...	...	I	...	...	...	...
74575*	39.6	−32 50	3.7	B1	223	+ 7	...	+16D*	...	II*	...	...	...	...
83953*	9 36.7	−23 8	4.7	B3ne	224	+22	...	...	...	I	...	...	...	...
84971	43.7	− 2 14	8.5	B3	208	+38	...	...	III	...	...	...	...	...
87015	57.2	+22 26	5.6	B3n	179	+53	...	+ 2E	II	I	...	...	...	...
87737*	10 1.9	+17 15	3.6	cA0	188	+52	...	+ 3A	...	.26A	.16A	...	...	...
87901*	3.0	+12 27	1.3	B8n	195	+50	...	...	...	I	...	...	...	...
89688	15.9	+ 2 47	6.5	B3n	210	+47	...	+ 6B	III	.18B	.13B	...	...	...
91316*	27.5	+ 9 49	3.8	cB0	204	+54	+ 5A*	+ 6B*	0.16C	.17A	.08A	...	...	...
97603*	11 8.8	+21 4	2.6	A2n	193	+68	...	...	...	I	...	...	...	...
97991	11.1	− 2 55	7.3	B2n	232	+52	...	− 1E	...	0.21C	0.18C	...	...	...
100600	29.5	+17 21	5.8	B3n	209	+70	...	...	...	I*	...	...	...	...

102647*	11^h44^m0	+15° 8′	2.2	A2n	222°	+71°	...	...	...	*	...	...	...	...
104337	55.8	−19 6	5.3	B5	256	+42	...	...	...	(I)	...	...	...	...
108662	12 23.9	+26 28	5.4	(Aop)	203	+86	...	...	...	I	...	...	...	...
116658*	13 19.9	−10 38	1.2	B2n	285	+50	...	...	I	I	...	...	...	...
120307*	43.5	−41 11	3.5	B2	283	+19	...	...	...	I	...	...	...	...
120315*	43.6	+49 49	1.9	B3n	65	+65	...	...	I	I	...	...	...	...
120324*	43.6	−41 59	3.3	B3ne	283	+18	...	...	...	I	...	...	...	...
122980*	59.9	−40 42	4.5	B3	286	+19	...	...	...	I	...	...	...	...
125823*	14 16.8	−39 3	4.6	B8	290	+19	...	...	...	I	...	...	...	...
127972*	29.2	−41 43	2.6	B3ne	291	+16	...	...	...	I	...	...	...	...
132058*	52.0	−42 44	2.8	B3	294	+13	...	...	...	I	...	...	...	...
132200*	52.7	−41 42	3.4	B2	295	+14	...	...	...	I	...	...	...	...
133029	57.2	+47 40	6.2	Aop	46	+57	...	...	...	(I)	...	...	...	...
134759*	15 6.5	−19 25	4.7	B9p	311	+31	...	...	...	I	...	...	...	...
135485	10.2	−14 19	8.3	B3	316	+34	...	...	III	...	...	...	...	...
136298*	14.8	−40 17	3.4	B3n	299	+13	...	...	...	I	...	...	...	...
138485*	27.3	−16 31	5.6	B5n	317	+30	...	...	I	I	...	...	...	...
138690*	28.5	−40 50	3.0	B3n	301	+11	...	...	...	I	...	...	...	...
138749*	28.9	+31 42	4.2	B5ne	16	+54	...	...	...	I	...	...	...	...
138764	29.0	− 8 51	5.2	B8	324	+35	...	−10E	...	II	...	...	...	...
140728	40.2	+52 40	5.5	(Aop)	49	+49	...	...	...	(I)	...	...	...	...
143018*	52.8	−25 50	3.0	B3n	315	+19	...	−18A	I	II	...	...	...	...
143275*	54.4	−22 20	2.5	B1n	318	+21	−12B	−13B	I	0.18B	0.12B	0.10C	...	...
144217*	59.6	−19 32	2.9	B1	321	+22	−14C	−13B*	I	.20B	.12B	.13B	...	0.20B
144218*	59.6	−19 32	5.1	B2	321	+22	...	−13C	I	.18B	.10B	.12B	...	.18B
144470*	16 1.0	−20 24	4.1	B2n	321	+21	...	−12B	I	.25A	.19A	.20B	...	.21B
145389*	5.6	+45 12	4.3	B9	37	+46	...	...	...	I	...	...	...	...
145502*	6.2	−19 12	4.3	B3n	322	+21	−10B	−12B	0.06C	.24B	.18B	.12B	...	.24B
147165*	15.1	−25 21	3.1	B1	319	+16	...	− 8A	II	0.21A	0.15A	0.26B	...	0.41B
147394*	16.7	+46 33	3.9	B8	39	+44	...	...	...	(I)	...	...	...	...

TABLE 6—*Continued*

HD	R.A. 1900	Dec. 1900	Mag.	Spec.	l	b	Velocity (Km/Sec)		Intensity Equivalent Width (Angstroms)					
							Ca	*Na*	K	D2	D1	λ 5780	λ 5797	λ 6284
147888	$16^h19^m.4$	−23°14′	6.6	B3±	322°	+16°	...	− 9C	...	0.24B	0.18B	...	...	...
147889	19.4	−24 14	8.0	B3	321	+16	...	−12D	...	III	...	...	...	...
147933*	19.6	−23 13	5.2	B3n	322	+16	...	− 8B	III	.20B	.15B	0.18A	0.03C	0.28B
147934*	19.6	−23 13	5.9	B3n	322	+16	...	− 9C	III	.26B	.14B	.32B	...	0.25C
148184*	21.2	−18 14	4.8	B3e	326	+20	−15E	−16A	0.06C	III	...	...	...	...
148688	24.7	−41 36	5.5	B1e	308	+ 3	...	+17D*	...	.60C*	.42C	.26B	...	...
149038*	27.0	−43 50	5.2	O9	307	+ 1	...	+ 2D	...	III	...	...	...	...
149363	29.1	− 5 56	8.0	O9	338	+25	−11E	...	0.17C	...	...	...	...	...
149382	29.2	− 3 48	9.0	B3	340	+27	...	...	II	...	...	...	...	...
149438*	29.7	−28 1	2.9	B1	319	+11	...	−17C	...	II	...	...	...	...
149757*	31.7	−10 22	2.7	B0n	334	+22	...	−18B	...	.26A	.18A	...	...	...
149881	32.4	+14 40	6.6	B1	359	+35	−18E*	−17C	III*	.16C	.08C	...	...	...
151804	44.5	−41 4	5.4	O9f	311	+ 1	...	− 8C	...	.48B	.39B	...	...	0.50B
151932	45.3	−41 41	6.6	Oc	311	0	−20	−17C	...	.53B	.56B	.36B	...	0.56C
151985*	45.6	−37 51	3.6	B2	314	+ 3	...	...	...	I	...	...	...	...
152234	47.0	−41 39	5.3	B0	311	0	...	− 6C	...	.57B	.42B	...	...	...
152236*	47.0	−42 12	4.9	cB1eq*	311	0	...	−11C	...	.76B	.70B	.42B	.14C	1.02C
152408	48.0	−41 0	6.0	O6f*	312	0	...	−10D	...	.82B	.67B	.34C	...	0.56C
154090*	58.2	−33 59	4.9	cB1eα	319	+ 3	...	− 2B	...	.52A	.38A	.12C	...	0.19C
155806	17 8.7	−33 26	5.5	O8e	320	+ 2	...	+ 1C	...	.34B	.22B	...	...	...
156247*	11.4	+ 1 19	var.*	B5	350	+20	...	−21C	...	III	...	...	...	...
157857	20.7	−10 55	7.4	O7	341	+12	−15D	− 6C	III	.40A	.31A	.34C	...	0.44B
160233	33.7	+ 4 24	8.6	B3	356	+17	...	...	III	...	...	...	...	...
160529	35.3	−33 27	6.7	cA4eα	323	− 3	...	(−22)B*	...	0.90B*	0.80B	0.57A	0.17B	1.36B
160762*	36.6	+46 4	3.8	B3	39	+30	...	−13D	...	II*	...	...	...	...

161912*	17^h43^m1	−40° 4′	4.9	cA3	318°	− 8°	...	−10C	...	0.70B	0.48B	0.18B	...	0.74B
161961	43.4	− 2 9	8.2	Bo	351	+11	−15E	...	IV	...	...	...	...	...
162978	48.7	−24 52	6.1	Bo	332	− 1	−16E	− 9B	0.15C	.32B	.25B	.35B	...	0.41B
164284*	55.3	+ 4 22	4.8	B5ne	358	+12	...	−16C	I	.18B	.16B	...	...	...
164353*	55.6	+ 2 56	3.9	cB7	357	+11	...	−13C	...	.40B	.28B	.12B	0.02C	0.20B
164402	55.8	−22 46	5.7	Bo	335	− 1	− 5D	−14C	.28C	.22C	.19C	.14C	...	...
164432	56.0	+ 6 16	6.2	B2	0	+13	...	−17C	III	.42C	.32C	...	...	...
164492*	56.3	−23 1	6.9	O7	335	− 2	...	−13D	...	.20C	.12C	...	...	...
164637	57.0	−22 43	6.6	Bo	335	− 2	−15E	− 3E	.19C	III	...	...	...	...
164794*	57.7	−24 22	5.9	O5	334	− 2	...	−19C	III	.38B	.24B	...	...	0.44B
165174	59.6	+ 1 55	6.1	B2n	357	+10	− 5	−12B	...	.43A	.35A	.26B	.07B	0.39B
165516	18 1.2	−21 27	6.2	Bo	337	− 2	− 6D	−16C	.40B	.31C	.26C	...	...	...
N Sgr*	2.1	−34 21	...	Q	325	− 8		−10D	...	.80C	.63C	...	...	...
165763	2.5	−21 16	7.8	Oa	337	− 2	...	+ 4D	...	.52C	.53C	...	...	0.30C
165784	2.6	−21 28	6.6	cA2	337	− 2	...	− 5B	...	.70A	.56A	.70A	.12B	0.84B
165921	3.2	−24 1	7.7	Bo	335	− 4	...	+ 2D	...	(III)	...	...	...	...
166182	4.4	+20 48	4.3	B2	15	+17	−21C*	−24D	.18B*	.16B*	.06B	...	...	...
N Her*	4.7	+45 51	...	Q	40	+26	−21A	−18B	...	I	...	...	...	...
166937*	7.8	−21 5	4.0	cB8ea	338	− 3	...	− 7B	...	III	...	...	...	...
167264	9.3	−20 46	5.4	Bo	338	− 3	...	oC	...	.29B	.24B	.24B	...	0.36B
167771	11.6	−18 30	6.4	O8	340	− 3	...	− 6C	...	.42C	.29C	.16C	...	0.31C
167815	11.8	−19 42	7.6	B2	339	− 3	...	−11D	...	.48C	.27C	.27C	...	...
169454	19.6	−14 2	6.8	cBoe	345	− 2	...	− 4B	...	.78B	.74B	.40B	.12B	1.00B
172367	34.7	− 7 20	9.7	Bo	353	− 2	− 8E	...	.42B	...	...	...	...	...
175191*	49.1	−26 25	2.1	B3n	337	−14	...	...	I	I	...	...	...	...
175514	50.6	+ 9 13	8.5	Bon	9	+ 2	+ 3B	...	.54B	...	...	...	...	...
176304	54.5	+10 0	6.5	B2	11	+ 1	−20	− 3C	(IV)	0.67B	0.57B	0.27B	0.10C	0.38B
177003	57.7	+50 24	5.2	B3	48	+19	−21E	...	...	I	...	...	...	...
177756*	19 0.9	− 5 2	3.6	B9n	358	− 7	...	...	...	I	...	...	...	...
178175	2.4	−19 27	5.4	B3ne	345	−14	− 7C	...	0.20C	...	...	...	...	...

TABLE 6—*Continued*

HD	R.A. 1900	Dec. 1900	Mag.	Spec.	l	b	Velocity (Km/Sec)		Intensity Equivalent Width (Angstroms)					
							Ca	*Na*	K	D2	D1	λ 5780	λ 5797	λ 6284
178849	19h 5m.1	+34°35′	6.6	B3	34°	+11°	...	+ 4C	...	0.16C	0.11C	...	...	...
180163*	10.4	+38 58	4.5	B5	38	+12	...	−16D	...	.19C*	.04C	...	...	...
180968	13.5	+22 51	5.4	Bon	24	+ 4	−13C	− 9C	0.12C	.26B	.22B	...	...	0.18C
183143	23.0	+18 5	6.9	cB9eα	21	− 1	...	− 1B	...	.73A	.62A	0.84A	0.18B	1.88B
184171	28.1	+34 14	4.8	B5	35	+ 6	...	−17E	III	II	...	...	...	...
184279	28.6	+ 3 34	6.8	B2e	9	− 9	−10	− 9C	III	.49B	.38B	.08C	...	0.29B
184915*	31.5	− 7 15	5.0	Bon	0	−15	−14E	...	.16B	...	...	...	...	...
185859	36.1	+20 15	6.4	Bo	24	− 2	− 8C	−11C	.33B	.30B	.26B	.20B	.13B	0.32B
185936	36.5	+13 35	5.8	B5	19	− 6	...	−13B	...	.14B	.12B	...	...	0.11C
186610	40.3	− 3 24	9.1	B3	4	−15	...	...	III	...	...	...	...	...
186618	40.4	+47 1	8.3	B1n	49	+11	−15C	...	.17C	...	...	...	...	...
187320	44.3	+19 24	7.6	B2n	25	− 4	− 7C	...	.30B	...	...	...	...	...
187567	45.5	+ 7 39	6.4	B3ne	15	−10	− 2E	...	IV	IV	...	...	...	...
187879	47.2	+40 20	5.6	B2	43	+ 6	−17	−18C	...	.47B	.36B	...	...	0.22B
188001	47.9	+18 25	6.3	O7f	24	− 6	−10E	− 5C	III	III	...	...	...	...
190066	58.1	+21 52	6.6	cBo	27	− 6	− 6	− 6B	...	.40B	.34B	.27B	.10C	0.48C
190429*	59.8	+35 45	(7.2)*	O5n	40	+ 2	− 8C	− 6C	.41B	IV	...	...	...	...
190429*	59.8	+35 45	(7.8)*	O9n	40	+ 2	− 7C	− 5C	III	IV	...	...	...	...
227415	20 0.1	+35 16	9.9	B3	40	+ 1	−14C	− 9D	.65B	IV	...	...	...	...
227460	0.6	+35 59	10.0	B3	40	+ 2	− 8C	−17D	.36B	.76B	.66B	...	...	...
190603	0.7	+31 56	5.7	cBoeβ	37	0	− 9B	−13A	IV	.68A	.67A	.58B	0.26C	1.02B
227586	1.8	+35 20	9.4	B1	40	+ 1	−15C	...	.66B	...	...	...	...	...
190864	1.9	+35 19	8.2	O6	40	+ 1	−15B	− 4D	.52B	.80B	.73B	.25C	...	...
227611	2.0	+35 37	9.5	Bne*	40	+ 1	−14C	−12D	.40B	.84B	.78B	...	...	...
190918	2.2	+35 31	7.0	O9f	41	+ 1	−13C	− 7B	0.50A	0.77B	0.57B	0.22B	...	...

190919	20h 2m2	+35°24′	7.3	cB1	40°	+ 1°	−15B	− 6D	0.53C	III				
*	2.2	+35 31	(8.0)*	B0	41	+ 1	−10B	− 9D	.72B	0.86B	0.68B	0.28B		
*	2.2	+35 29	(8.9)*	B5	40	+ 1		− 9D		0.86B	0.70B	.28C		0.50C
227634	2.3	+35 29	7.6	B1	40	+ 1	−17D		.42B					
227696	2.8	+35 27	9.0	B2	40	+ 1	−12C		.48B					
227767	3.6	+35 18	9.6	B2	40	+ 1	−10D		.41B					
191201	3.6	+35 26	7.1	B0	40	+ 1	−12D	− 5D	III	IV				
227836	4.3	+35 50	10.9	B2e	41	+ 1	− 3D	+ 6D	.46C	1.48C	1.37C			
227877	4.6	+35 10	9.5	B3n	40	+ 1	−15E		.39C					
191495	5.1	+35 14	8.1	B1	40	+ 1	−12A	− 5E	.42B	IV				
227960	5.4	+35 45	10.0	B0	41	+ 1	− 6C		.52B					
191566*	5.5	+35 11	(8.7)*	B2	40	+ 1	− 7C	−15E	.44B	0.40B	0.40B			
191567*	5.5	+35 11	(7.7)*	B2	40	+ 1	− 8C	− 7D	III	0.48C	0.44C			
191612	5.7	+35 26	8.2	O7	40	+ 1	−10A	−14D	.33B	III				
228007	5.9	+35 28	10.1	B3n	41	+ 1	−13C	+ 2E	.44C	IV				
228041	6.2	+35 12	9.6	B(3)ne	41	0	− 7C		.41B					
191765	6.5	+35 53	7.8	Ob	41	+ 1	−10E	−12D		0.73B	0.56B			
228104	6.9	+35 35	9.8	B(3)ne	41	0	−12D		.40B					
191917	7.2	+35 39	7.8	B1	41	+ 1	− 8D	−11D	.29B	0.88B	0.70B	.24B		.36C
192044	7.8	+26 11	5.9	B8ne	33	− 5				I				
192103	8.1	+35 54	7.9	Oa	41	0	−22D	−18D	III	1.*	0.6*			
192163	8.4	+38 3	7.4	Ob	43	+ 2	−18	−17C		0.49B	0.41B			.56B
192639	10.8	+37 3	7.0	O7f	43	+ 1	−13	−16D		(III)				
192641	10.8	+36 21	7.9	Oa	42	0	−17	− 7D		III				
193077	13.3	+37 7	8.0	Oc	43	0	−20	−17D		0.39C	0.34C	.28C		
193237*	14.1	+37 43	4.9	B1eq	44	0	−15C	−15A		0.36A	0.34A	.14B		.47B
193322	14.6	+40 25	5.8	O8	46	+ 2	−13	−13B		0.53A	0.46A			.32A
193793	17.1	+43 32	6.8	Oa	49	+ 3	−16C	− 8B	0.49B	0.74B	0.66B			.84A
193911	17.7	+24 7	5.4	B8ne	33	− 8		− 4B	III	0.20B	0.16B			
194279*	19.7	+40 26	7.0	B0*	46	+ 1	−13	−13C		0.83B	0.68B	0.46B	0.11B	0.94B

TABLE 6—*Continued*

HD	R.A. 1900	Dec. 1900	Mag.	Spec.	l	b	Velocity (Km/Sec)		Intensity Equivalent Width (Angstroms)					
							Ca	*Na*	K	D2	D1	λ 5780	λ 5797	λ 6284
195592	20^h27^m2	+43°59′	7.2	Boe	50°	+ 2°	−14	−10C		0.60B	0.48B	0.42B	0.10B	0.66B
195810*	28.4	+10 58	4.0	B7	23	−18				I				
197345*	38.0	+44 55	1.3	cA2ea	52	+ 1		− 7A		.5*	.4			
198183*	43.5	+36 7	4.5	B5ne	46	− 5		−11B		.16B	.12B			
198478*	45.5	+45 45	4.9	cB2ea	53	+ 1	−21B	−14B	0.50B	.44A	.39A	.25A	.07C	.40B
199478	52.4	+47 2	5.8	cB8ea	55	+ 1		−15C		.74B	.58B	.32B	.10C	.44B
199579	53.1	+44 33	6.0	O6	54	0	− 8E	−17C		.70B	.58B	.11B		.16C
200120*	56.4	+47 8	4.9	B3ne	56	0		−22D		I				
202850*	21 13.5	+38 59	4.3	cAo	52	− 8		− 8A		.47C	.34C	.18C		.30C
202904*	13.8	+34 29	4.4	B3ne	49	−11		−15C		.14B	.05B			
203025*	14.6	+58 10	6.4	B3e	66	+ 6	−16C	−18B	.35C	.76A	.64A	.18B		.34B
203064*	14.8	+43 31	5.1	O8n	55	− 4	−14A	−16B*	.27B	.30B	.26B			
203374	16.7	+61 25	6.6	Bone	68	+ 8	−17	−15D		III				
203664	18.6	+ 9 30	8.3	B2n	30	−29	− 7E		.27B					
204964	27.0	+59 56	7.5	B2	68	+ 6	−11A		III					
205139	28.3	+60 1	5.5	Bo	68	+ 6	−18E		III					
205196	28.6	+57 4	7.4	Bo	66	+ 4	−20E		III					
205618	31.4	+29 18	8.4	Bne	48	−17	−12D		.13C					
205686	31.9	+61 51	8.5	B3	70	+ 8	−13C		III					
205794	32.6	+57 1	8.7	B3	67	+ 4	−11C		.33C					
206165*	35.2	+61 38	4.9	cB2	70	+ 7	−17C	−20B	III	.45A	.39A	0.20B	0.08C	.34C
206183	35.3	+56 32	8.1	Bo	67	+ 3	− 8E		.30B					
206267	35.9	+57 2	5.6	O6n	67	+ 3	−18B	−20C	III	.55C	.47C			.26C
206327	36.3	+61 6	8.5	B2	69	+ 6	−18D		.37C					
206773	39.3	+57 17	7.0	Bone*	67	+ 3	−18C	−13C	0.20C	0.57B	0.44B			0.30C

207198	21^h42^m2	+61°59′	6.0	O9	71°	+ 7°	−20C		0.25C					
207260*	42.6	+60 40	4.5	cA2	70	+ 6		−19C		0.85C	0.78C	0.38C	0.08C	0.88C
207308	42.9	+61 50	7.9	B2	71	+ 7	−15C		III					
207538	44.6	+59 14	7.0	O9	69	+ 4	−12	−12C	(IV)	0.37B	.30B	.30B	.15C	.20C
207673	45.6	+40 40	6.5	cA0	58	−10		−16B		0.92B	.77B	.40B	.13B	.56B
207757*	46.2	+12 9	7.6	Bep	38	−32	0	−27C*		III*				
207951	47.8	+61 20	8.1	B2	71	+ 6	−12D		0.38C					
208392	50.9	+62 8	7.1	B3ne	72	+ 6	−14C		III					
208440	51.1	+62 6	8.8	B2	72	+ 6	−12E		0.28C					
208761	53.4	+62 25	8.7	B3n	72	+ 6	−10D		III					
209339	57.6	+62 0	6.5	B0	72	+ 6	−14	−17C	III	0.37B	.34B	.27B		.30B
209454	58.4	+61 4	7.7	B3n	72	+ 5	−14D		0.26B					
209481	58.7	+57 31	5.5	O9n	70	+ 2	−17C		0.18B					
209744	22 0.6	+59 19	6.7	B2n	71	+ 3	−23C		0.18B					
209975	2.1	+61 48	5.2	O9	73	+ 5	−13B	−12B	0.28B	0.41B	.38B	.21B		.28B
210129	3.1	+21 13	5.7	B8ne	48	−28		+ 1D		II				
210352*	4.8	+60 38	(8.2)*	B2	72	+ 4	− 9E		0.30C					
210352*	4.8	+60 38	(9.2)*	B5	72	+ 4	− 7E							
210478	5.6	+60 30	7.3	B2	72	+ 4	− 2E		III					
210809	7.9	+51 56	7.7	O8	68	− 3	−21	−26D		0.68B	.62B			.58B
210839*	8.1	+58 56	5.2	O6nf	71	+ 3	−13C	−15B*	0.31C	IV				
N Lac*	12.0	+55 7		Q	70	− 1	−14A*	−10A*	0.26A	0.46A	.36A	.22A		
212044	16.4	+51 21	7.1	B2e	68	− 5	−16D		III					
212455	19.3	+54 44	8.4	cB3	71	− 2	−31C	−30B	1.35B	1.04A	.87A	0.45A	0.12B	0.78B
212571*	20.2	+ 0 52	4.6	B1ne	35	−46	−14C	0C	0.09B	0.24C	.18C			
212593	20.4	+48 58	4.6	cB8	68	− 7		−13C		III				
214167*	31.4	+39 7	6.6	B2	65	−17	−14E	−14B		0.24B	.16B			
214168*	31.4	+39 7	5.8	B3ne	65	−17	−12D	−15B	0.11B	0.26B	.18B			
214432	33.0	+38 55	8.1	B3n	65	−17	−14C		0.26C					
214680*	34.8	+38 32	4.9	O9	65	−17	−15E	−13B		0.30A	0.21A			

TABLE 6—*Continued*

HD	R.A. 1900	Dec. 1900	Mag.	Spec.	l	b	Velocity (Km/Sec)		Intensity Equivalent Width (Angstroms)					
							Ca	*Na*	K	D2	D1	λ 5780	λ 5797	λ 6284
215227.....	22^h38^m6	+44°12′	8.7	Boe	68°	−13°	−16C	....	0.36B	....	....	......	......	......
216916.....	51.9	+41 4	5.5	B3	69	−17	− 7C	−12E	III	(III)	....	......	......	......
217050.....	52.7	+48 9	5.2	B3ne	72	− 9	−11C	−10B	.27B	0.52A	0.35A	......	......	0.17B
218376.....	23 2.4	+58 53	4.9	cB1	78	− 1	−13C	−10C	.14C	0.37B	0.34B	0.16C	......	0.28B
221253*....	25.4	+58 0	4.9	B3n	80	− 3	−15D	− 4C	II	0.16B	0.10B	......	......	......
223385*....	44.0	+61 40	5.6	cA2ea	83	0	....	−28A	....	1.39A	1.15A	.53A	0.12B	1.15A
223501.....	45.0	+61 39	8.2	B3e	83	+ 1	−10E	....	III	....	....	......	......	......
223960.....	48.9	+60 18	7.0	cA0ea	84	− 1	....	−27C	....	1.42A	1.12A	.46A	.14B	0.94A
223987.....	49.2	+61 3	7.6	B0*	84	0	−30B	−30C	.68B	1.04B	0.74B	.41C	......	0.80B
224055.....	49.7	+61 17	7.2	cB3ea	84	0	−30A	−23B	.85C	1.15A	0.82A	.56B	.17B	1.00B
224151*....	50.5	+56 53	6.0	B0	83	− 4	−18A	−20A	.30B	0.62A	0.50A	.21A	.05A	0.52A
224404.....	52.5	+59 28	6.4	B8n	84	− 2	....	−11C	....	0.22B	0.13B	.18C	......	0.16B
224424.....	52.7	+59 9	7.8	B0ea*	84	− 2	−14B	−18D	.46C	0.77B	0.58B	......	......	......
224559.....	53.8	+45 52	6.5	B3ne	82	−15	−14	−14B	....	0.27A	0.20A	......	......	0.18C
224572*....	53.9	+55 12	4.9	B2n	83	− 6	−10B	−15C	.10C	0.50C*	0.37C	......	......	......
224599.....	54.1	+59 29	10.2	B3n	84	− 2	−26C	....	.72B	....	....	......	......	......
224905.....	56.6	+59 54	9.2	B3n	85	− 2	− 9B	....	.56A	....	....	......	......	......
225094.....	58.3	+63 5	6.3	cB2ea	85	+ 1	−16B	−15C	.67B	0.70B	0.57B	.23B	.08B	0.64B
225146.....	58.8	+60 33	8.6	B0	85	− 1	−23B	−19D	0.95B	1.17B	0.89B	.50B	0.10C	1.14B
225160.....	58.9	+61 40	8.6	O8ea	85	0	−19C	−20D	IV	0.86B	0.78B	0.38C	......	0.68B

NOTES TO TABLE 6

HD		
698	......	The classification as a c star is doubtful. According to J. A. Pearce (*M.N.*, **92**, 884, 1932), the interstellar K line in this interesting binary "has an estimated intensity of 0.6 that of the stellar K line," whereas a spectrogram taken at Mount Wilson shows that the interstellar D lines are several times as intense as the stellar D lines.
886	γ Peg	
2626	......	The D lines, although fairly sharp, may possibly be stellar.
2905	κ Cas	
4768	......	H and K, probably blend of stellar and interstellar lines, although star is classified cB3.
5394	γ Cas	See Table 7.
8065	......	The stellar velocity is -76 km/sec, sufficient to separate the stellar and interstellar *Ca* II lines.
12953	......	The stellar lines are very similar to those of α Cygni. The much greater intensity of the D lines is probably due to the interstellar components.
14489	i Per	
14542	......	On one spectrogram the stellar and interstellar *Ca* II lines are blended; on another, the stellar component, owing partly to a change in its displacement, appears to the violet of the interstellar component.
18978	τ^3 Eri	
19356	β Per, Algol	
20756	τ Ari	The D lines may be stellar.
22192	ψ Per	
22928	δ Per	
23180	o Per	See Table 7.
24398	ζ Per	See Table 7.
24534	X Per	Magnitude probably about 6.0. D3 is bright. On the Mount Wilson spectrograms, H and K look like interstellar lines. Plaskett has considered them stellar.
24760	ϵ Per	
24912	ξ Per	See Table 7.
25940	c Per	
28446	......	Both components of ADS 3274.

NOTES TO TABLE 6—*Continued*

HD			
	29248	ν Eri	
	30614	9 (a) Cam	See Table 7.
	30836	π^4 Ori	The *Na* lines may be partly stellar. See Table 7.
	31293	AB Aur	See *Mt. W. Contr.*, No. 462; *Ap. J.*, **77**, 103, 1933.
	34078	AE Aur	
	34578	. . . . . .	The D lines probably consist of both stellar and interstellar components, with the interstellar component the more intense.
	35411	η Ori	
	35439	25 Ori	
	35468	γ Ori	
	35497	β Tau	
	35708	o Tau	
	36371	χ Aur	
	36486	δ Ori	See Table 7.
	36822	ϕ^1 Ori	
	36861	λ Ori Br	See Table 7.
	36862	λ Ori Fr	
	37022	θ^1 Ori C	Brightest star in Trapezium.
	37041	θ^2 Ori Br	
	37042	θ^2 Ori Fr	
	37043	ι Ori	See Table 7. On the Mount Wilson spectrogram the D lines do not appear quite so sharp as most interstellar lines, but the effect may be accidental.
	37128	ϵ Ori	Beals finds the K line double, the velocities of the components being +8 and +23 km/sec, respectively. The duplicity is confirmed by a high-dispersion spectrogram taken at Mount Wilson on which the measured velocities are +9 and +25 km/sec. The mean of these values, +17 km/sec, appears in Table 6. See Table 7.
	37468	σ Ori	
	37490	ω Ori	
	37742	ζ Ori Br	See Table 7.
	37743	ζ Ori Fr	

HD 37795	α Col	
38771	κ Ori	On a high-dispersion spectrogram the K line appears double, the velocities of the components being 0 and +24 km/sec, respectively.
41117	χ^2 Ori	
44743	β CMa	
45725	β Mon	Preceding and brightest component. D lines perhaps partly stellar.
45726	β Mon	Intermediate component.
45727	β Mon	Following component.
47129	......	Plaskett's very massive star. *M.N.*, **82**, 447, 1922.
47839	S Mon	See Table 7.
50013	κ CMa	
53138	o^2 CMa	
53367	......	The Victoria observers consider the *Ca* II lines stellar and record a velocity from one plate of −3 km/sec. See *Pub. Dom. Ap. Obs.*, **5**, 44, 1931. The Mount Wilson data appear to indicate that the lines are interstellar.
57060	29 CMa	
57061	τ (30) CMa	
58343	......	There may be stellar emission of low intensity near the K line.
58350	η CMa	D2 may be blended with *C* II.
58715	β CMi	
62623	l Pup	
63462	o Pup	
66811	ζ Pup	
68980	r Pup	
74575	α Pyx	Lines of terrestrial water-vapor are present and may interfere with the measurement of the D lines.
83953	I Hya	
87737	η Leo	
87901	α Leo	
91316	ρ Leo	Beals finds the K line double, the velocities of the components being −11 and +17 km/sec, respectively. The duplicity is confirmed by a high-dispersion spectrogram taken at Mount Wilson on which the measured velocities are −10 and +19 km/sec. The mean of these values, +5 km/sec, appears in Table 6. See Table 7.

NOTES TO TABLE 6—*Continued*

HD 97603	δ Leo	
100600	......	The very faint D lines may be stellar.
102647	β Leo	Broad stellar lines having very low contrast with the continuous spectrum occupy the position of the D lines. No interstellar lines are seen.
116658	α Vir	
120307	ν Cen	
120315	η UMa	
120324	μ Cen	
122980	χ Cen	
125823	a Cen	
127972, 3	η Cen	
132058	β Lup	
132200	κ Cen	
134759	ι Lib	
136298	δ Lup	
138485	ζ Lib	
138690	γ Lup	
138749	θ CrB	
143018	π Sco	
143275	δ Sco	
144217	β Sco Br	See Table 7.
144218	β Sco Fr	
144470	ω^1 Sco	
145389	ϕ Her	
145502	ν Sco	
147165	σ Sco	
147394	τ Her	
147933	ρ Oph S Br	
147934	ρ Oph N Fr	

HD 148184	χ Oph	
148688	......	The measured displacement of the D lines appears anomalous. Some gross error is feared.
149038	μ Nor	
149438	τ Sco	
149757	ζ Oph	
149881	......	The intensity of the K line (measurements by Beals and Williams) is abnormally high compared with that of the D lines; but the data on line displacements, as well as the spectral type of the star, indicate an interstellar origin of the calcium lines.
151985	μ^2 Sco	
152236	ζ^1 Sco	D3 is bright.
152408	......	D3 is bright.
154090	k Sco	
156247	U Oph	An eclipsing binary, magnitude 5.7–6.4. See Otto Struve, *Ap. J.*, **72,** 199, 1930.
160529	......	The sodium lines appear double, the probable explanation being that the component toward the red is interstellar, while that toward the violet, which is less intense, is caused by stellar absorption displaced as in P Cygni. The measured displacement of the interstellar line should be used with caution.
160762	ι Her	D2 may be blended with *C* II.
161912	ι^2 Sco	
164284	66 Oph	
164353	67 Oph	
164492	......	In the Trifid nebula. See note in *Mt. W. Contr.*, No. 569; *Ap. J.*, **86,** 28, 1937.
164794	9 Sgr	In M8. See note in *Mt. W. Contr.*, No. 569.
N Sgr 1936	......	Observed on October 8, 1936.
166182	......	Although the spectral class is B2, the K line may be partly stellar. D2 is probably blended with *C* II.
N Her 1934	......	For measurements of the calcium velocity, see *Pub. A.S.P.*, **47,** 208, 1935. The interstellar D lines were observed only before the development of component II. See *Mt. W. Contr.*, No. 530; *Ap. J.*, **82,** 413, 1935.
166937	μ Sgr	
175191	σ Sgr	
177756	λ Aql	

NOTES TO TABLE 6—*Continued*

HD 180163	η Lyr	D2 probably blended with *C* II.
184915	κ Aql	
190429	......	Both components of the double star ADS 13312. Magnitudes from ADS.
227611	......	Spectrum nearly continuous.
......	......	20^h2^m2, $+35°31'$, 8.0, B0, BD $+35°3955$. βGC 9916F. Magnitude from BD.
......	......	20^h2^m2, $+35°29'$, 8.9, B5, BD $+35°3956$. βGC 9919D. Magnitude from BD.
191566, 7	......	Both components of the double star ADS 13429. Magnitudes from ADS.
192103	......	Not reliable.
193237	P Cyg	
194279	......	In NGC 6910. Possibly a c star.
195810	ϵ Del	
197345	α Cyg	The D lines are believed to be chiefly interstellar, the superposed star lines probably supplying not more than 20 per cent of the total intensity. See note on page 278. The equivalent widths in Table 6 are our estimates for the interstellar lines.
198183	λ Cyg	
198478	55 Cyg	
200120	f^1 Cyg	
202850	σ Cyg	
202904	υ Cyg	
203025	......	Barnard found this star to be involved in nebulosity.
203064	A Cyg	See Table 7.
206165	9 Cep	
206773	......	D3 has emission on both edges.
207260	ν Cep	
207757	......	BD$+11°4673$. See *Mt. W. Contr.*, Nos. 381, 450; *Ap. J.*, **69**, 330, 1929; **75**, 413, 1932. The D lines may be stellar.
210352	......	Both components of the double star ADS 15660. Magnitudes from ADS.
210839	λ Cep	See Table 7.

N Lac 1936	......	Calcium observed between June 18 and July 4, 1936. Sodium observed between June 20 and June 30, 1936. See Table 7.
HD 212571	π Aqr	
214167	8 Lac S Fr	
214168	8 Lac N Br	
214680	10 Lac	
221253	AR Cas	
223385	......	Boss 6111.
223987	......	This may be a c star.
224151	......	Boss 6142. See *Mt. W. Contr.*, Nos. 535, 536; *Ap. J.*, **83**, 121, 126, 1936.
224424	......	The relatively low intensity of the continuous spectrum toward the violet confirms the large color excess found by Stebbins and his associates (unpublished).
224572	σ Cas	The surprisingly high intensity of the D lines needs confirmation.

In Table 7 are collected all measurements of displacements of interstellar D lines made at other observatories that have come to our attention. The general agreement between these values and those determined at Mount Wilson is good.

TABLE 7

DISPLACEMENTS OF INTERSTELLAR D LINES MEASURED AT OTHER OBSERVATORIES

HD	Star	Other Obs.	Mt. W.	Ref.
		km/sec	km/sec	
5394	γ Cas	−1	−3 B	2
23180	o Per	+12	....	2
24398	ζ Per	(+23)*	+12 A	2
24912	ξ Per	+13	+10 A	3
30614	9(α) Cam	−1	....	3
30836	π^4 Ori	†	+21 C	2
36486	δ Ori	+18	....	1
36861	λ Ori	+17	+20 C	3
37043	ι Ori	+24	....	3
37128	ϵ Ori	+18	+20 A	4
37742	ζ Ori	+17	+18 B	4
47839	S Mon	+11	+16 A	3
91316	ρ Leo	{−4	+6 B	2
		{−1	....	4
144217	β Sco	−9	−13 B	1
203064	A Cyg	−17	−16 B	3
210839	λ Cep	−16	−15 B	3
....	N Lac 1936	{−9	−10 A	5
		{−9	....	6

* Considered stellar by Miss Heger.

† Miss Heger states that "the D lines unquestionably oscillate but there is not sufficient evidence to show whether or not their amplitude is less than that of the other lines."

1. M. L. Heger, *Lick Obs. Bull.*, **10**, 59, 1919.
2. *Ibid.*, p. 141, 1921.
3. J. S. Plaskett, *Pub. Dom. Ap. Obs.*, **2**, 287, 1924.
4. C. S. Beals, *M.N.*, **96**, 661, 1936.
5. J. A. Pearce, *Pub. A.A.S.*, **8**, 250, 1936.
6. N. T. Bobrovnikoff, *Contr. Perkins Obs.*, No. 6, p. 29, 1937.

Table 8 lists all stars for which the measured intensity of 0.5 (D2 + D1) or of λ 6284 exceeds 0.80 A, and in addition 7 bright stars selected because the detached lines in their spectra are unusually intense for the apparent magnitude. These are strategic objects to observe in a search for additional interstellar lines.

TABLE 8

STARS WITH STRONG INTERSTELLAR LINES

HD	Star	R.A. 1900	Dec. 1900	Mag.	Spec.	l	b	Intensity K*	Intensity $\frac{D2+D1}{2}$	Intensity λ 6284
								E.A.	E.A.	E.A.
3940	......	0^h36^m9	$+63°45'$	7.4	cB8	90°	+2°	......	0.50	0.94
4717	......	44.2	+62 37	8.8	cA1	90	+1	......	0.98	1.16
4768	......	44.6	+59 7	8.0	cB3	91	−3	......	0.82	0.78
4841	......	45.4	+63 14	7.1	cB5	90	+1	......	0.68	0.97
9105	......	1 24.6	+62 51	7.5	cB5(e)	95	+1	......	0.89	1.00
12953	......	2 1.7	+57 57	5.9	cA2ea	101	−2	......	0.85	0.65
13476	......	6.6	+58 6	6.5	cA0	101	−2	......	1.00	0.81
13744	......	8.9	+57 50	7.8	cA0	102	−2	......	0.90	0.78
13745	......	8.9	+55 32	8.0	B1n	102	−4	......	0.81	0.65
13841	......	9.8	+56 34	7.2	cB2	102	−3	0.72	0.96	0.60
13854	......	9.9	+56 36	6.4	cB1ea	102	−3	0.75	0.82	0.62
14010	......	11.1	+63 58	7.0	cB8	100	+4	......	0.87	0.85
14134	......	12.1	+56 40	6.7	cB3ea	102	−3	0.80	0.87	0.58
14143	......	12.2	+56 43	6.7	cB1	102	−3	0.91	1.10	0.94
14433	......	14.8	+56 47	6.5	cA2	103	−3	......	0.81	0.88
14535	......	15.8	+56 47	7.5	cA2	103	−3	......	0.97	0.99
14542	......	15.9	+56 56	7.0	cB9	103	−3	......	0.98	0.78
14947	......	19.5	+58 25	8.0	O5f	103	−1	......	0.66	0.84
15316	......	22.8	+57 22	7.3	cA2	104	−2	......	1.08	0.96
15497	......	24.6	+57 15	7.2	cB7	104	−2	......	1.44	1.38
15785	......	27.2	+60 6	8.4	B2±	103	+1	......	0.75	0.82
16778	......	36.3	+59 24	7.7	cB9	104	+1	......	0.85	0.88
20041	......	3 8.2	+56 45	5.9	cA0	109	+1	......	0.61	0.87
21389	......	21.9	+58 32	4.8	cA0ea	110	+3	......	0.70	1.00
39970	......	5 50.9	+24 14	6.0	cB9	153	+1	......	0.46	0.92
43384	......	6 10.8	+23 46	6.3	cB3	156	+5	0.50	0.54	0.88
43836	......	13.3	+23 19	7.0	B9	156	+5	......	0.47	0.86
152236	ζ^1 Sco	16 47.0	−42 12	4.9	cB1eq	311	0	......	0.73	1.02
160529	......	17 35.3	−33 27	6.7	cA4ea	323	−3	......	0.85	1.36
165784	......	18 2.6	−21 28	6.6	cA2	337	−2	......	0.63	0.84
169454	......	19.6	−14 2	6.8	cB0e	345	−2	0.60	0.76	1.00
183143	......	19 23.0	+18 5	6.9	cB9ea	21	−1	......	0.68	1.88
190603	......	20 0.7	+31 56	5.7	cB0eβ	37	0	0.39	0.68	1.02
227611	......	2.0	+35 37	9.5	Bne	40	+1	0.40	0.81	......
227836	......	4.3	+35 50	10.9	B2e	41	+1	(0.46)	1.43	......
193793	......	17.1	+43 32	6.8	Oa	49	+3	0.49	0.70	0.84
194279	......	19.7	+40 26	7.0	B0	46	+1	0.78	0.76	0.94
207260	ν Cep	21 42.6	+60 40	4.5	cA2	70	+6	......	0.82	0.88
207673	......	45.6	+40 40	6.5	cA0	58	−10	......	0.85	0.56
212455	......	22 19.3	+54 44	8.4	cB3	71	−2	1.35	0.96	0.78

* The intensities of the K line are from measurements by Beals, Williams, and Sanford.

TABLE 8—*Continued*

HD	Star	R.A. 1900	Dec. 1900	Mag.	Spec.	l	b	Intensity		
								K*	$\frac{D2+D1}{2}$	λ 6284
								E.A.	E.A.	E.A.
223385	....	$23^h44^m.0$	+61°40′	5.6	cA2eα	83°	0°	......	1.27	1.15
223960	....	48.9	+60 18	7.0	cA0eα	84	−1	......	1.27	0.94
223987	....	49.2	+61 3	7.6	B0	84	0	0.68	0.89	0.80
224055	....	49.7	+61 17	7.2	cB3eα	84	0	.85	0.99	1.00
225146	....	58.8	+60 33	8.6	B0	85	−1	0.95	1.03	1.14
225160	....	58.9	+61 40	8.6	O8eα	85	0	......	0.82	0.68

Supplementary List of Bright Stars

HD	Star	R.A. 1900	Dec. 1900	Mag.	Spec.	l	b	K*	$\frac{D2+D1}{2}$	λ 6284
								E.A.	E.A.	E.A.
2905	κ Cas	$0^h27^m.3$	+62°23′	4.2	cB0eα	89°	0°	0.31	0.53	0.49
21291	....	3 21.0	+59 36	4.4	cB9	109	+4	......	.54	.48
36371	χ Aur	5 26.2	+32 7	4.9	cB3	144	+1	.46	.40	.64
41117	χ^2 Ori	5 58.0	+20 8	4.7	cB1eα	157	+1	.42	.41	.62
147165	σ Sco	16 15.1	−25 21	3.1	B1	319	+16	......	.18	.41
198478	55 Cyg	20 45.5	+45 45	4.9	cB2eα	53	+1	.50	.42	.40
225094	....	23 58.3	+63 5	6.3	cB2eα	85	+1	0.67	0.64	0.64

Carnegie Institution of Washington
Mount Wilson Observatory
June 1937

THE SPECTRUM OF H_2 FROM λ 4225 TO λ 4756

NORTON A. KENT AND REGINALD G. LACOUNT

ABSTRACT

The wave-lengths of 435 lines of H_2 have been measured on plates taken with a 21-foot concave grating at the California Institute of Technology. The results have been compared with the measurements by Gale, Monk, and Lee, and by Finkelnburg.

This paper is a continuation of data given in a previous paper.[1] The apparatus employed was the same as that described therein, and the wave-lengths were determined in a similar manner.

In Table 1, λ is the integer value of the wave-length in Ångstroms; F, Finkelnburg's fractional value; G, that obtained by Gale, Monk, and Lee; L, the Lacount[2] interferometer value; M_w, the writers' weighted mean determination; N, the number of "sets" of measurements entering into the calculation of M_w; PE, the probable error of the weighted mean, M_w; and ν, the "vacuum" wave-number[3] in m^{-1} obtained from M_w or from L, when the latter is present; b indicates that the line was broad; d, that the line was double and that the setting was made on the center of gravity; v, that there existed a weak, unresolved line on the violet side of the line measured.

With the interferometrically determined wave-lengths, L, the grating determinations, M_w (shown in parentheses and based on the iron standards), are listed for comparison. The maximum deviation of M_w from L is 0.006 A, the average, 0.003 A. The Gale, Monk, and Lee interferometer determinations are marked by an asterisk in column G of the Table. The average probable error of the mean for the values of M_w for the 435 lines listed is 0.001 A.

The writers' values agree, in general, more closely with those of Gale. The average difference between G and M_w, without regard to sign, is 0.008 A; that between F and M_w, 0.014 A.

A comparison of the 12 interferometer values, L, with M_w reveals

[1] *Ap. J.*, **84**, 585, 1936.

[2] Obtained by Lacount with the same apparatus as that described in the article by Kent and Lacount, *Phys. Rev.*, **51**, 241, 1937.

[3] Calculated from Kayser's table.

TABLE 1

λ	*F*	*G*	*I*	*L*	M_w	*N*	*PE*	ν
4225	...	546	0	...	551	1	...	2365891
26	790	736	0	...	752	1	...	2365219
27	355	377	2	...	386	2	001	2364864
28	860	812	1	...	830	1	...	2364057
30	998	(31)002	1	...	(31)016	1	...	2363394
32	683	670	2	...	682	2	002	2361905
32	925	892	1	...	899	2	001	2361784
33	408	407	4	...	416	2	002	2361514
33	893	818	3	...	824	3	002	2361268
37	...	545	1	...	565	2	001	2359184
37	907	...	2	...	(38)033	1	...	2358923
42	476	470	0	...	473	1	...	2356452
43	129	125	1	...	139	4	002	2356085
43	348	326	2	...	338	5	001	2355974
46	672	691	2	...	705	2	001	2354106
46	997	988	0	...	(47)002	1	...	2353942
53	301	289	3	...	301	4	001	2350456
54	040	029	1	...	046	3	001	2350044
55	267	221	0	...	224	1	...	2349394
60	...	343	0	...	337	1	...	2346574
61	...	668	1	...	682	1	...	2345833
62	794	778	1	...	790	2	003	2345224
65	146	162	1	...	179	2	002	2343910
67	902	906	1	...	935	1	...	2342397
77	475	480	1	...	474	4	003	2337173
79	387	416	2	...	420	4	001	2336110
80	724	740	1	...	756	3	002	2335381
81	814	816	1	...	818	2	002	2334802
86	068	035	0	...	043	1	...	2332501
87	570	613	0	...	611	1	...	2331647
89	637	641	3	...	643	2	001	2330543
90	099	114	2	...	116	4	001	2330286
95	425	423	1	...	431	5	000	2327403
95	667	637	1	...	648	2	002	2327285
98	034	027	0	...	008	1	...	2326007
4303	437	423	4	...	429	6	000	2323077
03	849	877	3	...	*{889	1	...	2322829
03	944	967	1	...	973	1	...	2322784
05	577	...	1	...	458	1	...	2321982
05	822	818	1	...	826	2	000	2321784
06	273	276	3	282	(283	3	002)	2321538
07	...	495	0	...	513	1	...	2320875
08	618	635	2	...	637	3	002	2320269
11	715	701	1	...	716	5	001	2318612
12	364	394	0	...	401	2	001	2318244
12	924	873	2	...	883	2	002	2317985
17	203	...	3	...	b317	1	...	2315605
18	012	004	1	...	002	4	002	2315238
18	261	220	2	...	225	4	001	2315117
27	360	362	1	...	368	2	002	2310226
27	939	927	5	934	(931	4	002)	2309924

* Doublet just resolved in one case. Four others show an unresolved doublet with maximum density at 0.921 ($PE=0.002$).

TABLE 1—*Continued*

λ	*F*	*G*	*I*	*L*	M_w	*N*	*PE*	ν
4329	662	644	1	......	661	1	....	2309003
30	167	....	00	......	275	1	....	2308675
30	406	401	1	......	405	1	....	2308608
31	389	375	0	......	382	1	....	2308085
32	628	619	3	......	620	6	001	2307426
34	662	697	0	......	672	1	....	2306334
35	532	519	3	......	524	6	001	2305880
36	304	309	1	......	324	2	001	2305455
39	538	534	1	......	554	1	....	2303739
39	845	817	1	......	835	1	....	2303590
40	466	470	Hγ	......	466	4	001	....
43	....	600	1	......	607	1	....	2301589
46	643	661	1	......	671	1	....	2299967
47	609	....	00	......	500	2	002	2299528
52	182	119	0	......	183	1	....	2297054
53	427	412	1	......	422	3	002	2296400
54	498	540	3	544	(541	2	001)	2295808
58	344	....	3	......	334	2	001	2293812
61	937	915	0	......	931	3	002	2291921
63	452	....	2	......	b609	1	....	2291039
66	674	650	1	......	670	1	....	2289433
67	709	726	1	......	738	2	001	2288873
68	216	....	1	......	251	3	001	2288605
70	289	278	0	......	285	3	001	2287539
70	771	766	2	......	772	4	002	2287385
71	002	990	1	......	(72)000	3	002	2286642
77	684	....	2	......	677	1	....	2283677
79	397	403	4	......	402	4	001	2282778
79	961	955	1	......	963	3	002	2282486
82	194	181	1	......	191	3	002	2281325
83	....	494	2	......	497	2	001	2280645
84	....	193	1	......	189	1	....	2280285
84	443	456	1	......	455	1	....	2280147
86	261	249	1	......	260	3	000	2279208
87	343	285	1	......	298	1	....	2278669
88	878	888	1	......	897	1	....	2277839
89	095	084	3	......	091	4	001	2277738
89	461	452	0	......	458	1	....	2277548
90	899	900	4	......	905	4	002	2276797
91	738	726	1	......	742	4	001	2276363
92	101	093	2	......	100	3	002	2276178
92	930	891	1	......	900	2	004	2275763
94	337	346	1	......	347	1	....	2275014
94	769	753	00	......	783	2	000	2274788
96	905	893	0	......	902	1	....	2273692
98	091	081	1	......	093	3	001	2273076
98	242	239	1	......	246	3	004	2272997
99	669	662	1	......	671	1	....	2272261
4400	....	830	3	......	d803	2	001	2271677
01	....	094	0	......	090	2	001	2271528
01	402	406	0	......	412	1	....	2271362
01	651	645	0	......	659	1	....	2271235
02	470	462	0	......	477	1	....	2270813

TABLE 1—*Continued*

λ	F	G	I	L	M_w	N	PE	ν
4403	639	625	1	......	637	1	......	2270215
04	184	165	1	......	171	2	001	2269938
04	......	607	2	......	615	2	003	2269711
10	487	478	2	......	496	3	001	2266685
10	650	618	3	......	628	3	001	2266617
12	252	253†	8	......	256	7	002	2265780
12	472	484	2	......	484	5	001	2265663
13	505	499	2	......	500	3	002	2265141
14	209	218	4	......	217	5	002	2264773
14	553	536	1	......	526	1	......	2264615
14	......	994	3	......	v997	3	002	2264374
16	220	217	2	......	226	4	001	2263743
16	485	480	1	......	477	2	003	2263615
17	338	342	5	......	337	6	001	2263174
18	665	673	1	......	671	5	001	2262490
19	490	494	4	......	493	5	000	2262070
19	838	818	1	......	833	3	001	2261896
20	306	304	4	......	300	6	000	2261657
20	928	915	1	......	920	2	001	2261340
21	186	163	2	......	168	2	001	2261213
22	631	647	1	......	655	3	001	2260453
22	......	772	1	......	785	1	......	2260386
22	989	988	2	......	991	2	002	2260281
23	253	248	3	......	252	5	001	2260148
24	936	......	00	......	924	1	......	2259294
25	150	151	2	......	154	2	003	2259176
25	900	895	2	......	902	5	001	2258794
26	109	108	0	......	115	2	001	2258686
27	738	750	0	......	749	3	002	2257852
28	076	050	00	......	082	1	......	2257682
28	787	792	1	......	782	1	......	2257326
29	560	......	00	......	556	1	......	2256931
31	......	378	1	......	......	......	......	......
31	411	......	1	......	d453	2	001	2255965
31	......	494	1	......	......	......	......	......
32	361	362	1	......	350	1	......	2255508
33	066	......	00	......	054	1	......	2255150
33	826	876	1	......	894	2	002	2254723
34	278	278	1	......	271	2	001	2254531
34	574	573	1	......	572	2	001	2254378
34	981	991	2	......	985	3	000	2254168
35	878	885	1	......	888	2	001	2253709
36	192	205	00	......	188	1	......	2253557
37	653	643	0	......	647	2	001	2252816
38	217	206	3	......	205	2	001	2252533
38	637	629	2	......	636	3	002	2252314
39	427	429	1	......	423	2	002	2251915
41	419	404	2	......	416	2	001	2250904
42	875	852	2	......	857	3	004	2250174
44	220	213	3	......	220	6	001	2249484
45	245	246	7	......	246	5	001	2248965
45	636	634	1	......	627	1	......	2248772

† Measured with the interferometer.

TABLE 1—*Continued*

λ	*F*	*G*	*I*	*L*	M_w	*N*	*PE*	ν
4446	813	815	0	......	824	2	001	2248167
47	550	553	9	......	v555	5	004	2247797
47	928	932	6	......	931	4	001	2247607
49	379	....	00	......	367	2	000	2246882
49	512	502	0	......	514	2	004	2246808
49	919	913	6	......	918	6	001	2246604
50	349	350	0	......	351	2	001	2246385
50	817	816	5	......	828	3	001	2246144
51	357	346	1	......	350	3	002	2245882
52	119	097	0	......	115	2	001	2245495
52	503	482	0	......	497	2	001	2245303
52	775	767	3	......	776	3	001	2245162
53	160	141	3	......	158	6	002	2244970
55	451	461	0	......	487	2	002	2243796
55	664	666	2	......	686	3	003	2243696
55	959	955	2	......	957	2	002	2243559
56	....	548	1	......	581	1	....	2243240
56	650	665	3	......	650	2	006	2243211
56	872	851	4	......	855	4	001	2243107
57	044	030	3	......	037	2	005	2243016
57	568	577	1	......	577	2	002	2242744
58	332	295	1	......	304	2	001	2242378
58	....	732	3	......	....	....	....	....
58	779	....	3	......	750	2	000	2242154
58	....	859	3	......	876	2	000	2242091
59	....	118	2	......	133	3	000	2241961
59	464	464	1	......	460	2	002	2241797
60	189	190	0	......	177	4	002	2241437
60	971	965†	10	967	(963	4	000)	2241042
61	989	914	1	......	909	2	002	2240567
63	870	876	1	......	870	3	001	2239582
64	235	221	2	......	223	3	002	2239405
64	....	352	1	......	347	1	....	2239343
67	141	145	8	......	144	8	001	2237941
67	716	748	0	......	729	1	....	2237648
68	299	280	2	......	285	2	001	2237369
69	563	544	0	......	556	2	001	2236733
70	729	715	1	......	700	1	....	2236161
71	....	516	2	......	517	3	001	2235752
71	574	....	....	......	....	....	....	....
71	....	608	1	......	612	3	002	2235705
71	953	961	3	......	956	4	002	2235533
74	269	261	6	......	258	5	002	2234383
76	379	329	1	......	338	2	002	2233344
77	073	071	5	......	074	5	002	2232977
77	836	823	1	......	825	1	....	2232603
77	997	....	00	......	985	2	001	2232523
78	981	987	3	......	987	4	002	2232023
79	343	393	1	......	389	1	....	2231823
79	....	692	2	......	694	2	000	2231671
81	272	263	2	......	261	2	001	2230891
81	919	919	1	......	906	2	001	2230570
82	....	075	1	......	083	2	003	2230481

TABLE 1—*Continued*

λ	F	G	I	L	M_w	N	PE	ν
4482	......	253	0	......	251	2	000	2230398
85	873	832	2	......	842	2	001	2228613
86	094	084	8	......	084	6	001	2228492
87	145	103	0	......	109	1	......	2227983
87	824	813	4	......	816	8	001	2227632
88	574	548	1	......	549	2	000	2227269
89	214	234	1	......	248	2	002	2226922
90	458	451†	9	453	(450	2	000)	2226325
90	864	852	1	......	850	2	001	2226127
91	741	738	0	......	736	2	003	2225688
91	937	975	1	......	969	1	......	2225572
93	693	688	5	......	692	7	002	2224720
95	310	313	1	......	323	2	002	2223913
96	666	672	1	......	679	3	003	2223242
97	096	101	3	......	114	2	000	2223027
97	569	577	3	......	580	3	003	2222797
98	108	108†	10	......	106	7	001	2222537
98	523	523	4	......	523	8	001	2222330
99	198	204	00	......	206	1	......	2221993
99	548	554	2	......	555	4	002	2221821
4500	046	050	1	......	053	2	003	2221575
01	595	597	1	......	602	2	000	2220811
01	960	960	6	......	959	4	001	2220635
02	598	600	2	......	614	2	000	2220311
02	736	743	2	......	745	2	000	2220247
04	464	467	2	......	476	3	002	2219394
04	928	916	1	......	927	4	002	2219172
05	635	631	6	......	631	4	003	2218825
09	076	103	2	......	111	2	000	2217112
10	898	904	5	......	905	3	005	2216230
11	......	332	1	......	360	1	......	2216007
11	705	690	4	......	696	4	004	2215842
11	857	888	0	......	892	1	......	2215746
12	876	871	1	......	870	3	004	2215266
13	837	828	3	......	828	2	002	2214795
14	319	313	3	......	322	2	001	2214553
15	166	182	2	......	192	2	000	2214126
15	579	562	3	......	568	4	002	2213942
17	424	428	3	......	434	3	001	2213028
17	......	722	1	......	732	1	......	2212882
17	887	898	2	......	904	2	001	2212797
19	142	122	3	......	134	2	001	2212195
19	969	959	3	......	965	2	001	2211788
21	......	417	3	......	......	......	......	......
21	464	......	4	......	b456	4	002	2211059
21	......	488	3	......	......	......	......	......
22	323	314	0	......	316	2	002	2210638
22	830	872	1	......	882	1	......	2210362
22	987	960	1	......	975	1	......	2210316
23	184	193	2	......	195	3	001	2210209
24	149	139	7	145	(139	1	.....)	2209745
24	958	883	1	......	897	1	......	2209377
27	136	183	3	......	175	4	002	2208266

TABLE 1—*Continued*

λ	F	G	I	L	M_w	N	PE	ν
4529	085	079	5	......	076	3	003	2207339
29	246	266	2	......	272	2	000	2207243
30	972	890	1	......	901	1	....	2206450
31	190	193	3	......	198	2	002	2206305
31	953	947	1	......	956	2	001	2205936
33	....	055	5	......	b097	1	....	2205381
33	153	128	4	......	b124	1	....	2205368
34	151	157	7	......	158	4	001	2204865
34	464	468	1	......	472	1	....	2204713
34	620	627	6	......	627	4	001	2204637
35	902	906	2	......	904	2	001	2204016
37	755	731	4	......	745	2	001	2203122
37	904	880	2	......	899	2	003	2203048
38	314	311	2	......	310	3	001	2202848
39	163	162	5	......	169	3	001	2202431
41	114	118	2	......	121	2	001	2201484
42	928	954	1	......	959	1	....	2200594
43	702	692	5	......	691	4	001	2200239
45	455	....	00	......	489	1	....	2199369
47	232	234	1	......	246	1	....	2198519
47	946	967	5	......	966	2	000	2198171
49	906	896	3	......	896	5	001	2197237
50	992	983	5	......	980	5	001	2196715
51	411	378	1	......	376	2	002	2196524
51	712	724	3	......	714	4	001	2196361
52	424	423	2	......	426	3	003	2196017
52	624	....	00	......	630	1	....	2195919
54	164	158†	10	......	160	3	000	2195181
57	125	125	4	......	135	4	002	2193748
57	417	393	5	......	401	3	001	2193620
58	312	318	4	......	322	5	001	2193177
58	610	606	4	......	612	5	001	2193037
58	837	837	1	......	846	1	....	2192925
59	068	....	1	......	123	1	....	2192792
60	192	206	2	......	217	2	001	2192266
60	650	594	0	......	599	1	....	2192082
61	128	148	1	......	147	3	002	2191819
62	228	222	4	......	227	5	001	2191300
62	....	453	1	......	451	2	006	2191192
63	732	728	3	......	736	4	001	2190575
64	713	690	1	......	704	1	....	2190111
64	948	909	0	......	932	1	....	2190001
65	577	544	3	......	555	2	001	2189703
67	759	753	0	......	778	2	002	2188637
68	133	130†	10	......	131	6	001	2188467
68	616	617	1	......	620	3	001	2188233
72	235	225	2	......	229	5	001	2186506
72	720	710†	8	......	712	6	002	2186275
75	880	878	8	......	880	4	001	2184762
76	559	535	1	......	551	2	003	2184441
76	733	732	1h	......	735	1	....	2184354
78	023	015	6	......	016	5	001	2183742
78	536	558	1	......	574	2	001	2183476

TABLE 1—*Continued*

λ	*F*	*G*	*I*	*L*	M_w	*N*	*PE*	ν
4579	462	454	5	......	458	4	002	2183055
79	996	994†	10	994	(993	4	003)	2182799
81	546	538	4	......	539	4	001	2182063
82	596	592†	10	594	(594	4	002)	2181561
83	902	880	2	......	890	3	001	2180944
84	487	499	5	......	501	5	001	2180653
88	680	678	3	......	680	4	002	2178668
89	916	....	0	......	935	1	....	2178072
90	205	....	0	......	212	1	....	2177940
91	835	806	2	......	813	3	002	2177181
93	581	579	0	......	596	2	003	2176336
94	752	740	0	......	753	1	....	2175788
95	136	166	1	......	169	2	001	2175591
96	854	....	00	......	873	1	....	2174785
97	216	206	4	......	209	4	001	2174626
98	495	493	3	......	496	4	001	2174017
4600	853	856	1	......	870	2	001	2172895
05	377	364	2	......	364	2	001	2170775
07	....	091	1	......	096	2	004	2169959
07	417	403	4	......	409	4	001	2169811
13	122	116	4	......	118	3	003	2167126
14	580	588	3	......	591	4	003	2166434
16	496	488	00	......	505	2	001	2165536
17	524	528	10	......	528	4	001	2165056
18	....	126	1	......	138	3	001	2164770
18	304	304	5	......	310	5	001	2164690
18	659	600	2	......	598	3	001	2164554
20	747	756	5	......	758	4	002	2163543
22	735	....	00	......	758	1	....	2162700
24	092	097	1	......	103	2	002	2161978
25	315	311	5	......	‡{319	5	002	2161410
25	....	584	3	......	593	5	002	2161381
27	984	986†	10	......	988	4	002	2160163
28	732	708	1	......	716	2	002	2159823
29	703	673	2	......	689	2	000	2159369
30	125	127	1	......	144	1	....	2159157
31	069	074	1	......	103	2	003	2158710
31	466	460	8	......	469	5	001	2158539
31	847	849	9	......	850	5	002	2158362
33	....	693	0	......	§695	2	001	2157502
34	030	032†	10	031	(035	3	002)	2157346
34	594	595	5	......	604	3	001	2157079
34	....	708	2	......	718	1	....	2157026
38	491	465	1	......	500	1	....	2155268
39	891	898	1	......	895	2	001	2154620
40	480	478	1	......	492	1	....	2154343
42	675	668	1	......	692	1	....	2153322
43	844	850	1	......	883	1	....	2152771
45	352	344	3	......	349	4	001	2152090
48	592	585	1h	......	576	1	....	2150596

‡ Faint broad line bridges region between.

§ Broad, and interferes somewhat with 4634.035.

TABLE 1—*Continued*

λ	F	G	I	L	M_w	N	PE	ν
4649	315	273	0	......	284	1	....	2150269
49	512	502	1	......	516	3	001	2150161
50	377	381	1	......	389	3	001	2149758
50	929	950	0	......	965	3	001	2149491
51	519	505	1	......	513	2	001	2149238
52	997	999†	6	......	(53)007	5	001	2148548
53	188	196	2	......	204	4	001	2148457
54	064	056	3	......	057	3	002	2148064
57	861	861	2	......	861	2	000	2146309
58	790	784	1	......	790	2	002	2145881
60	100	099	1	......	b114	3	003	2145272
60	390	395	5	......	402	5	002	2145139
61	391	402	8	......	402	4	002	2144679
62	812	811†	8	810	(816	2	003)	2144031
64	617	634	1	......	644	2	001	2143188
65	595	585	6	......	587	4	001	2142755
65	....	770	00	......	778	1	....	2142664
67	080	083	3	......	090	2	001	2142165
67	796	791	4	......	801	4	002	2141739
69	275	278	3	......	287	2	001	2141057
69	976	(70)015	2	......	(70)020	2	004	2140721
70	....	652	4	......	658	3	001	2140429
70	847	808	0	......	811	2	000	2140359
71	301	305†	7	308	(309	2	003)	2140131
71	710	710	1	......	718	2	000	2139943
72	090	080	1	......	097	1	....	2139769
73	095	097	3	......	106	2	005	2139307
73	....	233	1	......	236	2	001	2139247
74	....	530	4	......	v517	3	002	2138662
74	960	958	7	......	967	4	001	2138456
75	309	312	4	......	312	4	001	2138298
79	093	092	5	......	093	4	002	2136570
80	....	432	5	......	429	3	003	2135960
81	354	354	2	......	364	3	001	2135534
82	341	341	6	......	348	5	001	2135085
83	653	640	1	......	653	3	003	2134490
83	830	824†	8	......	830	5	001	2134409
84	650	654	4	......	656	4	001	2134033
86	145	142	3	......	143	4	002	2133355
86	774	772	6	......	784	4	003	2133065
88	439	438	2	......	442	4	002	2132310
90	180	184	7	......	185	5	001	2131518
92	040	040	5	......	048	3	001	2130671
99	787	832	1	......	851	1	....	2127134
4701	723	723	2	......	729	3	000	2126284
02	581	562	5	......	574	4	002	2125902
05	262	260	3	......	251	1	....	2124693
08	502	489	2	......	500	2	002	2123226
09	535	536†	10	538	(538	2	004)	2122759
11	064	067	3	......	064	3	001	2122071
13	922	930	6	......	929	4	002	2120781
14	357	308	1	......	330	2	001	2120601
18	836	810	1	......	838	3	002	2118575

TABLE 1—*Continued*

λ	F	G	I	L	M_w	N	PE	ν
4719	039	043†	10	......	043	5	001	2118483
19	......	300	1	......	289	3	001	2118372
21	003	000	1	......	003	2	000	2117603
21	539	542	3	......	548	3	003	2117359
23	041	032†	10	......	035	4	002	2116692
23	850	838	1	......	847	3	000	2116328
24	828	820	4	......	827	4	002	2115889
26	149	144	1	......	157	2	002	2115294
27	......	741	1	......	755	1	......	2114579
28	900	887	1	......	912	2	005	2114062
30	759	754	2	......	764	3	002	2113234
32	727	725	2	......	733	2	004	2112355
38	762	707	1	......	698	1	......	2109696
40	992	985†	5	......	985	4	002	2108679
42	094	109	3	......	114	4	002	2108176
42	780	780	6	......	781	5	002	2107880
43	391	383	5	......	385	4	002	2107612
45	323	314	2	......	313	2	005	2106755
46	042	968	1	......	(45)977	2	007	2106460
50	......	729	1	......	733	3	001	2104352
51	581	575	2	......	578	2	003	2103978
55	376	405	2	......	403	2	002	2102285
56	107	097	0	......	097	1	......	2101979
56	......	948	5	......	946	3	004	2101603

that the sum of the positive values of $L - M_w$ is 0.020 A and that the sum of the negative is 0.012 A, showing an average deviation of 0.003 and 0.002 A, respectively, which indicates an approximately random distribution of differences. For $L-G$ the sums are $+0.034$ and -0.002 A; for $L - F$, $+0.066$ and -0.024 A.

It is the writers' intention to publish the wave-lengths of lines in other regions as soon as possible.

Grateful acknowledgment is made to Dr. G. H. Dieke, who, while in California, assisted the senior writer materially in the long exposures necessary; to Dr. W. Uyterhoeven for a brief continuation of the work after the senior writer's departure; to numerous Boston University students who have assisted in the computations; to the Rumford Committee of the American Academy of Arts and Sciences for its generous financial assistance; and to the Elizabeth Thompson Science Fund for the loan of a calculating machine.

CALIFORNIA INSTITUTE OF TECHNOLOGY, 1927
AND
BOSTON UNIVERSITY
June 1937

PHOTOCHEMISTRY OF PLANETARY ATMOSPHERES

RUPERT WILDT

ABSTRACT

All polyatomic molecules detected in planetary atmospheres are highly sensitive to ultraviolet solar radiation. Their photochemical decomposition must be followed by secondary chemical reactions, reuniting the products of dissociation, in order to maintain the observed stationary composition of the atmospheres. The stability of methane and carbon dioxide is reasonably accounted for, but that of ammonia remains unexplained at present. The existence of methane and the failure to detect any other hydrocarbon indicate the presence of plenty of hydrogen on the giant planets, and most probably there is no carbon monoxide, carbon dioxide, or hydrogen sulphide at their surfaces. Small amounts of sundry molecules, not observed so far, are certain to be formed in consequence of the photochemical processes, and eventually these compounds may be detected under favorable circumstances.

In a short note attention was called to the role photochemical processes play in planetary atmospheres, but information about the very reactions involving the main atmospheric constituents was still scanty then.[1] A more detailed discussion seems profitable now, since numerous investigations have been completed meanwhile, dealing not only with the absorption spectra of polyatomic molecules in the far ultraviolet and the corresponding photochemical dissociations but also with the secondary chemical reactions of free atoms and simple radicals. These secondary reactions are of great importance to an understanding of the net result the primary photochemical process leads to. They are difficult to predict, and the final elaboration of a net reaction scheme, fitting the experimental results, is an intricate problem of chemical kinetics, still controversial in many cases.

The principal task, from the astrophysical point of view, is to explain how a stationary state can be maintained in atmospheres containing molecules highly susceptible to photochemical decomposition by ultraviolet solar radiation, like ozone, carbon dioxide, ammonia, methane, etc. For the ozone in the earth's stratosphere this problem may be regarded as solved quantitatively, at least with respect to the order of magnitude of the stationary concentration of ozone. For the other gases mentioned and for some related com-

[1] R. Wildt, *Nature*, **134**, 418, 1934.

pounds, apparently less prominent, a qualitative solution will be attempted here. Which primary photochemical process is preponderant in a mixture of atmospheric gases depends on the energy distribution of the incident radiation and on the respective absorption coefficients, and, therefore, indirectly on the atmospheric level. For example, the decomposition of ozone by the absorption of visual solar radiation (Chappuis-bands) shifts the photochemically maintained stationary state of the stratosphere to lower ozone concentrations, compared to the hypothetical state produced by the action of ultraviolet sunlight alone. On the other hand, carbon dioxide, occurring in traces in the troposphere, is prevented from decomposing photochemically by the protective ultraviolet absorption of the vast mass of oxygen in the upper atmosphere. Evidently, careful consideration is to be given to the relative abundance of the atmospheric constituents and to their vertical distribution. The variety of secondary reactions increases greatly with the number of possible partners. For this reason the proposed reaction schemes leave room for some criticism. But the presence of atmospheric constituents not detectable by spectroscopic means may be postulated or refuted by the ensuing secondary reactions, i.e., by purely chemical arguments. It is indeed believed that the presence of a considerable amount of hydrogen in the atmospheres of the giant planets can be established in this way, which fortunately corroborates certain general cosmogonic conceptions.

In order to illustrate the photochemical efficiency of a continuous spectrum like that of sunlight, it is appropriate to express the energy density as a function of the frequency of radiation. The familiar form of the emission power of a black body

$$E_\lambda = 2\pi c^2 h \lambda^{-5} \left(e^{\frac{ch}{\lambda kT}} - 1\right)^{-1} \tag{1}$$

has to be replaced by

$$E_\nu = 2\pi \frac{h}{c^2} \nu^3 \left(e^{\frac{h\nu}{kT}} - 1\right)^{-1} . \tag{2}$$

It is easy to derive the energy maximum on the frequency scale

$$\nu_{\max} = a \cdot \frac{kT}{h} = a^* \cdot T , \tag{3}$$

where $\alpha = 2.8214$ is the root of the transcendental equation

$$\frac{\alpha}{3} + e^{-\alpha} = 1 . \qquad (4)$$

On introducing the customary wave-numbers (unit cm^{-1}), the numerical value of the constant is $\alpha^* = 1.97$ cm^{-1} $degree^{-1}$, which reveals that the maximum number of quanta of solar radiation ($T = 6000°$ K) is close to 11,820 cm^{-1}, or 8450 A. By substituting

$$\frac{h\nu}{kT} = x \text{ and } \frac{E_\nu}{2\pi} \cdot \frac{c^2h^2}{k^3T^3} = y , \qquad (5)$$

Planck's function (2) may be normalized:

$$y = \left(\frac{e^\alpha - 1}{\alpha^3}\right) \cdot \frac{x^3}{e^x - 1} . \qquad (6)$$

This normalized function is displayed by Figure 1, the abscissae being proportional to the wave-numbers and the ordinates to the number of quanta. Whether the energy distribution of solar radiation follows a black-body curve throughout the far ultraviolet cannot be ascertained, and the existence of an ultraviolet "window," situated beyond the Lyman continuum, has been much discussed recently. Nevertheless, Figure 1 illustrates two facts. On a frequency scale the Planck function has its steeper gradient on the infrared side of the energy maximum, and the number of quanta decreases rapidly throughout the range from 40,000 to 80,000 cm^{-1} for solar radiation.

To start with the gaseous elements, there is no reason to suppose that their photochemical dissociation makes any significant contribution to the chemistry of planetary atmospheres; oxygen is to be excepted from this statement and will be dealt with later. The existence of free halogen molecules can be ruled out for their great chemical affinity. The monatomic noble gases have very high ionization potentials, and even in the ionized state they seem to be chemically inert. The limiting wave-lengths of the photochemical decomposition of molecular nitrogen and hydrogen are 1370 A and 850 A, respectively. Since all planetary atmospheres are known to

contain polyatomic molecules strongly absorbing much greater wave-lengths, both hydrogen and nitrogen are probably well shielded. The best chance for the photochemical decomposition, or at least excitation, of molecular nitrogen seems to be given in the atmosphere of Mars, which should contain the smallest amount of polyatomic molecules among all planetary atmospheres, judged by

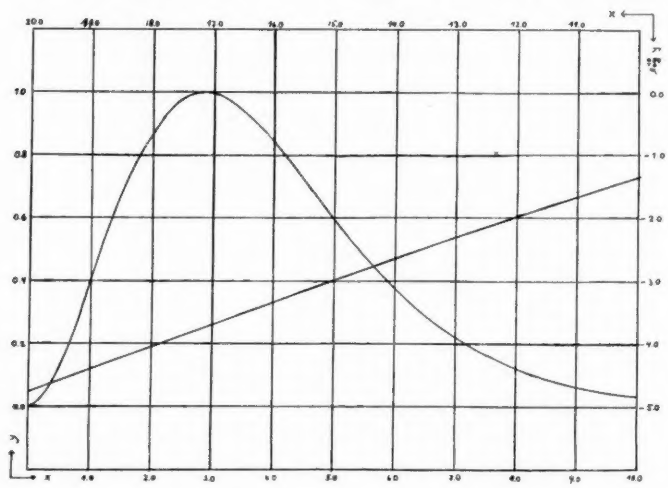

FIG. 1.—Graph of the normalized Planck function, eq. (6). The upper and the right-hand scales refer to the almost straight curve, giving $\log^{10} y$ as function of x in the range from $x = 10.0$ to $x = 20.0$. For a temperature of 6000° K, the following abscissae and wave-numbers correspond to one another:

$x = 2.39$	$N = 10{,}000\ \mathrm{cm}^{-1}$	$x = 9.45$	$N = 40{,}000\ \mathrm{cm}^{-1}$
4.77	20,000	14.32	60,000
7.16	30,000	19.00	80,000

the spectroscopic evidence. Of course, all planets are likely to be surrounded by ionospheres similar to the terrestrial one, but their masses should be exceedingly small compared with the bulk of the atmospheres. The consideration of ionospheric phenomena on other planets would go beyond the scope of this paper. But it seems worth while to point out that luminescence of an aurora-like character may also occur in the atmospheres of other planets. In the experiments made by Terenin and his collaborators,[2] the photochemical decomposition of various inorganic and organic compounds produces ex-

[2] H. Neuimin and A. Terenin, *Acta physicochemica U.S.S.R.*, **5**, 465, 1936.

cited radicals, like OH, CN, NH_2, which exhibit strong fluorescence both in the ultraviolet and the visual region.[3] It is very tempting to ascribe to atmospheric luminescence the discrepancies between the planetary diameters observed in the light of different wave-lengths. But, as long as the physiological and photographic influences affecting the planetary diameters have not been cleared up completely, every suggestion of this kind seems premature.

The photochemical decomposition of oxygen molecules yields unexcited atoms alone or 50 per cent of excited atoms, according to the wave-length employed:

$$\lambda < 1950 \text{ A}: O_2 + h\nu \rightarrow O\,(^3P) + O\,(^3P)\,,$$
$$\lambda < 1760 \text{ A}: O_2 + h\nu \rightarrow O\,(^3P) + O\,(^1D)\,.$$

In the earth's stratosphere this process is followed by partial recombination and by the formation of ozone, which subsequently decomposes, both photochemically and thermally. The terrestrial ozone equilibrium may be dismissed by referring to the most recent treatment along theoretical lines.[4] No other planetary atmosphere is known, thus far, to contain spectroscopically observable amounts of either oxygen or ozone. But it is of interest to note that in an atmosphere containing only very little oxygen, say about 5 g cm^{-2}, the ozone layer would be formed close to the ground and, therefore, might attack chemically the planetary crust. Such may have been the case on Mars, in an earlier stage of evolution. For this and other cosmochemical implications, see a paper[5] giving a more detailed discussion of oxygen and ozone in planetary atmospheres.

PHOTOCHEMISTRY OF SIMPLE HYDROCARBONS

The low-pressure bands of methane start at λ 1300, and at higher pressure they extend to a limit around λ 1450. From there to λ 850 the absorption is entirely continuous, and therefore all excited states up to the first ionization potential (approximately 15 volts) appar-

[3] Such phenomena presumably have some bearing upon the luminescence of cometary gases. The writer intends to take up the chemistry of cometary matter in a later paper.

[4] O. R. Wulf and L. S. Deming, *Terr. Magn. and Atm. El.*, **41**, 299 and 375, 1936.

[5] R. Wildt, *Nachrichten Gesell. Wiss. Göttingen* (Math. Phys. Kl. [N.F.]), **1**, 1, 1934.

ently are repulsive.[6] The low-pressure absorption of ethane consists of extremely diffuse bands starting at λ 1350 and going down below λ 1000. With increase in pressure the limit moves to λ 1500 or even to λ 1600. On account of the extreme diffuseness of the ethane bands it is assumed that, as in methane, all upper electronic states are unstable.[7] In ethylene, absorption has been observed from about λ 1980 to λ 1200, which consists of numerous well-defined bands.[7,8] For acetylene, rather weak absorption has been reported between λ 3150 and λ 2870, and strong photochemical action is known to result from absorption in the region between λ 2300 and λ 1900, where the bands are perfectly sharp.[7,9] A third extensive system of more or less diffuse bands covers the range from λ 1520 to λ 1050. Naturally, the observed limits of absorption depend very much on the gas pressure and the length of the absorbing layer. According to another investigator,[10] the continuous absorption of 15 cm of methane under standard conditions extends up to λ 1820. In any case, the sequence $CH_4 - C_2H_6 - C_2H_4 - C_2H_2$ indicates the shift of the absorption limit to greater wave-lengths. Beside methane no other hydrocarbon has thus far been identified by the spectroscope in the atmospheres of the giant planets. But ammonia has been found on both Jupiter and Saturn. Since this gas absorbs from λ 2300 downward and, therefore, partly protects the methane, the following discussion of the decomposition of methane has direct bearing only upon the atmospheres of Uranus and Neptune, where all ammonia is probably frozen out because of the lower temperature. The complications arising from the fact that the products of the simultaneous decomposition of methane and ammonia are likely to react on each other will be taken up in a later section. Adel and Slipher[11] estimate the amounts of methane on Uranus and Neptune to be approximately 4 and 25 mile-atmospheres, which may be a lower limit only for the possible pressure-broadening of the comparison spectra. By division

[6] A. B. F. Duncan and J. P. Howe, *J. Chem. Phys.*, **2**, 851, 1934.

[7] W. C. Price, *Phys. Rev.* (2), **47**, 444, 1935.

[8] G. Scheibe and H. Grieneisen, *Zs. f. phys. Chem.*, B, **25**, 52, 1934.

[9] G. B. Kistiakowski, *Phys. Rev.* (2), **37**, 277, 1931.

[10] A. Rose, *Zs. f. Phys.*, **81**, 758, 1933.

[11] *Phys. Rev.* (2), **47**, 787, 1935.

of these numbers through the height of the homogeneous atmosphere (RT/gM) of methane one gets the partial pressure of methane at the base of the atmospheres, provided these consist exclusively of methane. If, however, as is most likely, the atmospheres of Uranus and Neptune contain a large surplus of hydrogen, this gas would determine the effective distribution of atmospheric density, and the height of the homogeneous atmosphere of hydrogen would be the appropriate divisor (about 30 miles for Uranus and 25 miles for Neptune). On this assumption the partial pressure of methane may be 0.1 and 1 atmosphere for Uranus and Neptune, respectively. For Uranus this partial pressure is of the order of the vapor pressure of methane at the generally assumed surface temperature of the planet (90° K). For Neptune the surface temperature ought to be at least 110° K in order to maintain the observed amount of methane in the gaseous state. This surface temperature seems by no means impossible, in view of the powerful infrared absorption of 25 mile-atmospheres of methane.

On irradiation of methane by Schumann ultraviolet light, the primary process is the formation of hydrogen atoms and methyl radicals;

$$CH_4 + h\nu \rightarrow H + CH_3 .$$

The detailed investigation of the quantum yield and of the final reaction products is still under way, but a preliminary announcement has been made which states that in pure methane the secondary reactions produce mainly H_2 and C_2H_2, also small amounts of C_2H_6 and traces of C_2H_4 and of higher gaseous hydrocarbons.[12] Most fortunately, sufficient information is available about the behavior of both hydrogen atoms and methyl radicals which have been produced and studied independently from the photochemical primary process. These experiments lead to the expectation that the foremost secondary reactions should be recombinations by way of triple collisions:

$$H + H + M \rightarrow H_2 + M ,$$
$$CH_3 + CH_3 + M \rightarrow C_2H_6 + M ,$$

[12] W. Growth and H. Landenklos, *Die Naturwissenschaften*, **16**, 796 and 828, 1936.

provided the reactions go on in an inert atmosphere, which does not furnish any chemical acceptors to the radicals. Neither hydrogen atoms nor free methyl groups react with surplus methane, according to Bonhoeffer and Harteck.[13] The recombination of free methyl groups, produced in an atmosphere of helium or nitrogen, has been followed quantitatively by Paneth.[14] When he replaced the inert carrier gases by hydrogen, the formation of ethane was suppressed almost completely, and methane was re-formed by the reaction

$$CH_3 + H_2 \rightarrow CH_4 + H \ .$$

For further data concerning this reaction, consult a recent paper by Patat.[15] It would seem now that for maintaining a stationary concentration of methane the presence of an ample supply of hydrogen would be a sufficient guaranty. This has indeed been concluded both from general cosmogonic reasoning[16] and from more specific evidence based upon the interpretation of the density distribution in the interior of the giant planets.[17] Therefore it may be held that the purely thermal reaction between CH_3 and H_2 frustrates the photochemical decomposition of methane in the atmospheres of Uranus and Neptune.

This statement is not invalidated by the observations, quoted above, on the formation of higher hydrocarbons during the photochemical decomposition of pure methane. This may result from several processes of the following type, sometimes called "disproportionation":

$$CH_3 + CH_3 \rightarrow CH_4 + CH_2 \ ,$$

and from subsequent additions, like

$$CH_2 + CH_2 \rightarrow C_2H_4 \ .$$

[13] K. F. Bonhoeffer and P. Harteck, *Grundlagen der Photochemie*, 1933; K. H. Geib and P. Harteck, *Zs. f. Phys. Chem.*, (Ser. A), **170**, 1, 1934.

[14] F. A. Paneth, W. Hofeditz, and A. Wunsch, *J. Chem. Soc.*, **1**, 372, 1935.

[15] F. Patat, *Zs. f. phys. Chem.*, B, **32**, 274, 1936.

[16] D. H. Menzel, *Pub. A. S. P.*, **42**, 228, 1930.

[17] R. Wildt, *Nachrichten Gesell. Wiss. Göttingen* (Math. Phys. Kl. [N.F.]), **1**, 67, 1934.

Also it should be noted that these higher hydrocarbons are likely to decompose photochemically in their turn, all the more since they absorb at greater wave-lengths than methane. Acetylene polymerizes under the influence of ultraviolet light, and the reaction product is precipitated in solid form. Therefore, the absence of acetylene from planetary atmospheres is easily accounted for. To the writer's knowledge, the photochemical decomposition of ethane has not yet been studied, but it may be presumed that a breaking-up of the *C–C* bond would be found to be the primary process. Then the methyl radicals would react with surplus hydrogen, forming methane, and ethane would prove to be photochemically unstable in a hydrogen atmosphere. Much work has been done on the photochemical decomposition of ethylene,[18] but the interpretation of the experimental results is still beset with difficulties. Pending evidence to the contrary, it would not seem likely in any way that ethylene could resist the combined action of hydrogen and ultraviolet radiation. Moreover, another type of secondary reaction will tend toward the destruction of all higher hydrocarbons in the planetary atmospheres. As pointed out before, hydrogen atoms originate in the re-formation of methane and disappear by recombination, which is a comparatively slow process for the triple collisions involved. Therefore, a small stationary concentration of hydrogen atoms ought to exist in the atmospheres of the giant planets. But hydrogen atoms are known to attack violently all hydrocarbons, methane excepted, and to cause hydrogenation, breaking of carbon chains, and, principally, dehydrogenation.[19] Even if this process be a very slow one, it should have led to complete destruction of the higher hydrocarbons within a time which is short compared with the age of the planets. So it is very gratifying to realize that methane holds a rather exceptional position with respect to its stability. Otherwise one would fail to understand the absence from planetary atmospheres of other simple hydrocarbons, all of which have vapor tensions only slightly smaller than that of methane and, therefore, could not possibly be frozen out completely. The formation of methane in the cooling of a primeval

[18] R. D. McDonald and R. G. W. Norrish, *Proc. R. Soc., London*, A, **157**, 480, 1936.

[19] K. F. Bonhoeffer and P. Harteck, *Zs. f. phys. Chem.*, **139**, 64, 1928; H. von Wartenberg and G. Schultze, *ibid.*, B, **2**, 1, 1929.

atmosphere rich in hydrogen and carbon oxides, as suggested by Russell,[20] implies the simultaneous synthesis of small amounts of higher hydrocarbons, and apparently it is only by the photochemical processes and secondary reactions outlined above that the other hydrocarbons have been destroyed during a more advanced stage of evolution. It may be added here, too, that hydrogen sulphide, in addition to its photochemical decomposition, is rapidly disintegrated by hydrogen atoms, solid sulphur being precipitated.

PHOTOCHEMISTRY OF AMMONIA AND RELATED COMPOUNDS

It is well known that the absorption spectrum of ammonia at ordinary temperatures and pressures starts at about λ 2200 and extends into the far ultraviolet. With pressures of the order of 1 mm or less, the bands down to λ 1665 are all diffuse because of predissociation. Below λ 1665 all the bands are very sharp and show rotational fine structure. True continuous absorption, in distinction to that produced by pressure broadening, does not begin until about λ 1200. At λ 1150 and below, the continuous absorption is so strong that no more bands could be measured accurately. Sharp bands exist, however, as far down as λ 1085.[21] Two ways of photochemical decomposition have been observed in the laboratory, and a third one seems to be energetically possible, namely:

$$\lambda < 2200\,\text{A}:\ NH_3 + h\nu \rightarrow H + NH_2\,,$$
$$\lambda < 1700\,\text{A}:\ NH_3 + h\nu \rightarrow H + NH_2^*\,,$$
$$\lambda < 1900\,\text{A}:\ NH_3 + h\nu \rightarrow H_2 + NH^*\,.$$

The NH_2^* are excited radicals which show strong fluorescence between λ 4000 and λ 6000, emitting the so-called α-bands of ammonia observed in discharges through streaming ammonia vapor. The resonance bands λ 3360 and λ 3370 of the molecule NH have been sought in vain. So the third process, which would cause the emission of the NH bands, can be ruled out because of experimental evidence. The first process should be preponderant in the atmospheres of Jupiter and Saturn, where the second is probably inhibited by the

[20] *Science*, **81**, 1, 1935.

[21] A. B. F. Duncan, *Phys. Rev.* (2), **47**, 822, 1935.

competing absorption of methane in the very range of wave-lengths required. Now the quantum yield of the first process is about 0.25 at room temperature and varies only slightly with the partial pressure of ammonia. Evidently ammonia is re-formed at a considerable rate, by the secondary reactions. But it has not yet been established beyond doubt which course the secondary reactions take, despite extensive experimental investigations. In all experiments part of the ammonia is destroyed irreversibly, the final products being molecular hydrogen and nitrogen. No reaction scheme can be conceived at present which would prevent any irreversible decomposition of ammonia and, therefore, would serve to maintain the presumably stationary composition of the atmospheres of Jupiter and Saturn. Even the presence of surplus hydrogen is of no direct help. By analogy to the re-formation of methane, one might expect a reaction

$$NH_2 + H_2 \rightarrow NH_3 + H\ ,$$

which would imply a dependence of the quantum yield on the partial pressure of hydrogen admixed to the ammonia. The early experiments by Warburg prove the contrary. With due regard to the entire experimental material, an opinion may be ventured here as to the direction in which a solution of the astrophysical problem may be sought. But it is realized that any final verdict needs the support of further experiments.

Farkas and Harteck[22] succeeded in measuring the stationary concentration of hydrogen atoms in decomposing pure ammonia and explained their results by the following set of secondary reactions:

a) $$NH_3 + H \rightleftarrows NH_4\ ,$$

b) $$NH_4 + NH_2 \begin{cases} \rightarrow 2\,NH_3 \\ \rightarrow NH_3 + H_2 + NH\ , \end{cases}$$

c) $$NH + NH \rightarrow N_2 + H_2\ .$$

At room temperature the equilibrium (*a*) is entirely on the side of the ammonium radical. The quantum yield is determined by the ratio of the alternative reactions (*b*) and (*c*), and in order to get the

[22] *Zs. f. phys. Chem.*, B, **25**, 257, 1934.

observed value (0.25) it has to be assumed that (*b*) proceeds three times faster than (*c*) at room temperature. Melville[23] made the interesting observation that in a mixture of ammonia and hydrogen the quantum yield of the photolysis of ammonia is very efficiently reduced by the addition of hydrogen atoms. Farkas and Harteck suggest that this effect is caused by the fact that in Melville's experiments NH_2 and NH_4 are no longer present in approximately equimolal amounts, on account of the increased association of NH_3 with the added hydrogen atoms, and that, therefore, the surplus NH_4 may enter reactions like the following, or similar ones:

$$NH_4 + NH \rightarrow NH_3 + NH_2 ,$$

consuming the fatal NH molecules which otherwise would decompose irreversibly. Now it will be remembered that a stationary concentration of hydrogen atoms is set up in a mixture of hydrogen and methane on irradiation by ultraviolet light. Thus it may be that the very presence of methane in the atmospheres of Jupiter and Saturn prevents the ammonia from decomposing irreversibly, by a mechanism closely related to that which operates in Melville's effect. Whether this is true or not is hard to ascertain at present for lack of knowledge of the extinction coefficients of methane and ammonia in the overlapping region of absorption, among other reasons.

It should not be overlooked that other investigators[24] have proposed a rather different reaction scheme, involving the intermediate formation of hydrazine molecules. Since they did not measure the stationary concentration of hydrogen atoms during decomposition, their interpretation is necessarily at variance with that given by Bonhoeffer and Harteck and can scarcely claim the same significance. Hydrazine is decomposed by ultraviolet light too:

$$\lambda < 2500 \text{ A}: \quad N_2H_4 + h\nu \rightarrow NH_2 + NH_2 ,$$

$$\lambda < 1600 \text{ A}: \quad N_2H_4 + h\nu \rightarrow NH_2 + NH_2^* ,$$

where the excited radical emits the α-bands of ammonia referred to before. The so-called Schuster bands of ammonia, λ 5643 and λ 5681,

[23] *Trans. Faraday Soc.*, **28**, 885, 1932.

[24] R. A. Ogg, P. A. Leighton, and F. W. Bergstrom, *J. Amer. Chem. Soc.*, **56**, 322, 1934.

are now ascribed to a transition from an excited stable state of the hydrazine molecule to a repulsive one.[25] Their absence from the fluorescence accompanying the photochemical decomposition of hydrazine by Schumann ultraviolet light, as established by Terenin, does not favor the conception of a transitory formation of hydrazine. Besides, only rapid destruction by a subsequent reaction could protect hydrazine from being frozen out. The exceedingly low-vapor tension of this compound at the surface temperatures of Jupiter and Saturn is by far the strongest argument against its appearance in the foregoing scheme of the photolysis of ammonia. However, the occurrence of methylamine in the atmospheres of the same planets should be envisaged. Traces of the radicals CH_3 and NH_2 will certainly recombine, and since in the range of temperature with which we are concerned here the vapor tension of $CH_3 \cdot NH_2$ is about one-tenth that of ammonia, there is little danger of condensation. Whether these traces can be detected by the spectroscope is a different question. It would be worth while to look for the rotation-oscillation bands of methylamine in the spectra of Jupiter and Saturn, although they may conceivably be difficult to disentangle from the heavy absorption of methane and ammonia. The electronic absorption spectrum of methylamine extends from λ 2400 downward, but the corresponding photochemical process has not yet been investigated.

Furthermore, researches should be noted here concerning the reaction of decomposing ammonia with ethylene or carbon monoxide. Although these experiments are of an orienting character only, most probably they preclude the existence of either of these gases in the atmospheres of Jupiter and Saturn. The hydrogen atoms originating in the photolysis of ammonia are found to induce polymerization of ethylene.[26] In principle this is the same process as discussed before, in view of the hydrogen atoms formed by the reaction of CH_3 with H_2. The photochemical reaction of ammonia with carbon monoxide[27] yields formamide ($HCO \cdot NH_2$) as a primary product, which then undergoes secondary reactions and decomposes photochemically too.

[25] R. W. Lunt, J. E. Mills, and E. C. W. Smith, *Trans. Faraday Soc.*, **31**, 792, 1935.

[26] H. S. Taylor and H. J. Emeléus, *J. Amer. Chem. Soc.*, **53**, 3770, 1931.

[27] Emeléus, *Trans. Faraday Soc.*, **28**, 89, 1932.

Less than 5 per cent of the ammonia reacting yields the normal products N_2 and H_2. Since the main reaction product is deposited in condensed form, the atmospheres of Jupiter and Saturn should be depleted of carbon monoxide by this time. This conclusion is the more remarkable since the presence of carbon monoxide is difficult to exclude on spectroscopic evidence and its vapor tension, nearly as high as that of nitrogen, would favor its persistence in the gaseous state. In addition, it may be mentioned here that the presence of carbon dioxide in the atmosphere of Jupiter is hard to reconcile with that of ammonia because these gases associate, forming ammonium carbaminate,

$$2NH_3 + CO_2 \rightleftarrows NH_4 \cdot CO_2 \cdot NH_2 \, .$$

The dissociation tension of this solid compound is exceedingly small compared with the vapor tension of either pure ammonia or pure carbon dioxide. Although the dissociation tension of ammonium carbaminate has not yet been measured at temperatures lower than room temperature, it can be estimated that the surface temperature of Jupiter, usually assumed to be about 150° K, would have to be increased by at least 100° in order to maintain the spectroscopically observed amount of ammonia in equilibrium with the corresponding amount of gaseous carbon dioxide and solid ammonium carbaminate. The analogous argument and about the same numerical estimate applies to the presence of hydrogen sulphide, which also would associate with ammonia, forming $NH_4 \cdot SH$.

PHOTOCHEMISTRY OF SOME GASEOUS OXIDES

The atmosphere of Venus seems to be composed almost entirely of carbon dioxide, and the amounts of oxygen and water vapor must be less than one-thousandth and one-tenth, respectively, of the amounts present in the earth's atmosphere. The estimates of the total mass of carbon dioxide are based on the strength of the absorption bands situated in the near infrared. They vary between 400 meter-atmospheres and 2 mile-atmospheres. Since oxygen is practically absent, the carbon dioxide is exposed to the destructive

action of ultraviolet sunlight, which brings about the following primary process:

$$\lambda < 1800\ \mathrm{A}: \quad CO_2 + h\nu \rightarrow O + CO\,.$$

In the highest atmospheric layers carbon monoxide may dissociate photochemically in its turn:

$$\lambda < 1200\ \mathrm{A}: \quad CO + h\nu \rightarrow C + O\,,$$

but throughout the bulk of the atmosphere carbon monoxide will be protected by the absorption of carbon dioxide. The most important secondary reaction should be the partial recombination of the oxygen atoms, which would be followed by a speedy photochemical dissociation of the oxygen molecules. Carbon monoxide molecules are not known to associate in any way. Thus the problem is reduced to the oxidation of carbon monoxide by photochemically produced oxygen atoms, which has been studied by several investigators. The extensive work by Popov[28] has little bearing on the astrophysical problem because in his experiments the oxidation took place under very low pressure, and, therefore, the homogeneous reaction was negligible beside that on the wall. Jackson[29] used pressures up to several hundred millimeters, and his experiments cover a wide range of temperatures (300°–700° K). At room temperature oxygen atoms react with oxygen molecules, forming ozone at least one hundred fifty times more rapidly than with carbon monoxide molecules, forming carbon dioxide. At high temperatures the dry oxidation is practically independent of temperature and total pressure. With water vapor present, the reaction is no longer independent of pressure and has a large temperature coefficient. A mechanism involving OH and H was suggested by Jackson in order to explain the effect produced by water vapor. Recently it has been proved[30] that the photochemical oxidation of carbon monoxide is a chain reaction, and various reaction schemes have been suggested. A final choice between these is not yet possible. Still it may be safely concluded that the photolysis

[28] *Acta physicochemica U.S.S.R.*, **3**, 223, 1935.

[29] W. F. Jackson, *J. Amer. Chem. Soc.*, **56**, 2631, 1934.

[30] L. Holzapfel, Inaugural-Dissertation, Universität Berlin, 1936.

of carbon dioxide in the atmosphere of Venus is followed by a re-oxidation of the carbon monoxide. The presumably high temperature at the surface of Venus—on account of the greenhouse effect of the carbon dioxide—and the presence of traces of water vapor, which cannot be ruled out at present, may be helpful agents. Water vapor itself decomposes photochemically according to the following equation:

$$\lambda < 1800\,\text{A}:\ H_2O + h\nu \rightarrow OH + H\,.$$

Since the limiting wave-length of photolysis is approximately the same for water vapor and carbon dioxide, these compounds should be decomposed simultaneously in an atmosphere containing both of them. This may lead to a subsequent formation of formaldehyde, which in laboratory experiments has been observed to originate from the reaction between carbon monoxide and photochemically produced hydrogen atoms. The same process may occur in the atmosphere of Venus. Formaldehyde has been detected by chemical methods in the earth's atmosphere,[31] but its photochemical origin has not yet been ascertained there. Formaldehyde displays a strong electronic absorption spectrum in the astronomically accessible ultraviolet. Therefore it would be of interest to look for it in the spectrum of Venus.

Laboratory experiments give some evidence of the photochemical oxidation of nitrogen.[32] Oxidation of nitrogen is a large-scale phenomenon in terrestrial thunderstorms. But apparently the oxides are destroyed rapidly, since their stationary concentration is almost immeasurably small. Under these circumstances it is improbable that nitrogen oxides should be detected spectroscopically in the atmospheres of the other terrestrial planets, all of which contain traces of oxygen, at best.

PRINCETON UNIVERSITY OBSERVATORY
June 1937

[31] N. R. Dhar and A. Ram, *Nature*, **132**, 819, 1933.

[32] V. Kondratjev, *Acta physicochemica U.S.S.R.*, **3**, 247, 1935.

NOTE ON THE TEMPERATURE OF VENUS

ARTHUR ADEL

ABSTRACT

The distribution of intensity of absorption in the fine structure of the CO_2 bands in the spectrum of Venus provides an independent approach to the problem of the planet's temperature. The temperature of the surface appears to be greater than 50° C.

Information regarding the temperatures of planetary atmospheres is generally sought through the determination of the distribution of energy in the reflection and emission spectra of the planets. There is, however, another method which is not so incumbered by the effects of the earth's atmosphere and which is quite ideally suited to those planets whose spectra include absorption bands characteristic of their atmospheres: Venus contains carbon dioxide; Jupiter and Saturn, methane and ammonia; Uranus and Neptune, methane. For, in a planetary atmosphere, the distribution of molecular population over the various vibrational and rotational states is strictly determined by the prevailing temperatures. In consequence the distribution of intensity of absorption in the fine structure of the bands is also governed by the temperature, and is in most instances a very simple function of the latter.

For the solution of the problem one requires, however, definitive, high-dispersion spectra to make possible the unambiguous selection of the fine-structure lines displaying the maximum intensity of absorption. With the possible exception of a reproduction of a portion of the spectrum of Venus, such data are not available.[1] The spectrum alluded to, while scarcely adequate for the present need, will suffice for purposes of illustration.

The reproduced region of the spectrum of Venus displays the two carbon dioxide absorption bands

$$\left\{ 5\nu_3 + \begin{pmatrix} \nu_1 \\ 2\nu_2 \end{pmatrix} \right\}_L$$

[1] W. S. Adams and T. Dunham, Jr., *Pub. A.S.P.*, **44**, 243, 1932.

and

$$\left\{5\nu_3 + \binom{\nu_1}{2\nu_2}\right\}_U ,$$

with centers at 12672.4 and 12774.7 cm^{-1}, respectively.[2] Each of these bands possesses a converging high-frequency branch and a diverging low-frequency branch, but no zero branch. Apropos of the congestion in the high-frequency branches, the diverging branches are more convenient for study. Moreover, the short wave-length band (12774.7 cm^{-1}) is apparently the more easily examined of the two. The theoretical intensity of the jth line in the negative branch of this band is given by the expression

$$I = \int_{\nu} a_\nu d\nu = C_1 j e^{-\sigma j(j+1)} ,$$

where

$$\sigma = \frac{h^2}{8\pi^2 AkT} ,$$

A being the moment of inertia of the carbon dioxide molecule. The theoretical intensity cannot be directly observed, but the minimum percentage transmission can be.[3] The minimum percentage transmission $T_{\min}$ and the theoretical intensity are related by the expression

$$d\{\log T_{\min}\} = C_2 j e^{-\sigma_x j(j+1)} dx ,$$

which applies to a layer of the Venusian atmosphere of thickness dx and temperature T_x. The value of T_x determines the value of j for which the function $T_{\min}$ is a minimum. For the entire atmosphere we have

$$\{\log T_{\min}\}^2 = C_2 j \int_0^\infty e^{-\sigma_x j(j+1)} dx .$$

It is sufficient to point out that this function (or $T_{\min}$ for the entire atmosphere) will also be a minimum for a certain value of j and that

[2] Arthur Adel and D. M. Dennison, *Phys. Rev.*, **43**, 716; **44**, 99, 1933.

[3] D. M. Dennison, *ibid.*, **31**, 503, 1928.

this will correspond to a value of T lower than the surface temperature of the planet and higher than the temperature of the outer layers of the planet's atmosphere. In other words, we may write

$$\{\log T_{\min}\}^2 = C_2 j e^{-\sigma_e j(j+1)} ,$$

where σ_e contains this effective temperature.

From the water-cell transmissions made in 1922 by W. W. Coblentz and C. O. Lampland,[4] D. H. Menzel[5] has calculated an effective noonday temperature of 50° C. for the surface of Venus. We should therefore expect to find the value of j corresponding to 50° C. greater than the value of j at which maximum absorption occurs in the negative branch of

$$\left\{ 5\nu_3 + \begin{pmatrix} \nu_1 \\ 2\nu_2 \end{pmatrix} \right\}_U .$$

From the expression

$$C_2 j e^{-\sigma_e j(j+1)}$$

it follows that the maximum intensity of absorption relates the effective temperature with the ordinal number of the line in question in the manner

$$j \cong \frac{2\pi}{h} \sqrt{AkT} .$$

For $T = 273° + 50° = 323°$, and $A = 70.2 \times 10^{-40}$ gm cm^2, we find $j \cong 18$. Since alternate fine-structure lines are completely forbidden by the selection rules, we expect to find the maximum intensity of absorption somewhere between the center of the band and the ninth appearing line. Although it is difficult to ascertain from the reproductions exactly where the maximum absorption occurs, careful examination indicates that 50° C. is probably too low a value for the temperature of the surface of the planet Venus.

Lowell Observatory
Flagstaff, Arizona
July 1937

[4] *Pop. Astr.*, **30**, 551, 1922.

[5] *Ap. J.*, **58**, 65, 1923.

NOTES

THE NUCLEAR STAR CLUSTER IN 30 DORADUS

Recent photographs made with the 60-inch reflector of the Boyden Station permit a further description of the gaseous nebula 30 Doradus, which shares with the "axis" the distinction of being the most conspicuous feature of the Large Magellanic Cloud. In particular the photographs reveal the nature and richness of the remarkable cluster of blue stars that lies in the heart of the nebulosity. In neither linear dimensions nor total luminosity is 30 Doradus closely approached by any gaseous nebula of the galactic system. The nebulosity, NGC 5195, at the end of a spiral arm of Messier 51, may be, however, of comparable dimensions, luminosity, and general structure.

The position for 1900.0 of 30 Doradus, which is known also as the looped nebula and as NGC 2070, is $\alpha = 5^h 39^m.4$, $\delta = -69^\circ 9'$, $\lambda = 246^\circ$, $\beta = -31^\circ$.

In spectral characteristics 30 Doradus resembles the great Orion nebula (NGC 1976). The nebular lines, N_1 and N_2, and the hydrogen lines predominate, but a close study of the spectrum as a whole is not possible because of the large dimensions of the nebula. An examination by Miss Cannon shows faintly and diffusely the *O* II pair of lines at λ 3727, not hitherto recorded for 30 Doradus, but conspicuous in the Orion nebula.

The nebulosity, both dark and bright, extends to great distances from the center. The total diameter is about $25'$, corresponding to 600 light-years, which is about one hundred times the diameter of the Orion nebula and perhaps five times the diameter of W. H. Pickering's spiral of faint nebulosity that spreads throughout the whole constellation of Orion. The variable HV 2740, which is $5'$ from the center, is apparently irregular; an earlier indication that it was a Cepheid with period of 23.0 days, showing a large deviation from the period-luminosity curve,[1] has been rejected after further study. Half

[1] *Harvard Bull.*, No. 883, 1931.

PLATE VII

South

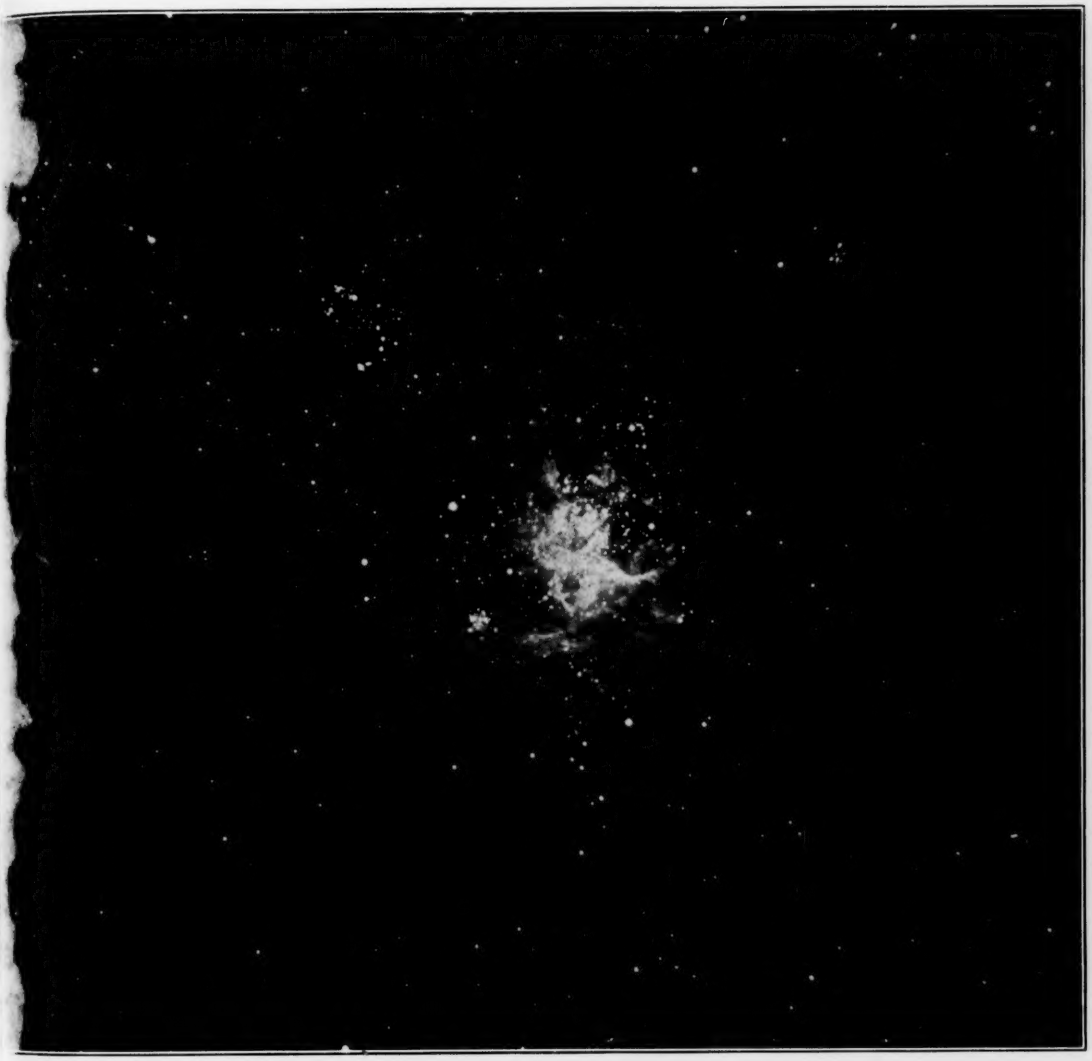

30 Doradus, in the Large Magellanic Cloud

Photographed by J. S. Paraskevopoulos, with the 60-inch reflector at the Boyden Station of Harvard Observatory. nlarged 2.7 times. Scale, 1 mm = 70."2. Exposure, 50 minutes.

a dozen other variables have been found within the bounds of the nebula by Mrs. S. F. Lindsay, but types have not yet been determined. The total photographic absorption produced by the nebula probably exceeds one magnitude.

Five clusters of the galactic type are apparently involved in the nebulosity. The richest is the loose, elongated cluster at the center. Its major and minor axes are approximately sixty and forty-five light-years. Estimates of magnitude are difficult because of the irregular nebulous background and the Eberhard effect. An examination of the nuclear cluster on seven plates of different exposure-times gives for the number of stars brighter than various magnitude limits:

m_{pg}	N_m	m_{pg}	N_m
12	10	17	300
15	50	19+	1000

A comparison of photographs on blue- and red-sensitive plates indicates that all of the cluster stars are blue. Their exceedingly high luminosities are, of course, responsible for the incited radiation of the large nebula in which they are involved. Even with no allowance made for the strong absorption within the nebula, their absolute magnitudes range from positive values up to -5 and brighter.

In the nuclear area Miss Cannon has classified the spectra of five stars.[2] Some are fainter than the fourteenth magnitude, but all are of spectral class O.

It is of interest to note that, notwithstanding the large number of stars in the nuclear cluster and their exceedingly high luminosity, they contribute altogether but a small portion—perhaps 10 per cent—of the total light of 30 Doradus, which is a naked-eye object. Estimates made at the Lick Observatory[3] and at Harvard place the integrated apparent magnitude of the nucleus stars and nebulosity at about 6.0; a Harvard estimate of the integrated magnitude of the whole nebula, with the small contribution from the involved clusters, gives the value 4.0.[4]

[2] *Ibid.*, No. 891, 1933; *Harvard Ann.*, **76,** 28, 1916.

[3] *Lick Obs. Pub.*, **13,** 109, 1918; see also *ibid.*, pp. 187–89.

[4] *Harvard Circ.*, No. 271, 1925. In this paper, through a misprint, the total diameter is given as 40 parsecs; it should read 140 parsecs, the value indicated by the plates then available.

The accompanying photograph was made on January 17, 1937, with an exposure time of fifty minutes on a Cramer Hi-Speed Special plate. The original photograph shows objects fainter than the nineteenth magnitude.

HARLOW SHAPLEY
JOHN S. PARASKEVOPOULOS

HARVARD OBSERVATORY
September 1937

THE PHOTOELECTRIC COLOR OF THE ZODIACAL LIGHT

ABSTRACT

The mean color of the zodiacal light as observed with a photoelectric photometer at McDonald Observatory is +0.28 mag. on Becker's system of photoelectric colors. This color corresponds to spectral type G1, which is very near the color of the sun. It is concluded that there is no Rayleigh scattering in the zodiacal cloud and hence the number of very small meteoric particles is negligible.

Colorimetric measures of the zodiacal light are data which will be useful in an analytical discussion of the physical properties of the medium producing the illumination. It is generally believed that the zodiacal light is produced by the scattering of sunlight by meteoric particles concentrated in the plane of the ecliptic and extending beyond the orbit of the earth. According to the theories of scattering, if the particles are small—say one-quarter of the wave-length of light—the radiation scattered by them will follow Rayleigh's law, that is, the zodiacal light in this case should be as much bluer than the sun as is the daytime sky. If the particles are large compared with the wave-length of light, then the scattering is that of pure reflection and is independent of the wave-length of the incident light. For intermediate sizes the law of scattering is somewhat complicated and is a function of various powers of the wave-length.

The color of the zodiacal light has been measured by one of us[1] with a photoelectric photometer at the Yerkes Observatory. The results were not consistent, indicating that possibly the color of the zodiacal light changed from time to time. It was stated, however, that a part of this variation might be due to the light from the night sky, since the colorimetric determinations were for the total light, that is, the auroral light, the scattered light, and the light of the unresolved stars, plus the zodiacal light.

[1] *Ap. J.*, **80**, 61, 1934.

In view of the large variations found in that work it seemed wise to take additional observations of the color of the zodiacal light under better conditions for measurements at such large zenith distances. We have observed this color at the McDonald Observatory, with the photoelectric photometer used and described by Elvey and Roach.[2] Owing to the high elevation, 2070 m, the sky is quite uniform and free from haze at large zenith distances. The method of observing was quite different since with the alt-azimuth arrangement of the photoelectric sky photometer it was quite easy to make a series of observations across the zodiacal-light cone at a given zenith distance. The observations near the ends of the run gave the sky correction to be applied to the zodiacal light, since the auroral and scattered light is constant for a given zenith distance. In this manner nothing but the zodiacal light was included in the observations for color. Since the observations were taken sufficiently far from the Milky Way, there was very little differential effect from the unresolved stars between the areas used for the sky background and the region of the zodiacal light. The colors were calibrated and corrected for extinction by observations on eight bright stars of various spectral classes. This number of stars is not sufficient to establish independently the relationship between color and spectral type, but there are enough data to determine the color equation between our observed colors and the photoelectric colors of stars measured by W. Becker.[3] The resulting color equation for reducing our observations to Becker's system is

$$\text{Color}_{\,(\text{Becker})} = 0.37 + 0.74 \times \text{Color}_{\,(\text{obs})} .$$

The accompanying tabulated results are for the evening zodiacal light. The mean color of the zodiacal light is -0.12 mag, which

Date	Color
1937 Mar. 1	−0.10 mag
29	.10
30	.15
Apr. 3	−0.15
Mean	−0.12

[2] *Ibid.*, **85**, 213, 1937.

[3] *Veröff. Sternwarte Berlin-Babelsberg*, **10**, Nos. 3 and 6, 1933.

when reduced to Becker's system is equal to +0.28 mag. This color, when referred to his diagram showing the dependence of color upon spectral type, corresponds to spectral class G1.

Since the foregoing color of the zodiacal light is very similar to that of the sun, we can conclude that there is practically no Rayleigh scattering in the cloud of meteoric material and hence the number of very small particles is negligible.

C. T. Elvey
Paul Rudnick

McDonald Observatory
Fort Davis, Texas
July 23, 1937